

January 2013

Phenotypic Characterization of the Pancreatic-Derived Factor (PANDER) Knockout Mouse on Pure C57BL/6 Background

Shari Moak

University of South Florida, slmoak@mail.usf.edu

Follow this and additional works at: <http://scholarcommons.usf.edu/etd>

 Part of the [Biology Commons](#)

Scholar Commons Citation

Moak, Shari, "Phenotypic Characterization of the Pancreatic-Derived Factor (PANDER) Knockout Mouse on Pure C57BL/6 Background" (2013). *Graduate Theses and Dissertations*.
<http://scholarcommons.usf.edu/etd/4830>

This Thesis is brought to you for free and open access by the Graduate School at Scholar Commons. It has been accepted for inclusion in Graduate Theses and Dissertations by an authorized administrator of Scholar Commons. For more information, please contact scholarcommons@usf.edu.

Phenotypic Characterization of the Pancreatic-Derived Factor (PANDER)
Knockout Mouse on Pure C57BL/6 Background

by

Shari Lynn Moak

A thesis submitted in partial fulfillment
of the requirements for the degree of
Master of Science
with a concentration in Cell and Molecular Biology
Department of Cell Biology, Microbiology, and Molecular Biology
College of Arts and Sciences
University of South Florida

Major Professor: Brant R. Burkhardt, Ph.D.
Sandra Westerheide, Ph.D.
Patrick Bradshaw, Ph.D.

Date of Approval:
October 31, 2013

Keywords: FAM3B, Liver, Glucose Tolerance, Type 2 Diabetes, Hepatic Insulin Signaling

Copyright © 2013, Shari Lynn Moak

DEDICATION

I would like to dedicate this thesis to my amazing family. First and foremost, my parents, who have been my biggest fans, support system, and source of utmost strength throughout my graduate career and life. I've truly been blessed to have such a perfect Mom & Dad and I wouldn't have been able to do this without your unwavering support emotionally, mentally, and financially. I am forever grateful for all that you both have done for me! Secondly, my wonderful siblings/sibling-in-laws and my beautiful nieces and nephews for always being there for me when I needed a hug, kiss, and an "I love you Auntie Shari!" to help me through the day. It meant the world to have such a strong family unit behind me and I definitely would not be here without the love and support from each and every one of you!

I would also like to thank my wonderful boyfriend, Dan. Not only have you been with me since before I even started graduate school, but you've been by my side every step of the way. Your invaluable support, guidance, shoulder to cry on when I had more bad days than good, understanding, and love have gotten me where I am today. I truly would not have been able to do this without you! Thank you for all that you are, all that you do for me, and the love that you continue to show through one of the most trying times in our lives together.

ACKNOWLEDGMENTS

I would like to genuinely thank Dr. Grace Dougan for being my biggest confidant and assisting me in every aspect of this thesis project. I would not have been nearly as level-headed or successful without your help, advice, and friendship! Also, a huge "thank you" to my committee members, Dr. Sandy Westerheide and Dr. Patrick Bradshaw, for all of their guidance and advice throughout this whole process. Lastly, I would like to thank my Major Professor, Dr. Brant Burkhardt, for always encouraging me to follow my dreams, to never give up when times are hard, and to believe in myself. Your wealth of knowledge and advice has allowed me to grow so much not only as a scientist but also as a person in the past 2 years and I can't thank you enough!

TABLE OF CONTENTS

LIST OF TABLES	iii
LIST OF FIGURES	iv
ABSTRACT.....	vi
CHAPTER ONE: INTRODUCTION	1
Typical Glycemic Regulation	1
Fed State Glycemic Regulation.....	1
Fasting State Glycemic Regulation.....	3
Insulin Signaling	4
Type 2 Diabetes (T2D).....	6
Discovery of PANcreatic-DErived Factor (PANDER)	9
Newly Discovered Structure of PANDER.....	10
Genomic Structure of PANDER.....	11
Regulation of PANDER Transcription	12
Regulation of PANDER Secretion.....	14
Summary of PANDER Animal Models.....	15
Hepatic Ad-PANDER Overexpressor and siRNA Knockdown.....	15
Ad-PANDER Overexpressor	16
PANDER Transgenic Overexpressor	17
PANDER Knockout Model.....	17
Role of PANDER in Glycemic Regulation	19
Role of PANDER in Type 2 Diabetes	20
Role of PANDER in Cancer.....	21
Other FAM3 Family Members.....	23
Project Summary and Specific Aims	25
CHAPTER TWO: INITIAL PHENOTYPING OF PANDER KNOCKOUT C57BL/6 MOUSE	28
Rationale	28
Experimental Design & Methods	29
Murine Colony Acquisition, Care, and Maintenance	29
Murine DNA Genotyping	30
Measurement of Fasting Glycemia.....	30
Body Weight Measurements	31
Measurement of Hormonal Analytes	31
Measurement of Plasma Corticosterones.....	32
Measurement of Plasma Triglycerides.....	33
Glucose Tolerance & Insulin Tolerance Testing.....	33
Confirmation of PANKO-C57 and WT Genotypes.....	34

PANKO-C57 Mice Exhibit Lower Fasting Glycemia Short and Long Term	35
PANKO-C57 Mice Display Increased Body Weights Longitudinally.....	37
Differential Expression of Metabolic Hormonal Analytes in PANKO-C57	38
Similar Corticosterone and Plasma Triglyceride Concentrations in PANKO-C57	40
PANKO-C57 Mice Display Enhanced Glucose Tolerance in Metabolic Tests	42
PANKO-C57 Mice Reveal Similar Insulin Sensitivity in Insulin Tolerance Test (ITT)	43
Summary of Initial PANKO-C57 Phenotypic & Metabolic Characterization.....	47
 CHAPTER THREE: HEPATIC INSULIN SIGNALING IN PANDER KNOCKOUT C57BL/6	
MOUSE	49
Rationale	49
Experimental Design & Methods	50
SDS-PAGE Western Blotting of Fasting and Fed Liver Protein.....	50
Measurement of Hepatic Triglyceride Content	52
Evaluation of Hepatic Glycogen Content.....	52
Measurement of PEPCK and G6Pase Expression via RT-PCR	53
Measurement of Plasma High-Density Lipoprotein (HDL) and Low-Density	
Lipoprotein (LDL) Cholesterol.....	54
Fasting PANKO-C57 Mice Exhibit Enhanced Hepatic Insulin Signaling	54
Insulin-Stimulation Enhances Hepatic Insulin Signaling in PANKO-C57	56
Decreased Fasting Hepatic Triglyceride Content in PANKO-C57 Mice.....	58
PANKO-C57 Mice Exhibit Increased Fed Hepatic Glycogen Stores.....	59
Gluconeogenic Enzyme Expression is Upregulated in Fed PANKO-C57 Mice	60
Higher HDL and Lower LDL Plasma Cholesterol in PANKO-C57 Mice.....	62
Summary of Hepatic Signaling Mechanisms in PANKO-C57 Mice	63
 CHAPTER FOUR: CONCLUSIONS	65
PANKO-C57 Compared to Previous PANDER Knockout/Knockdown Models	65
PANKO-C57 as an Improved PANDER Murine Model	66
Advantages.....	66
Limitations	68
PANDER's Role in Glycemic Regulation & Type 2 Diabetes Based on PANKO-C57	71
PANDER in the Fed State.....	71
PANDER in the Fasting State	73
PANDER in Type 2 Diabetes.....	75
Final Thoughts and Summary	78
 LITERATURE CITED	79
 APPENDICES	88
Appendix A: Primary Antibodies Utilized	88
Appendix B: 4005M Breeding Protocol for PANKO-C57 IACUC Approval.....	89
Appendix C: Experimental 4071 R Protocol IACUC Approval	90

LIST OF TABLES

Table 1: Summary of Western Results Comparing Hepatic Signaling in PANKO-C57 versus WT as a Heat Map Representation	63
Table 2: Comparisons of PANDER Knockout C57/129 & <i>db/db</i> siRNA Knockdown Murine Models to PANKO-C57	66
Table A1: Primary Antibodies and their Respective Catalog Numbers Used in SDS-PAGE in Chapter 3	88

LIST OF FIGURES

Figure 1: Fed State Network of Interactions in Normal Glycemic Regulation	3
Figure 2: Insulin Signaling Network in Insulin Sensitive Individuals.....	6
Figure 3: Secondary and Crystal Structure of PANDER.....	11
Figure 4: PANDER Gene Targeting Strategy.....	18
Figure 5: Luminex Multiplexing Concept & Protocol	32
Figure 6: PCR-Amplified PANKO-C57 and WT Allele Confirmations.....	35
Figure 7: Male PANKO-C57 Mice have Lower Fasting Glycemia Short and Long Term	36
Figure 8: Female PANKO-C57 Display Lower Average Fasting Glycemia Trend After Short and Long Term Fast	37
Figure 9: PANKO-C57 Mice Body Weight Measurements Trend Heavier than WT Mice	38
Figure 10: Longitudinal Serum Hormonal Analyte Concentrations in PANKO-C57 and WT Mice.....	40
Figure 11: Plasma Corticosterone and Triglyceride Levels in PANKO-C57 and WT Mice.....	41
Figure 12: GTT of PANKO-C57 Male and Female Mice Reveals Enhanced Glucose Tolerance.....	43
Figure 13: Male PANKO-C57 and WT Similarities of Blood Glucose in ITT	45
Figure 14: ITT Measurement of Insulin Sensitivity in Female PANKO-C57 and WT Mice.....	46
Figure 15: Overnight Fasting Hepatic Signaling in PANKO-C57 and WT Mice	55
Figure 16: Insulin-Stimulated Effect on Hepatic Signaling Protein Expression in PANKO-C57	57
Figure 17: PANKO-C57 Mice Hepatic Triglyceride Concentrations Fasted and Insulin Stimulated.....	59

Figure 18: Hepatic Glycogen Stores in PANKO-C57 and WT Mice.....60

Figure 19: Fasting and Insulin-Stimulated Relative Gene Expression of G6Pase and
PEPCK in PANKO-C57 Mice.....61

Figure 20: Plasma HDL/LDL Cholesterol Concentrations in PANKO-C57 and WT Mice62

Figure 21: PANDER’s Predicted Actions in the Fed State Based on PANKO-C57 Model72

Figure 22: PANDER’s Predicted Role in Glycemic Regulation in the Fasted State Based
on PANKO-C5774

Figure 23: PANDER’s Predicted Role in Insulin Resistance and Type 2 Diabetes.....76

ABSTRACT

PANcreatic-DErived Factor (PANDER), or FAM3B, is a 235-amino acid protein strongly expressed within and secreted from the endocrine pancreas. Research surrounding PANDER has revealed a large role for the protein in maintaining glucose homeostasis, as evidenced by several Ad-PANDER overexpressing murine models, our lab's pancreas-specific PANDER transgenic overexpressor, and most recently our mixed genetic C57/129J PANDER knockout (PANKO) mouse. However, PANDER's overall role in glycemic regulation and glucose homeostasis has yet to be studied in a purebred C57BL/6J PANDER knockout model. Here we present the first phenotypic characterization of our global PANDER knockout mouse on a C57BL/6J background (PANKO-C57) where we examined metabolics through glucose/insulin tolerance testing, fasting glycemia, and body weights, the concentrations of hormonal analytes along with lipids and corticosterones, and full elucidation of hepatic insulin signaling through the insulin signaling cascade. Overall, the PANKO-C57 mice exhibited increased body weights with enhanced glucose tolerance and lower fasting glycemia, similar peripheral insulin sensitivities, increased hepatic lipidemia, and enhanced hepatic insulin signaling at critical insulin signaling molecules. Taken together, the PANKO-C57 demonstrates that the disruption of PANDER results in selectively enhanced hepatic insulin signaling yet with increased lipidemia and overall body weight. These findings reveal a novel role for PANDER in differentially controlling lipogenesis and hepatic glucose production that may selectively impact overall glycemic control and potentially facilitate the onset and/or progression of type 2 diabetes.

CHAPTER ONE: INTRODUCTION

Typical Glycemic Regulation

Glycemic regulation, or the maintenance of glucose homeostasis within the body, is a process that is tightly regulated by not only numerous hormones but also by many organs including the brain, liver, pancreas, skeletal muscle, and even the intestines [1-4]. The brain, in particular, relies on glucose as its main source of energy and oxidation to function and conduct processes through all neuronal tissue. In conditions where glucose in the blood is low, or hypoglycemia, the brain's functions become abnormal and can ultimately lead to death [2]. However, by working cooperatively with the liver, pancreas, and skeletal muscle, the brain is allowed to operate properly while still allowing for optimal glucose homeostasis through glucose production and subsequent utilization [1-4]. It is most important that the maintenance of glycemia is tightly regulated especially in times of fasting and fed when blood sugar concentrations fluctuate so greatly. The balance of various hormones from the brain, gut, and pancreas secreted at optimal times in response to fluctuating blood glucose allow for maximal functioning of glycemic regulation and glucose homeostasis.

Fed State Glycemic Regulation

The balance between glucose entrance into and departure from the bloodstream is at the forefront of importance in maintaining proper glucose homeostasis. The primary source of circulating glucose is through ingestion of a meal (fed state/postprandial) and subsequent gastric emptying by digestive enzymes [1, 4, 5]. The regulation of postprandial circulating glucose appearance is due, in large part, to the action of 2 hormones referred to as incretins-

GIP (Glucose-dependent Insulinotropic Polypeptide, formerly Gastric Inhibitory Polypeptide) and GLP-1 (Glucagon-Like Peptide 1). GIP and GLP-1 are secreted from intestinal K-cells and L-cells, respectively, in response to oral ingestion of a meal that is rich in carbohydrates and/or fats [1, 4, 5]. Their mechanisms of action differ, however, in that although they both stimulate the biosynthesis and release of insulin from pancreatic β -cells, GLP-1 slows gastric emptying to properly correlate glucose appearance with timely release of insulin and prevents glucagon secretion whereas GIP works primarily in adipose tissue for fat metabolism [4, 5, 25]. Their levels under normal glycemic conditions differ, too, in that because GLP-1 is more physiologically relevant to humans, it fluctuates from levels being high postprandially and much lower when fasting [1]. Taken together, GIP and GLP-1 work cooperatively with insulin and glucagon to speed glucose disappearance to surrounding tissues and organs after oral nutrient uptake. Additionally, amylin, a neuroendocrine hormone secreted by pancreatic β -cells with insulin, works in concert with insulin to increase glucose disappearance and slow gastric emptying to prevent spikes in blood glucose [8]. Perhaps more importantly, amylin suppresses glucagon, a hormone secreted by pancreatic α -cells (and inhibited by insulin) in times of fasting when plasma glucose levels are low to enhance hepatic glucose production (HGP) [1, 8, 9]. By suppressing the action of glucagon postprandially, amylin chiefly regulates the appearance of endogenous glucose from the liver in addition to exogenous glucose from meal intake [1] (Summarized in Figure 1). Insulin, a potent anabolic hormone, also allows for glucose utilization through the process of glycolysis [2, 6]. When insulin is released from pancreatic β -cells through GLP-1 and GIP stimulation, there is a consequential rise in plasma insulin levels, triggering the uptake of glucose into cells for oxidation. When glucose is transported into muscle, liver, and fat cells through glucose transporters, it is shuttled through the oxidative process of glycolysis and The Citric Acid (TCA) Cycle to yield ATP for cellular energy [1, 4, 5, 8].

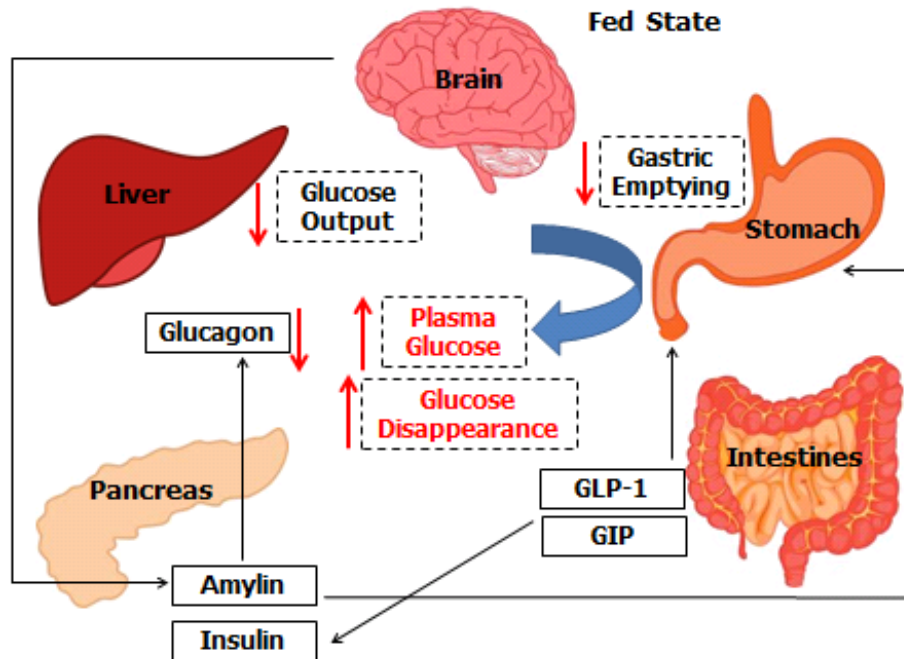


Figure 1: Fed State Network of Interactions in Normal Glycemic Regulation. Illustration representing the normal regulation of glycemia in the fed state, beginning with nutrient stimulation from the brain, stimulating the simultaneous release of amylin with insulin stimulated by GLP-1 and GIP. Amylin and GLP-1 slow gastric emptying and GLP-1 works with insulin to inhibit glucagon secretion in turn decreasing glucose output while plasma glucose and consequent glucose disappearance increases (adapted from Aronoff et al., 2004 [1])

Fasting State Glycemic Regulation

On the other hand, under fasting conditions when circulating glucose is scarce, the liver is utilized to upregulate glucose output into circulation through two discrete mechanisms. HGP is accomplished in the liver by breaking down glycogen through glycogenolysis and also via *de-novo* synthesis from amino acids and other carbon derivatives through gluconeogenesis [1, 2, 6]. First, glucose is stored within the liver (and muscle) as glycogen, a highly branched polymerized molecule with an α -(1, 6) linkage every 10 glucose residues that carries an average of 4 kcal of energy per gram of tissue [1, 2]. Under the control of the hormone glucagon (when plasma insulin levels are low) and in fasting conditions up to 8-12 hours, glycogenolysis is the primary source of glucose output from the liver [1, 9]. The hydrolysis of glycogen is initiated with the cleavage of a single glucose-1-phosphate molecule off of the branched polymer by

glycogen phosphorylase, activated by the binding of glucagon to its putative receptor on the plasma membrane. Then, the glucose-1-phosphate molecule is converted to glucose-6-phosphate, a gluconeogenic intermediate, to be acted on by glucose-6-phosphatase (G6Pase), where it is then converted to glucose and able to be transported out of the cell [1, 2]. After approximately 8-12 hours of prolonged fasting, the main source of hepatic glucose output switches from glycogenolysis to gluconeogenesis where amino acids, free fatty acids, and other fuel sources are used to synthesize glucose, still under the control of glucagon [2, 25]. Through the conversion of these fuel sources into pyruvate, oxaloacetate can then be formed and converted into phosphoenolpyruvate, the first gluconeogenic intermediate which will undergo steps that use ATP to form glucose. Insulin is another dominant regulator of glycogenolysis and gluconeogenesis in that the presence of insulin, signaling that glucose is in abundance in the body/plasma, both gluconeogenesis and glycogenolysis are inhibited [1, 2, 6]. In insulin sensitive individuals, when the release of insulin is triggered and binding of insulin to the insulin receptor on the hepatocyte membrane is accomplished, glucose is drawn into the cell to form glycogen and the formation of gluconeogenic precursors is inhibited [6]. Together, these 3 sources of circulating glucose allow for continued euglycemia in the fasting state when all other conditions inside the body are normal.

Insulin Signaling

The intricacies involved in the molecular aspect of insulin signaling is complex, beginning with the binding of insulin to its receptor at the cell membrane and activating a cascade of effects. When the release of insulin by the pancreatic β -cell is stimulated by an increase in blood glucose or by incretins, it signals the skeletal muscle and liver to 1) stimulate the uptake of glucose and 2) promote the formation of glycogen (glycogenesis) and halt gluconeogenesis by inhibiting the action of glucagon specifically on the liver [1]. Insulin does this by binding to

its tetrameric tyrosine-kinase Insulin Receptor (IR) where it becomes autophosphorylated, stimulating the phosphorylation of members of the Insulin Receptor Substrate (IRS) subfamily [6, 25]. Specifically, IRS-1 will physically interact with the p85 domain of Phosphatidylinositol-3'-Kinase (PI3K) immediately after it becomes tyrosine phosphorylated by IR, which then activates many downstream proteins, perhaps most importantly, Akt or Protein Kinase B (PKB) [6, 7, 22, 23]. The cascade of phosphorylation events through Akt allows for the exocytosis of Glucose Transporter (GLUT2 in the liver, GLUT4 in muscle and adipose tissue) from vesicles to subsequent translocation to the cell surface, allowing for the uptake of glucose into the cell [2, 6]. Simultaneously, Akt will phosphorylate Glycogen Synthase Kinase-3 (GSK3), effectively inactivating it and decreasing the rate of phosphorylation of Glycogen Synthase (GS), allowing for the synthesis of glycogen [6, 25]. Lastly, the binding of insulin to IR stimulates fatty-acid synthesis rather than degradation by activating various transcription factors such as Sterol Regulatory Element-Binding Protein 1 (SREBP-1) and enzymes including Acetyl CoA Carboxylase (ACC) and Fatty Acid Synthase (FAS) [3, 6]. Another protein important in hepatic insulin signaling is cAMP-Responsive Element Binding Protein (CREB) as it further controls hepatic glucose production (Summarized in Figure 2) [52, 54]. CREB is most important in the fasted state where the cyclic AMP (cAMP) family of proteins become activated by the binding of glucagon to the glucagon receptor and ultimately upregulate the phosphorylation of CREB, a transcription factor that activates the transcription of gluconeogenic enzyme G6Pase and Phosphoenolpyruvate Carboxykinase (PEPCK) [54, 55, 56, 57]. Insulin will also inhibit the transcription of certain gluconeogenic enzymes, mainly PEPCK and G6Pase by nuclear exclusion of the transcription factor Forkhead Box Protein O1 (FOXO1) [25, 26]. In conclusion, insulin sensitivity at the peripheral (muscle) and hepatic level allow for proper insulin signaling

resulting in glucose uptake through glucose transporters, fatty-acid synthesis through SREBP-1, and gluconeogenic enzyme suppression by FOXO1.

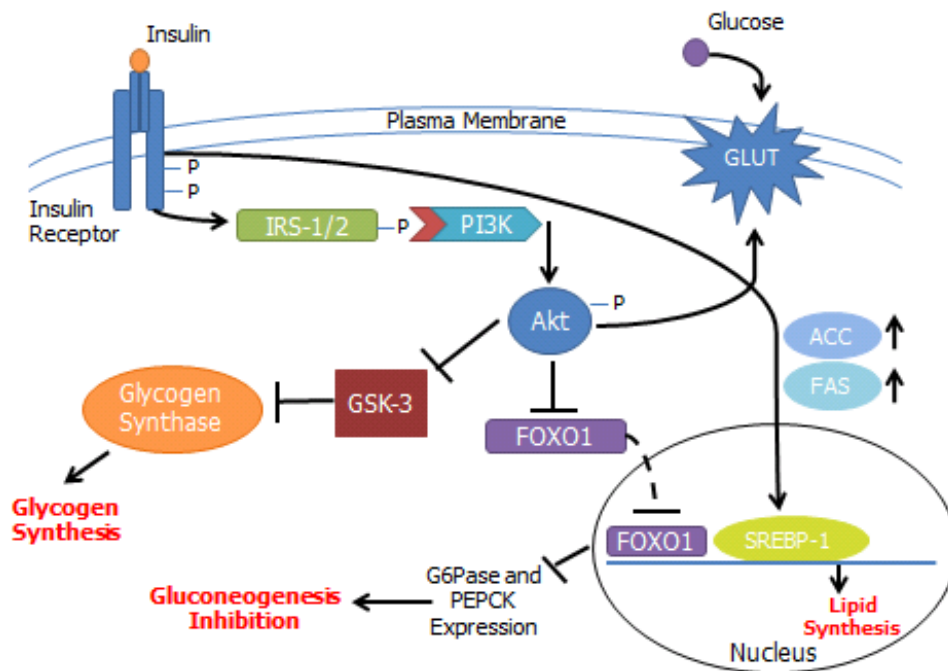


Figure 2: Insulin Signaling Network in Insulin Sensitive Individuals. Insulin signaling cascade, beginning with the binding of insulin to the Insulin Receptor at the plasma membrane, triggers a phosphorylation cascade that ultimately results in upregulation of glycogen synthesis, inhibition of gluconeogenesis, and upregulation of lipid synthesis along with GLUT translocation to plasma membrane and glucose uptake (adapted from Saltiel *et al.*, 2001 [6]).

Type 2 Diabetes (T2D)

As of 2012, globally, diabetes affected 371 million people, 50% of which continued to be undiagnosed [10]. What's more, the number of people across the world with diabetes is expected to rise to almost 440 million people by the year 2030. [11]. Here in the United States, according to the Center for Disease Control and Prevention (CDC), an estimated 25.8 million people, or 8.3% of the United States, has diabetes, 7 million of which were undiagnosed [12, 15]. Of all of the people with diabetes in the United States and across the world, 90-95% of them have type 2 diabetes [12, 13, 14]. Type 2 diabetes accounts for approximately 12-15% of all healthcare expenditures across the globe and has been a causative factor (if not the only

causative factor) in almost 250,000 US deaths [12, 14]. The global epidemic that is type 2 diabetes threatens to substantially worsen within the next 2 decades making the study of and prevention of this multi-faceted disease at the forefront of scientific interest today [13].

Type 2 diabetes, also known as “non-insulin dependent diabetes mellitus” or “adult-onset diabetes,” is a complex disease defined by insulin resistance/impaired insulin sensitivity due to impaired β -cell function and failure of target tissues to respond to secreted insulin [12, 14]. These defects result in constant hyperglycemia because of impaired glucose tolerance (IGT) and glucose utilization, increase in hepatic glucose production, dysregulation of insulin signaling, and an increase in circulating free fatty acids [13, 14]. Mechanistically, insulin resistance, considered a central problem in T2D, occurs beyond the Insulin Receptor (IR) in cells, as tyrosine phosphorylation of IR in type 2 diabetic patients is unaffected in skeletal muscle, the main site of glucose disposal [14, 16]. Instead, insulin-induced phosphorylation of IRS-1 and PI3-K, immediately downstream from IR, have been shown to be significantly reduced in type 2 diabetic patients with no change in either protein levels. Further, the same trend of decreased phosphorylation with no change in protein level was also characterized in regards to Akt in type 2 diabetic patient samples [16, 20]. Together, these indicate that defects exist in transmitting the phosphorylation signal when insulin binds to IR in the progression of type 2 diabetes [14, 16, 20, 21]. These abnormalities in insulin signaling ultimately result in a reduction of glucose transporter translocation to the cell surface, leading to a subsequent decrease in glucose uptake by the cell and plasma hyperglycemia [14, 19, 20]. Consequently, the worsening hyperglycemia (among other things) leads to an increased need for insulin production and secretion from the pancreatic β -cell. This sets in motion a vicious cycle of hyperglycemia and hyperinsulinemia, 2 well known type 2 diabetic hallmarks. These are in addition to the hyperlipidemia that is also present in T2D. However, over time, the β -cell can no

longer compensate for the increase in blood glucose levels and insulin secretion eventually decreases significantly along with an overall decrease in β -cell mass and increase in β -cell apoptosis [12, 14, 17, 18, 24].

The liver, another significant factor in the pathogenesis of type 2 diabetes, controls glycogenolysis and gluconeogenesis, both being the main source of glucose output in fasted conditions. Glucose homeostasis is significantly skewed when insulin signaling is disrupted specifically within the liver, as it results in a failure to suppress HGP and worsened glucose intolerance, both found in type 2 diabetes [25, 27, 28]. In fact, excessive HGP from the liver positively correlates with fasting hyperglycemia and HGP rates consistently increase with increasing hyperglycemia through T2D disease progression [28-31]. Insulin's direct effect on HGP suppression, through binding to its putative receptor on the hepatocyte membrane, is severely disrupted in insulin resistant states. Rising plasma hyperinsulinemia due to hepatic insulin resistance further contributes to continued glucose output by the liver and compensatory hyperglycemia [6, 28, 29, 30]. When insulin does not bind specifically to its hepatic IR because of decreased sensitivity, phosphorylation of IRS-1, PI3-K, and Akt does not occur, ultimately resulting in GSK-3 activation, glycogenolysis will occur, and FOXO1 will be allowed to enter the nucleus to transcribe gluconeogenic enzymes [6, 25, 26]. Furthermore, Michael *et al.* discovered that when hepatic insulin resistance is modeled where insulin is made unable to bind to hepatic IR, mRNA expression of both G6Pase and PEPCCK are significantly increased, indicating that HGP is highly upregulated [27]. The same group also reported that this insulin resistance, studied in liver-specific IR knockout mice, promotes overall hyperinsulinemia by simultaneously decreasing insulin clearance while also increasing insulin secretion [27].

Discovery of PANcreatic-DERived Factor (PANDER)

PANcreatic-DERived Factor (PANDER) was initially discovered in 2002 during a screen for new cytokines using an Ostensible Recognition of Folds (ORF) algorithm. This algorithm uses comparisons, such as known cytokines to an unknown sequence, to determine a protein's predicted secondary structure [32, 38]. Using a database of known sequences, the ORF algorithm uses sequence alignment of repetitive and non-repetitive sequences to establish proteins that are homologous in their secondary structures [32, 38]. That is, instead of using a protein's amino acid residue sequence, GORII parameters are used to calculate a protein's secondary structure string which is then used in sequence alignment [32, 34, 38]. In the search that uncovered PANDER, secondary structure probes from short chain cytokines like interleukin (IL)-2, -3, -4, growth hormone, etc. were utilized and the NCBI GenPept Database was used as the known library [34]. The 4-helix bundle secondary structure with up-up-down-down topology of these cytokines used as probes has remained highly conserved throughout the course of evolution [33, 34]. In addition to the 4-helix bundle and unique topology, 2 disulfide bridges linking the 4 helices at conserved cysteine residues are also signature to these cytokines, allowing them to be excellent candidates for structure-based studies such as the ORF algorithm [34]. A novel family of proteins entitled family with sequence similarity 3 (FAM3) was discovered from the ORF search with 4 putative gene members- FAM3A being the first discovered, followed by FAM3B, FAM3C, and FAM3D [34, 35, 36, 37]. All 4 family members consist of 224-235 amino acids and share 31.6-53.3% homology between, but no homology to known cytokines besides their predicted secondary structures, perhaps indicating the discovery of a novel cytokine subfamily [34, 39]. FAM3B, the second of the 4 genes discovered, is the longest FAM3 family member at 235 amino acids long and was later renamed "PANDER" because of its robust mRNA expression within the endocrine pancreas determined by northern

blot [34, 44]. PANDER mRNA is also expressed to lesser extents within the small intestine and prostate [34].

Newly Discovered Structure of PANDER

In early 2013, the three-dimensional crystal structure of murine PANDER was elucidated using sulfur singular anomalous dispersion (S-SAD) and X-ray data [40]. Johansson *et al.* showed using two different constructs of murine recombinant PANDER, unglycosylated (S)E30 PANDER and a truncated S46 PANDER, that 1) PANDER is, in fact, not a protein made of all α -helices and 2) its protein structure displays a globular β - β - α fold made of 2 anti-parallel β -sheets and a single layer of 3 short α -helices (Figure 3) [40]. Composed of 9 strands in total, the first β -sheet contains 4 strands, leaving 5 strands in the second β -sheet, creating a completely hydrophobic core within the protein structure [40]. The N-terminal tail of PANDER contains the disulfide bridges between cysteine residues that was initially believed to be at positions 63-69 and at positions 91-229 in the previous 4-helix model, but is in actuality at positions 63-91 and 69-229 [40, 43]. PANDER's N-terminus also contains the signal peptide in the first 30 amino acid residues, followed by the next 29 residues being hidden within the protein itself though they, along with the structural integrity of the β - β - α fold are essential to PANDER's overall functionality [40]. These new findings further contradict initial structure-function studies of PANDER which revealed that truncation of the entire N-terminus had no effect on PANDER function and action [43]. PANDER's new structure also revealed a highly conserved 4 water molecule-filled cavity that rests between the 2 β -sheets and has been shown to contribute to relative thermal stability of PANDER overall, contrary to evidence that such internal protein packing substantially destabilizes proteins [40, 42].

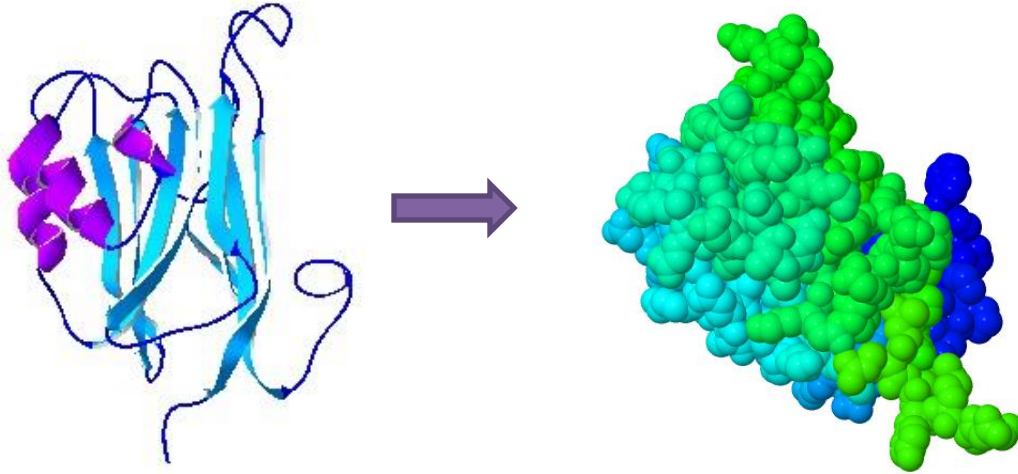


Figure 3: Secondary and Crystal Structure of PANDER. This figure illustrates the ribbon secondary structure (Left) of FAM3B (PANDER) depicting β -sheets in light blue with α -helices in purple (enhanced from Protein DataBase: 2YOQ) and the globular crystal structure form (Right) of the FAM3B protein (also adapted from PDB: 2YOQ) [40].

Perhaps the most telling feature of PANDER is that it bears no resemblance to not only other cytokines that were utilized in its discovery nor to its previously hypothesized 4-helix bundle structure, but also to any known protein. In fact, the protein that possesses the highest similarity to PANDER was Top7, a novel artificial protein that was specifically created to assess the boundaries of realizable proteins structures [40, 41]. Given that there are currently no known biological proteins that remotely share the same structure as PANDER, this is indication that PANDER could potentially represent a brand new structural class of signaling molecules with unique functions [40, 41].

Genomic Structure of PANDER

Initial characterization of PANDER in 2002 revealed that, genomically, human PANDER is present on chromosome 21q22 with a total of 8 exons over a 40 kb region and murine PANDER is located on chromosome 16B5-C4 [34, 45]. A typical signal peptide was also discovered both in the murine and human form of PANDER on the N-terminus with a hydrophobic leader sequence, indicating targeting to the endoplasmic reticulum (ER) for secretion from the cell [34,

52]. This processing of PANDER gives rise to a 23 kDa secreted PANDER product as opposed to the full-length 235 amino acid protein at 26 kDa, both detected in cell lysate and media from hepatocytes and β -TC3 cells infected with PANDER [34, 44, 52, 67]. Using the 5'- RNA Ligase Mediated-Rapid Amplification of cDNA Ends (RLM RACE) method, the PANDER transcriptional start site in insulin-producing pancreatic β -TC3 cells was identified 520 bp upstream from the translational start codon [45, 63]. Within the 5' flanking region of the PANDER gene at positions -99 and -48 upstream of the transcriptional start site are 2 TATA boxes and 3 A-box and E-box elements each from -335 to +491 bp, indicating a potential responsiveness of the PANDER promoter to glucose, much like that of the insulin promoter [45, 48]. Additionally, hepatocyte nuclear factor (HNF) 1 and 4, octamer binding protein-1 (Oct-1), and signal transducer and activator of transcription (STAT) 3, 5, and 6 binding sites were identified, indicating islet-specificity [45]. HNF-1 and HNF-4, though normal in the pancreas, regulate hepatocyte transcription and indicate expression within liver-derived cell lines as well, verified by an increase in PANDER promoter activity in BNL-CL2 liver-derived cell lines [45, 62]. In summary, the 5' untranslated region (5' UTR) of the PANDER gene contains not only the PANDER promoter and transcriptional start site, but all of the putative transcriptional factor binding sites that potentially give PANDER its tissue-specificity and nutrient responsiveness [34, 45, 49].

Regulation of PANDER Transcription

Following the lead of other various islet-specific proteins like insulin and glucagon mentioned previously, dominant control of their expression is exhibited at the transcriptional level by promoter elements and nutrient responsiveness [45, 46, 47]. This led to the further characterization of the regulatory regions and the islet-specific transcriptional elements that control PANDER expression at the transcriptional level.

First, Burkhardt *et al.* reported that the minimal element required for maximal promoter activity and PANDER gene expression happens to be in the +200/+491 region where all 3 E-box elements and a single A-box lie [45, 49]. Further, given that the PANDER promoter contains several E- and A-box elements and therefore could potentially be stimulated by glucose, glucose stimulation experiments were performed using various constructs of the PANDER promoter containing a number of those elements [45]. It was reported that the PANDER promoter was significantly upregulated by glucose in a dose-dependent manner and that treatment of β -TC3 cells with 22 mM D-glucose had the biggest increase in promoter activity when using luciferase plasmids under the control of the PANDER promoter [45]. This significant response of the promoter to glucose was also observed in murine pancreatic islets that were transfected with luciferase/PANDER plasmids but not in α -TC3 cells that secrete glucagon, indicating cell-type and nutrient specific expression of PANDER [45, 52]. The mechanism of the PANDER promoter's glucose responsiveness was found to be due to CREB-dependent pathway involving Ca²⁺, and either PKA or PKC where CREB phosphorylation was increased as well as PANDER gene expression in response to glucose [52, 65].

Cell-specificity was further conformed when *cis* elements within the promoter, A-boxes specifically, proved to be essential for binding an important transcription factor in pancreatic development, Pancreatic/Duodenal Homeobox-1 (PDX-1) [49, 50, 52]. Using chromatin immunoprecipitation (ChIP) and electromobility shift assay (EMSA), Burkhardt *et al.* showed that PDX-1 binds to all 3 of the A-boxes in the PANDER promoter in the -338 to +491 region and site directed mutagenesis of the 2 A-boxes in the -100 to +491 region completely deteriorated PANDER promoter activity [49, 52]. The same 2 A-boxes proved to be critical in the PANDER promoter's glucose responsiveness as their combined mutagenesis markedly reduced promoter activity [49, 52]. Additionally, 2 more β -cell specific transcription factors, V-

maf musculoaponeurotic fibrosarcoma oncogene homolog A (MafA) and β -cell E box Transactivator 2/NeuroD (BETA2/NeuroD) significantly upregulated activity of the PANDER promoter when combined with PDX-1, though PDX-1 alone had the greatest effect [49, 52, 64]. As a whole, PANDER transcription is regulated by β -cell specific transcription factors that bind to elements within the PANDER promoter and enhance promoter response to glucose stimulation, among other nutrients.

Regulation of PANDER Secretion

Just as PANDER transcription was enhanced by glucose, PANDER secretion has also been shown to be upregulated by glucose, for one. PANDER has been reported to co-localize with insulin in secretory granules of β -cells as shown by immunogold-labeling electron microscopy, and not only did glucose induce PANDER mRNA and protein expression in β -cells and islets, but it also increased PANDER secretion dose-dependently from β -cells almost 3-fold [52, 65, 66, 68]. The same effect was observed when PANDER was overexpressed in murine islets [66]. Interestingly, PANDER secretion from β -cells positively correlated with glucose-stimulated insulin secretion (GSIS) from the same cells, indicating the possibility that PANDER is likely co-secreted with insulin [66].

PANDER was also observed to be secreted from pancreatic α -cells, though secretion was not upregulated by increasing to decreasing glucose stimulation [52, 66, 69]. Carnegie *et al.* first reported that PANDER was present in pancreatic α -TC1-6 cells in granular cytoplasmic compartments and does not co-localize with glucagon [52, 69]. However, when stimulated with L-Arginine, the most robust known stimulator of glucagon secretion, PANDER secretion increased from α -TC1-6 cells significantly at up to 20 mM treatment in addition to a significant increase in glucagon secretion [52, 69, 70, 71]. What's more, when treated with low

concentrations of insulin (17 nM) alone or in combination with L-Arginine, PANDER secretion from α -TC1-6 cells was significantly increased (more so when treated with insulin alone), while still allowing for insulin-induced glucagon suppression [52, 69]. The mechanism for the unexpected upregulation of PANDER secretion from α -TC1-6 cells in response to insulin was reported to be attributed to the PI3K-Akt node of insulin signaling [69]. In general, PANDER is present in and secreted from pancreatic islets, α -cells, and β -cells in response to a variety of nutrient stimuli including glucose in β -cells and L-Arginine and insulin in α -cells, indicating a potential role for PANDER in glucose homeostasis functioning in glucoregulatory mechanisms [52].

Summary of PANDER Animal Models

Characterization of PANDER *in-vivo* has only recently begun within the past 3 years with numerous PANDER animal models being created. Not only are there PANDER knockout models, but also siRNA PANDER knockdown models, adenovirus-PANDER overexpressing models, and a recently characterized PANDER transgenic model to contribute to the characterization of PANDER's biological role *in-vivo*.

Hepatic Ad-PANDER Overexpressor and siRNA Knockdown

Li *et al.* developed a hepatic PANDER overexpressor by injecting adenoviral-PANDER (ad-PANDER) into the tail of C57BL/6 mice targeted for the liver [51, 62]. This hepatic-specific PANDER overexpression significantly increased hepatic steatosis with an increase in triglycerides within the serum and upregulation in both mRNA and protein expression of lipid metabolism genes including SREBP-1, FAS, and peroxisome proliferator-activated receptor γ (PPAR γ) [51, 52, 62]. In addition, plasma insulin levels were increased with disruption of phosphorylation of proteins in the hepatic insulin signaling cascade, specifically Akt, 5'

adenosine monophosphate-activated protein kinase (AMPK), and the transcription factor FOXO1, though unphosphorylated FOXO1 expression was the most markedly increased [51, 62]. Small-interfering RNA (siRNA) knockdown of hepatic PANDER was reported by the same group to reverse all of the above affects, but in *db/db* mice, a mouse strain used to model type 2 diabetes, not C57BL/6 mice [51, 52, 53]. Hepatic PANDER silencing also significantly reduced blood glucose levels and improved insulin resistance by decreasing expression of gluconeogenic enzymes and increasing phosphorylation of both Akt and AMPK while reducing the expression of FOXO1 [51, 52, 62]. Taken together, these ad-PANDER and siRNA knockdown models suggest that PANDER induces hepatic lipogenesis and insulin resistance primarily through a FOXO1 dependent pathway where PANDER decreases the phosphorylation of key insulin signaling proteins to aid in the increase in FOXO1 [51, 62].

Ad-PANDER Overexpressor

Wilson *et al.* also created a serum PANDER overexpressor using adenoviral gene delivery into the tail vein of male C57BL/6 mice [52, 54, 62]. This ad-PANDER model presented with increased fasting blood glucose levels and the compensatory hyperinsulinemia due primarily to elevated levels of corticosterone (murine glucocorticoids) and not glucagon, glycogen, or any other factor [52, 54]. Corticosterones/glucocorticoids have been shown to be present in higher concentrations in type 2 diabetic obese models and are reported to increase blood glucose levels through increasing gluconeogenesis and perpetuate insulin resistance *in vivo* [52, 54, 58, 59]. Ad-PANDER mice were also shown to be glucose intolerant during a glucose tolerance test (GTT), the result of the fasting hyperglycemia, as the mice were peripherally insulin sensitive [54, 62]. Further, PANDER overexpression in these C57BL/6 mice after an overnight fast and after being refed for 4-hours following an overnight fast resulted in an increase in mRNA expression of G6Pase and PEPCK, though only significant without being refed [52, 54, 62].

There was also no observed effect on the phosphorylation of Akt or GSK3 levels in the ad-PANDER mice, with the ad-PANDER mice revealing a decrease in liver triglycerides, contrary to the previously mentioned ad-PANDER murine model [51, 54]. In all, this specific ad-PANDER model suggests a role for PANDER as a causative agent of hyperglycemia in glucose homeostasis in the fasting state, by upregulating HGP through gluconeogenesis and increasing corticosterone levels [52, 54].

PANDER Transgenic Overexpressor

A PANDER transgenic (PANTG) mouse was created to specifically overexpress PANDER in the pancreas, specifically in the islets, using a portion of the PDX-1 promoter in B6SJLF1/J mice [50, 80, 81, 82, 96]. These mice initially presented with decreased β -cell mass and glucose intolerance on HFD, mimicking that of a type 2 diabetic model [80]. Further characterization of these PANTG mice using hyperinsulinemic-euglycemic clamp (HEC) studies which revealed a similar glucose disposal rate and peripheral sensitivity on both a HFD and normal chow compared to WT, but a significant increase in HGP and decrease in % HGP suppression, indicating insulin resistance at the hepatic level in PANTG mice [81]. These mice also presented with significantly higher fasting glycemia compared to WT mice in addition to glucose intolerance previously observed and an increase in overall weight gain [82, 96]. Mechanistically, the PANTG mice displayed a decrease in phosphorylation of AMPK previously shown in an ad-PANDER acute model with consequential hepatic hyperlipidemia [51, 82, 96]. This first genomically overexpressing PANDER murine model further supports PANDER's proposed enhancement of glucose intolerance and insulin insensitivity *in-vivo*.

PANDER Knockout Model

Lastly, in contrast to siRNA knockdown PANDER murine model, Cooperman *et al.* generated a global PANDER knockout (PANKO) model, devoid of any circulating PANDER, to aid

in elucidating PANDER's biological roles [52, 60, 61, 62]. This mouse, generated by replacing the first 2 exons of the PANDER gene including the transcriptional start site with a neomycin cassette in the reverse order (Figure 4), was backcrossed onto a C57/129 genetic background [60].

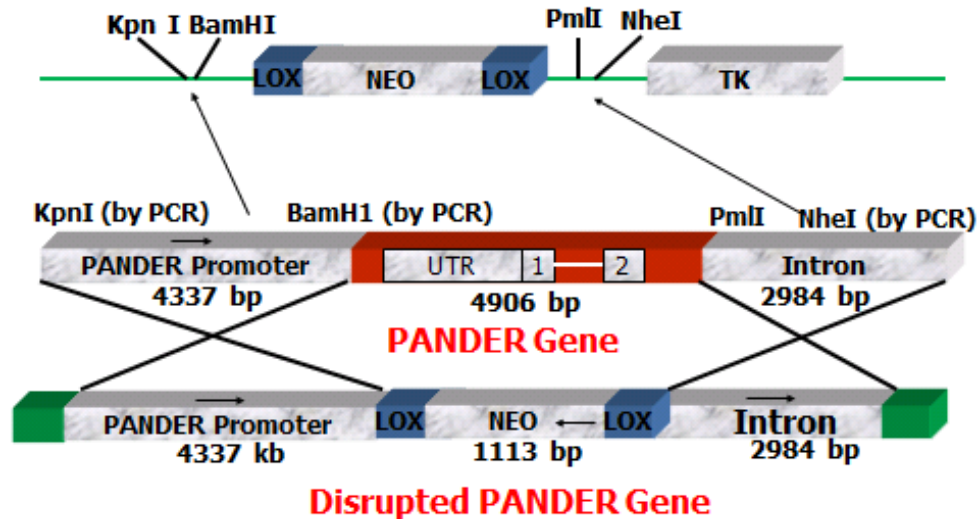


Figure 4: PANDER Gene Targeting Strategy. Illustration of the targeting strategy used when creating the PANKO mouse, where a region of the PANDER promoter, UTR, transcriptional start site, signal peptide, and first 2 exons were replaced with a Neomycin cassette in the reverse order. The Neomycin gene was flanked by a 4.3 kb and 2.9 kb arm of the PANDER gene, leading to its disruption (adapted from Cooperman *et al.*, 2010) [60].

In general, the PANKO mouse displayed glucose intolerance during a GTT due to an impairment in insulin secretion and abnormal Ca²⁺ handling within pancreatic islets suggesting that PANDER potentially affects calcium homeostasis in response to glucose [52, 60, 62]. Insulin levels were also elevated in the PANKO mice during a GTT, due primarily to a decrease in insulin clearance within the liver [60]. The increase in insulin levels was accompanied by similar levels of other hormones including leptin, c-peptide, glucagon, and amylin [60]. On the other hand, the same PANKO mice, under hyperinsulinemic-euglycemic clamp conditions, exhibited lower HGP and higher % HGP suppression, indicating a degree of hepatic insulin sensitivity compared to wild-type (WT) mice [52, 60, 62]. This is accompanied by a significant decrease in expression of G6Pase and PEPCCK after an overnight fast and no effect on blood

glucose levels [52, 54, 62]. When evaluated on a high-fat diet (HFD) for a 10 week duration, the PANKO C57/129J mice presented with significantly lower blood glucose levels after both a 24 and 48 hour fast and glucose intolerance during GTT [52, 61, 62]. Interestingly, insulin levels at all time points during a GTT were lower in PANKO mice compared to WT, where they were previously elevated when fed normal chow [60, 61, 62]. Fasting expression of G6Pase and PEPCK mRNA remained decreased even when PANKO mice were fed HFD, and overall weight along with food consumption were similar [61]. As a whole, it appears that the loss of circulating PANDER could act as a protectant against fasting hyperglycemia when being fed a HFD for a minimum of 10 weeks by suppressing expression of gluconeogenic enzymes [52, 61, 62].

Role of PANDER in Glycemic Regulation

In-vitro and *in-vivo* data regarding PANDER suggest a potential role in glycemic regulation, especially its response to nutrient stimulus. Interestingly, under physiological conditions of insulin sensitivity and normal glucose tolerance, PANDER promotes these normal processes by facilitating the secretion of insulin from β -cells, and insulin, as the dominate molecule, will suppress HGP regardless of PANDER's actions [52, 62]. As evidenced in the PANDER murine models summarized above, it is only where there is an excess of PANDER in a combination with one or more states of hyperglycemia, hyperinsulinemia, or hyperlipidemia, that PANDER begins to exert negative effects on overall glycemic regulation [39, 52, 62]. By using a type 2 diabetic murine model, the *db/db* mouse, where hepatic PANDER expression was silenced by siRNA, hepatic lipogenesis, insulin resistance shown by a decrease in phosphorylation through the insulin signaling cascade, and fasting hyperglycemia were all abolished and enhanced glucose tolerance was restored [51, 62]. Additionally, Wilson *et al.*

corroborated this evidence by measuring the serum PANDER levels in C57BL/6 mice considered to be young and lean and observed a decrease in serum PANDER both fed and fasting compared to aged, fat mice [54]. These aged, fat mice with natural elevated serum PANDER levels also had higher fasting blood glucose levels compared to young, lean mice, further indicating that under normal physiological conditions, PANDER will work to maintain normal glycemia and HGP [52, 54]. The PANTG mouse model also exhibits fasting hyperglycemia and decreased β -cell mass while on a HFD and increased hepatic triglyceride content compared to WT proving that increased PANDER works with lipids to promote hyperglycemia whereas in normal control mice, this is delayed, or even non-existent [52, 80, 82].

Role of PANDER in Type 2 Diabetes

Type 2 diabetes is generally defined by 3 hallmarks- hyperglycemia, hyperinsulinemia, and hyperlipidemia which all exacerbate the progression of the disease. Perhaps the most telling data regarding PANDER and its potential pathogenesis in type 2 diabetes is the effect that it has on the liver to induce all 3 diabetes hallmarks [62]. Not only does PANDER bind to the liver membrane shown through I^{125} labeling saturation studies, but its binding is highly specific though there has been no elucidation of the PANDER receptor [62, 72]. Further, treatment of hepatocellular liver carcinoma (HepG2) cells with PANDER inhibited insulin-stimulated signaling beginning at IR, through Akt, suggesting that PANDER induces hepatic insulin resistance [62, 72]. This is in addition to HEC studies on the PANTG corroborating evidence that hepatic insulin resistance is induced by PANDER and HGP was upregulated in ad-PANDER and PANTG models [81]. Hyperglycemia is also driven by PANDER in that not only is the PANDER promoter significantly stimulated by high glucose concentrations and HGP is higher *in-vivo*, but PANDER enhances the expression of G6Pase and PEPCK as evidenced through ad-

PANDER, PANKO models, and hepatocytes treated with PANDER exhibiting higher glucose production [45, 49, 52, 54, 61]. The combination of increased HGP in clamp studies and increased rate of gluconeogenesis with PANDER murine models having a higher fasting glycemia makes PANDER responsible for at least 1 diabetic hallmark- hyperglycemia.

Hyperinsulinemia, both a cause and consequence of hyperglycemia, is evident in the presence of PANDER as insulin stimulates the PANDER promoter and enhances PANDER secretion from α -cells [52, 69]. Hyperinsulinemia, in turn, creates a compensatory increase in glycemia through decreased insulin sensitivity and upregulating HGP, further increasing PANDER expression and secretion from β cells [52]. Hepatic steatosis, serum triglycerides, and expression of lipid metabolic genes are all upregulated in murine models overexpressing PANDER in addition to recent evidence claiming that palmitic acid, a long chain fatty acid molecule, significantly increases the expression of both PANDER mRNA and protein in murine β TC6 cells [51, 52, 90]. This signifies that not only does PANDER enhance circulating and hepatic hyperlipidemia, but it also promotes further hyperlipidemia. Taken together, all of the hallmarks that define T2D also define an increase in PANDER expression, secretion, and action, ultimately creating a vicious cycle of T2D initiation and progression aided by increased PANDER levels. This makes PANDER an attractive therapeutic drug target in the treatment of T2D to slow or even prevent the onset and progression of the metabolic abnormalities associated with T2D and restore glucose tolerance and insulin sensitivity [52, 62].

Role of PANDER in Cancer

Most recently, within the last year, PANDER has evolved to be a topic of interest of the realm of cancer research. PANDER was recently discovered in a number of human cancer cells including human hepatocellular carcinoma cells, lung carcinoma cells, and even human colon

cancer cells [75]. Interestingly, RNA interference (RNAi) experiments to silence PANDER expression resulted in apoptotic cell death of both human colon cancer cells and lung carcinoma cells, whereas the earliest PANDER experiments revealed that PANDER overexpression or treatment induced apoptosis of β -cells through the CDKN1A/caspase-3 network [43, 44, 67, 75, 76]. The silencing of PANDER by RNAi that subsequently lead to apoptosis in cancer cells was shown to be mediated by tumor protein 53 (p53), as it was significantly upregulated following PANDER silencing [75]. Further, phosphorylation of p53 was increased when PANDER was silenced, and when reversed, when p53 was silenced, PANDER-induced apoptosis was nearly completely reversed [75].

Down-regulation of PANDER mRNA and protein levels was observed in oral squamous cell carcinoma (OSCC) cells and primary patient samples compared to normal oral cells [73]. This downregulation of PANDER was attributed to microRNA (miRNA) upregulation in the 3' UTR of the PANDER gene, causing imperfect base pairing [73]. This was the first study that linked PANDER expression (down-regulated, in this case) to the carcinogenesis of a specific cancer type, oral squamous cell carcinoma, and characterized the cause of downregulation being that of miRNA upregulation [73]. A similar downregulation of PANDER expression was also observed in human gastric cancer where the lower PANDER mRNA levels in gastric cancer samples correlated to greater depth of tumor invasion [74, 77]. Li *et al.* performed the first studies evaluating the effects of the 7 different alternative splicing isoforms of PANDER in colon cancers, specifically in 6 colon adenocarcinoma cell lines and tissues [74]. One PANDER isoform, a 258 amino acid residue non-secretory form of PANDER (FAM3B-258), was found to be highly upregulated in its expression in not only colon cancer cell lines but also colorectal adenocarcinoma tissue samples, though tumor differentiation was poor [74]. Overexpression of FAM3B-258 in colorectal carcinoma cells was shown to enhance cell invasion and migration

through a Slug-dependent pathway, where the transcription factor Slug was highly expressed in the cells overexpressing FAM3B-258 [74]. Slug will work with another transcription factor, Snail, to downregulate to the expression of cell adhesion molecules and allow for invasion, both of which were upregulated in FAM3B-258 overexpression cells [74, 77, 78]. Additionally, FAM3B-258 enhanced colon cancer metastasis to the lung in nude mice, further confirming that FAM3B-258 works with Slug to aide in cancer cell invasion and migration [74]. In summary, though most research involving PANDER centers around its mechanism of action in glucose homeostasis and the pathogenesis of type 2 diabetes, PANDER's role in up/downregulating various cancers is quickly emerging, as well, especially in oral, gastric, and colorectal cancers.

Other FAM3 Family Members

When PANDER was discovered in 2002 (known as FAM3B at the time), it was only one gene in a family of 4 putative genes including FAM3A, FAM3C, and FAM3D [34]. Though FAM3B is arguably the most researched of all 4 genes, research on FAM3A, FAM3C, and FAM3D, though minimal, has begun to surface. First, FAM3D was initiall found to be highly expressed in the placenta and to a smaller extent in the small intestine, known to be very hyperproliferative, indicating that FAM3D could be important in cell proliferation [34]. In 2012, de Wit *et al.* revealed that FAM3D, the human ortholog of murine Oit1, was robustly expressed in the gastrointestinal tract of humans and was affected by nutrient stimulus [83]. Levels of FAM3D in human plasma was shown to be decreased after fasting, and more interestingly, after being on a HFD for 3 weeks, FAM3D levels were elevated postpradially after also being fed a HFD shake compared to subjects being on a LFD [83]. FAM3D has also been linked to diabetes mellitus in patients suffering with pancreatic adenocarcinoma, but has never been elucidated further [83, 84]. The expression pattern of FAM3D, though limited in extensive research, is similar to that of

PANDER and is affected by nutritional status in a similar manner, specifically in its response to HFD.

FAM3A, the first gene identified in the ORF algorithm, is composed of 230 amino acid residues and is expressed in a wide array of tissues, including the most robust expression in the heart, followed by the liver, pancreas, colon, and small intestine, among others [34, 39]. Zhou *et al.* is the only group thus far to report on FAM3A's activity in the liver, where they determined that PPAR γ overexpression enhanced FAM3A expression in HepG2 cells which was reversed with PPAR γ agonists in HepG2 cells and primary hepatocytes [35, 39]. The FAM3A promoter was also highly activated by PPAR γ and PPAR γ was shown to bind directly to its putative binding site in the FAM3A promoter, the peroxisome proliferator response element (PPRE) [35, 85]. Site-directed mutagenesis of PPRE deteriorated FAM3A's promoter response to PPAR γ and *in-vivo*, the upregulation of the FAM3A promoter resulted in an increased phosphorylation of Akt [35]. Like that of PANDER and FAM3D, FAM3A evidence suggests a potential role in controlling hepatic lipogenesis through PPAR γ and further control hepatic metabolism [35, 39].

FAM3C, also known as interleukin-like epithelial-mesenchymal transition (EMT) inducer (ILEI), as its name suggests, is integral in the process of EMT and breast cancer progression, much different than that of its other family members [40, 86]. Initial reports on FAM3C centered around its robust expression in the ear and the laminar retina, where it where it was identified as perhaps inducing nonsyndromic hearing loss [36, 37, 40, 86, 87]. FAM3C's name was changed to ILEI after Waerner *et al.* discovered that it was a molecule involved in EMT, where epithelial cells' transition to cancer begins, as evidenced in its altered expression and correlation to tumor metastasis [40, 86]. ILEI is expressed to its highest levels in the process of EMT and overexpression of ILEI exclusively in mammary epithelial cells promotes EMT and

tumor metastasis of the cells [86]. Further, transforming growth factor- β (TGF- β), a known EMT inductor, will enhance the activation of ILEI by inhibiting the action of heterogeneous nuclear ribonucleoprotein E1 (hnRNP E1) and TGF- β activated translation (BAT) element that work to suppress ILEI translation [40, 88, 89]. Through this TGF- β activation of ILEI, and conformation of ILEI's role in EMT shown through siRNA silencing, EMT progresses and the expression of ILEI (especially in the cytoplasm) correlates positively with breast cancer patient outcome [40, 88, 89]. FAM3C is the first member of the FAM3 family to have a suggested role in the progression of cancer, while FAM3A and FAM3D relate to PANDER in their roles in maintaining metabolic homeostasis. Nevertheless, the family with sequence similarity 3 has proven to be an integral part of normal human processes and all members have implications in the pathogenesis of diseases including cancer and type 2 diabetes mellitus.

Project Summary and Specific Aims

Type 2 diabetes (T2D), a disease affecting 371 million people around the world as of 2012, is expected to reach that of epidemic proportions by affecting just over 440 million people by the year 2030 [10, 11]. The effects that T2D has taken and has yet to take globally, nationally, and economically greatly exacerbate the need to further understand proteins involved in insulin signaling, their regulation, and how they contribute to the onset and progression of the disease. Pancreatic-Derived Factor, or PANDER, is a novel protein hormone discovered in 2002 that was shown to be highly expressed within pancreatic islets, co-secreted with insulin, and stimulated by glucose [34, 66]. For these reasons, in addition to the fact that PANDER binds to the liver membrane and inhibits the activation of critical insulin-signaling molecules, it is believed that PANDER plays a role in glucose homeostasis [72]. Initial acute murine studies show that C57BL/6 mice overexpressing PANDER hepatically exhibit impaired

glucose tolerance, elevated gluconeogenic gene expression, and increased hepatic lipogenesis [51, 54]. However, previous studies of PANDER knockout mice on a mixed genetic C57/129J background also revealed glucose intolerance, similar insulin sensitivity to WT, impaired insulin secretion from pancreatic β -cells, yet reduced mRNA expression of gluconeogenic enzymes [54, 60]. These results are further convoluted by a single report claiming knockdown of PANDER resulted in an attenuation in hepatic steatosis, insulin resistance, and hyperglycemia [51]. These novel contradictory findings further emphasize the importance of understanding PANDER's role in glucose homeostasis and hepatic insulin signaling in a genetically pure animal knockout model.

The following project being proposed will aim to determine the phenotype of the PANKO-C57 PANDER knockout mouse in addition to elucidating the mechanism of selective hepatic insulin resistance caused by PANDER shown in previous *in-vivo* and *in-vitro* data. Previous *in-vivo* studies have not provided a clear mechanism of PANDER's action in a pure-bred C57BL/6J murine model and therefore have reported conflicting results. Ultimately, by characterizing a PANDER knockout mouse on C57BL/6J background, perhaps one of the best understandings of how PANDER affects central cellular metabolic processes and its implications in type 2 diabetes will be uncovered. *Based on in-vitro data and initial characterization of the PANKO mouse on C57/129J mixed genetic background, we hypothesize that the PANKO-C57 mice will exhibit improved glucose tolerance and insulin sensitivity with enhanced hepatic insulin signaling. The specific aims to test this hypothesis are as follows:*

Specific Aim 1: Determine the overall glycemic regulation and metabolic characterization in the pure PANKO-C57BL/6 mouse

1.1: Determine fasting glycemia, hormonal, and plasma triglyceride differences between PANKO-C57 mice and WT mice

1.2: Characterize post-prandial differences between PANKO-C57 and WT mice via glucose and insulin tolerance testing

Specific Aim 2: Elucidate the mechanism of PANDER in hepatic signaling

2.1: Characterize the impact of PANDER on the PI3Kinase-Akt node of hepatic signaling

2.2: Determine the expression of gluconeogenic enzymes G6Pase and PEPCK

2.3: Measure differences in hepatic glycogen content and hepatic triglyceride content

CHAPTER TWO: INITIAL PHENOTYPING OF PANDER KNOCKOUT C57BL/6 MOUSE

Rationale

As presented previously, PANDER animal models, both transgenic and knockouts to date, have provided confounding evidence in terms of PANDER and its role in glyemic regulation, as a number of the models are acute. Transgenic mice overexpressing PANDER present with overall higher blood glucose levels and impaired hepatic insulin signaling at Akt [51, 54]. siRNA mediated knockdown of PANDER has been shown to enhance insulin signaling at the PI3K-Akt node in addition to decreasing hepatic lipogenesis [51]. However, a single report regarding a generated PANDER knockout mouse suggested glucose intolerance with a lower HGP and decreased expression of gluconeogenic enzymes, but this animal, though not acute, was on a genetically mixed C57/129 background, not optimal for phenotypic characterization [54, 60]. Compilation of discordant *in-vivo* data regarding PANDER begs a knockout model on a purebred C57BL/6 background for complete characterization and novel findings as to PANDER's complete role *in-vivo* [52].

The C57/129 PANKO mouse, after its standard initial characterization, was subsequently backcrossed for 8 generations onto the C57BL/6 background to allow for optimal phenotypic characterization, as C57BL/6 mice are the most widely used inbred mouse strain in scientific studies [91, 92]. This resulting congenic PANKO strain, after a total of 10 generations of backcrossing, ended up being approximately 99.9% homozygous at the specific affected null locus to any additional PANKO mice born, ensuring no interference from a mixed genetic background in phenotyping [91]. Once backcrossed on to C57BL/6 background, the mice were

backcrossed an additional generation at The Jackson Laboratory (Bar Harbor, ME) where they were submitted under strain name B6.129S6-*Fam3B*^{tm1Bkht/J} for maintenance before being shipped to Moffitt Cancer Center's Stabile Vivarium (Tampa, FL). The mice were further backcrossed one more additional generation upon arrival at Moffitt Cancer Center for murine colony derivation, allowing for the optimal 10 generation backcross on to the C57BL/6 background for maximum homozygosity in the colony [91].

By utilizing this PANDER knockout model on a C57BL/6 background, we hypothesized that the PANKO-C57 mouse would exhibit enhanced glucose tolerance complemented with an increase in insulin sensitivity shown through metabolic tests with lower fasting glycemia and hormonal levels to be evaluated using high-sensitivity assays [60].

Experimental Design & Methods

Murine Colony Acquisition, Care, and Maintenance

3 PANKO-C57 and 5 total C57BL/6 breeding pairs were obtained from Jackson Laboratory (Bar Harbor, ME) after being backcrossed an additional generation and genotype confirmed for animal husbandry and colony start-up. The mice were maintained in standard breeding cages with standard pellet bedding at Moffitt Cancer Center's Stabile Vivarium (Tampa, FL) given normal chow (Purina®) ad-libitum with constant access to water in accordance with approved breeding Institutional Animal Care and Use Committee (IACUC) protocol 4005 M. Any pups born were weaned at 3-4 weeks of age before being ear-tagged for identification and tail-snipped for DNA genotyping. Mice were then subsequently transferred to the approved Research protocol (4071 R) for experimentation. All maintenance and procedures conducted adhered to approved IACUC protocols at the University of South Florida and Moffitt Cancer Center (Appendix B & C).

Murine DNA Genotyping

DNA was extracted from all PANKO-C57 and WT pups at 3-4 weeks of age for conformation of respective genotype. 0.5 centimeter long tail snips were obtained from each mouse using a single edge razor blade (Fisher Scientific, Pittsburgh, PA). Tails snips were subsequently placed in Eppendorf tubes (Hauppauge, NY) with volumes indicated of Buffer ATL and Proteinase K at 56°C overnight for tail dissolving according to manufacturer's protocol in DNeasy Blood & Tissue Kit (Qiagen, Valencia, CA). DNA isolation was further completed according to manufacturer's protocol and concentrations/purities were determined using a Nanodrop (Thermo Scientific, Wilmington, DE). Eluted DNA samples were used in PCR amplification under standard cycling conditions where each sample was amplified using WT primers (-338 Kpn and -35 TA) and KO primers (-338 Kpn and KONEoP2) to confirm no heterozygous mice were present [45, 60]. DNA samples were subsequently run in a 1% agarose gel with 2 µl ethidium bromide for DNA visualization. Gels were visualized using Fuji LAS4000 imager (FujiFilm GE Healthcare, Pittsburgh, PA) and genotype was confirmed through presence of specific banding patterns base on WT (approx. 850-1000 bp) or KO (approx. 400-500 bp) primers used and compared to a standard 1 Kb Plus DNA Ladder (Invitrogen, Carlsbad, CA).

Measurement of Fasting Glycemia

4-5 month old male and female PANKO-C57 and WT C57BL/6 mice were fasted overnight (>16 hours, long-term) by removal of all food, leaving water, for blood glucose reading after the overnight fast. The same procedure was followed when short-term fasting glycemia was measured where male and female PANKO-C57 and WT mice were fasted for 4 hours by removal of food from cages. A TRUEtrack blood glucose meter (Walgreens) with respective strips was utilized to evaluate the glucose content of approximately 1 µl of blood

obtained via a tail vein puncture using a sterile lancet. All values and concentrations were analyzed via GraphPad Prizm (Version 5) and statistical significance ($p < 0.05$) between KO and WT was determined using 2-tailed Student t-test.

Body Weight Measurements

Body weights of PANKO-C57 and WT mice were measured (Beckman Digital Scale) in the mornings after feeding normal chow ad-libitum in 2-3 week increments. Weight measurements began at 8 weeks of age after being weaned and continued to 21-23 weeks of age. All weights were measured in grams and were analyzed by the mean and SEM for each group at each time point weight was measured. All weights were analyzed via GraphPad Prizm (Version 5) and statistical significance ($p < 0.05$) between KO and WT was determined using 2-tailed Student t-test.

Measurement of Hormonal Analytes

Evaluation of hormonal differences was conducted using a MAGPIX® Luminex (Austin, TX) Multiplexing Instrument and plasma (Figure 5). Blood was obtained via a submandibular vein poke from male PANKO-C57 mice at 2 months and 5 months of age along with WT male mice of the same ages using 18-gauge PrecisionGlide needles (BD Diagnostics, Franklin Lakes, NJ) and microvette tubes. Samples were kept on ice until processing. Samples were then centrifuged for 10 minutes at 13.2 rpm for plasma separation, the plasma supernatant removed and placed in an Eppendorf (Hauppauge, NY) tube, then stored at -80°C until use. The MAGPIX® panel that was used included antibody-immobilized beads for the following analytes: Amylin, Resistin, Glucagon, Insulin, C-Peptide, and Leptin. The assay was conducted using approximately 10-30 μl of fasting plasma used in triplicate in accordance with the manufacturer's protocol for the Mouse Metabolic Magnetic Bead Panel (Millipore, Billerica, MA). Results were then analyzed based on a Mouse Metabolic Hormone Standard provided with the

assay kit, using WT C57BL/6 plasma as a control, and xPONENT® data analysis system (Luminex). All values and concentrations were analyzed via GraphPad Prizm (Version 5) and statistical significance ($p < 0.05$) between KO and WT was determined using 2-tailed Student t-test.

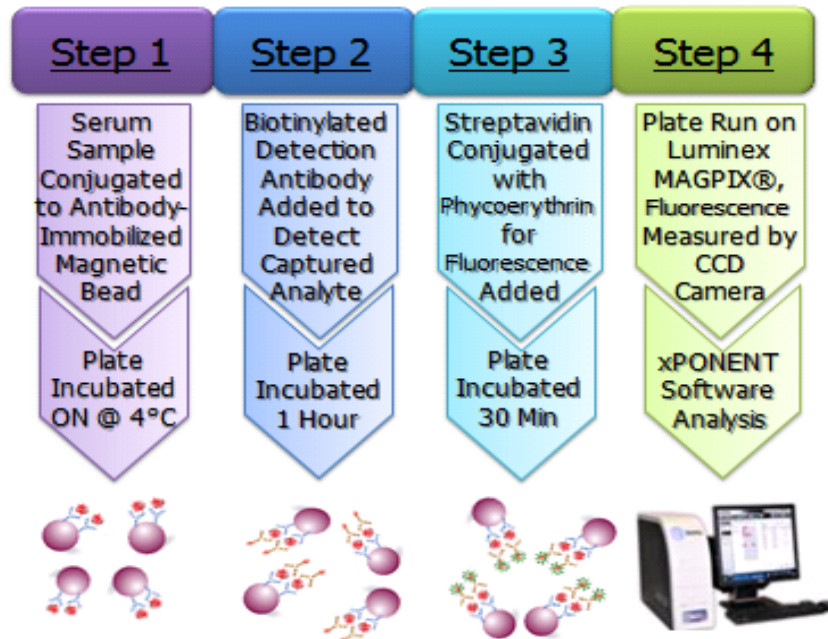


Figure 5: Luminex Multiplexing Concept & Protocol. This figure represents the concepts and 2-day protocol involved in the MAGPIX® Luminex system, beginning with conjugation of the serum sample added to the plate to the immobilized magnetic beads. Steps 2 and 3 are completed before quantitative measurement in Step 4 using xPONENT® analysis.

Measurement of Plasma Corticosterones

Corticosterone levels were measured longitudinally in serum from male PANKO-C57 and WT mice at 2 and 5 months of age after an overnight fast. Serum was obtained from mice as described above in *Measurement of Hormonal Analytes*. Corticosterone ELISA assay was performed according to manufacturer's protocol provided in the ENZO® Life Sciences Corticosterone ELISA Kit (ADI-900-097) (Farmingdale, NY). Results were obtained via VersaMax Microplate Reader (Molecular Devices, Sunnyvale, CA) with SoftMax® Pro software at a wavelength of 405 nm for optimal absorbance according to assay protocol. All values and

concentrations, presented in ng/mL, were analyzed via GraphPad Prizm (Version 5) and statistical significance ($p < 0.05$) between KO and WT was determined using 2-tailed Student t-test.

Measurement of Plasma Triglycerides

Plasma triglyceride content was evaluated by adhering to the manufacturer's protocol provided in Triglyceride Quantification Kit (Abcam- ab65336, Cambridge, MA) with plasma from male PANKO-C57 and WT mice at 2 months and 4-5 months of age obtained as described above. All samples were performed in triplicate. The assay was conducted at plasma dilutions of 1:10 and 1:50 using water as a control to ensure values were within the standard curve given with the kit. The protocol pertaining to the colorimetric assay was utilized and samples were analyzed using a VersaMax Microplate Reader (Molecular Devices) with SoftMax® Pro software at a wavelength of 570 nm for optimal absorbance. All values and concentrations, presented in nM, were analyzed via GraphPad Prizm (Version 5) and statistical significance ($p < 0.05$) between KO and WT was determined using 2-tailed Student t-test.

Glucose Tolerance & Insulin Tolerance Testing

For glucose-tolerance testing (GTTs), 4 month old male and female PANKO-C57 and WT mice were fasted overnight (>16 hrs) and injected intraperitoneally with 2 grams of glucose (Fisher Scientific) per kilogram of mouse body weight. Blood glucose levels were obtained as described above at 0, 15, 30, 60, and 120 minutes post glucose injection [60]. For insulin-tolerance testing (ITTs), 4 month old male and female PANKO-C57 and WT mice were fasted for 4 hours (approx. a week after GTT was completed) and injected intraperitoneally with 1.0 units of insulin (NovoLog®, Novo Nordisk, Plainsboro, NJ) per kilogram of mouse body weight. Blood glucose levels were measured as described previously at 0, 15, 30, 60, 90, and 120 minutes post-injection of insulin [60]. All numerical values were analyzed via GraphPad Prizm

using SEM and statistical significance ($p < 0.05$) was determined at each time point between KO and WT using 2-tailed Student t-test.

Confirmation of PANKO-C57 and WT Genotypes

Prior to experimentation, all pups born to PANKO-C57 or WT parents were genotyped using DNA extracted from tail snips and amplified using primers for the KO and WT alleles as described in Experimental Design & Methods. In all, 203 pups were born, and 219 mice including the parent generation were genotyped. Mice born to PANKO-C57 and WT parents were analyzed for the presence of both the WT allele using -338 Kpn Forward and -35 TA Reverse primers, and the KO allele using the -338 Kpn Forward and KONEoP2 Reverse primers as previously described [45, 60]. Amplification of the PANKO allele resulted in an approximately 500 bp product in PANKO-C57 mice, while amplification of the WT allele was confirmed in C57BL/6 WT mice by the appearance of a band between 850 and 1000 bp using the respective primer sets (Figure 6A). Further, the absence of either the PANKO or WT gene was confirmed in WT and PANKO mice, respectively, through PCR amplification and subsequent gel electrophoresis to ensure only homozygous mice were being used in experimentation. Negative amplification of the PANKO gene in WT mice was confirmed by the absence of a DNA fragment at approximately 500 bp in gel electrophoresis, when compared to positive (WT mouse with PANKO primers) and negative (WT mouse with WT primers) controls (Figure 6B). The same negative amplification was observed when attempting to amplify the WT allele in PANKO-C57 mice. The absence of DNA bands was observed in gel electrophoresis between 850 and 1000 bp, further indication that the PANKO-C57 mice were not heterozygous, but rather homozygous for knockout of the PANDER gene (Figure 6C). It was also confirmed that none of the WT mice that were genotyped and used in experimentation contained the KO allele, either.

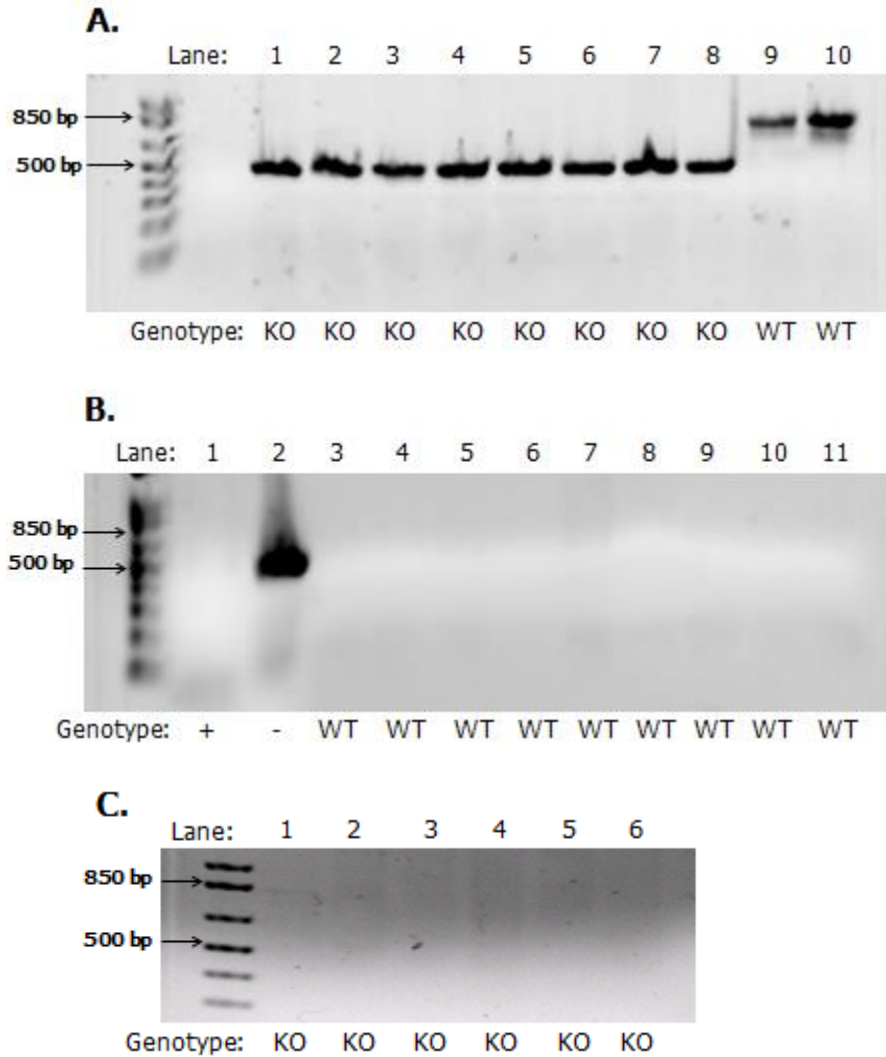


Figure 6: PCR-Amplified PANKO-C57 and WT Allele Confirmations. 1% agarose gel electrophoresis for genotype verification of PANKO-C57 and WT mice, using 1 Kb Plus DNA Ladder (Invitrogen) as standard in all figures, with 500 bp and 850 bp fragments labeled. (A) Lanes 1-8: depicting PANKO DNA fragment at around 500 bp, Lanes 9 & 10: showing WT fragment between 850 and 1000 bp. (B) Lanes 1 & 2: positive and negative control of WT mice with KO primers and WT mice with WT primers, respectively, and Lanes 3-11 confirming the absence of the KO gene as in the positive control. (C) Lanes 1-6: negative amplification of the WT allele in 6 KO samples. Shown by the absence of a fragment between 850 and 1000 bp in lanes 1-6.

PANKO-C57 Mice Exhibit Lower Fasting Glycemia Short and Long Term

Characterization of the PANKO-C57 began with analyzing fasting blood glucose levels after a short (4 hours) and long term (overnight, approx. 16 hours) fast to determine overall insulin sensitivity. As stated previously, siRNA knockdown PANDER mice presented with lower

blood glucose levels as well as PANKO mice on C57/129 background, but only on HFD after 24 and 48 hour fasts, and neither of these were global knockouts on C57BL/6 backgrounds [51, 52, 61, 62]. PANKO-C57 male mice at 4 months of age exhibited a significantly lower fasting glycemia compared to age and sex matched C57BL/6J WT mice after fasting for 4 hours where the average PANKO-C57 blood glucose was $169.3 \text{ mg/dl} \pm 6.9$ versus WT average blood glucose of $225.8 \text{ mg/dl} \pm 30.5$ ($P < 0.05$) (Figure 7A). This same trend, with an increased significance, was also observed after a long-term fast of the same age and sex matched PANKO-C57 and WT mice, where PANKO-C57 mice presented with an average blood glucose of $117.1 \text{ mg/dl} \pm 5.9$ versus WT average of $156.2 \text{ mg/dl} \pm 12.2$ (Figure 7B).

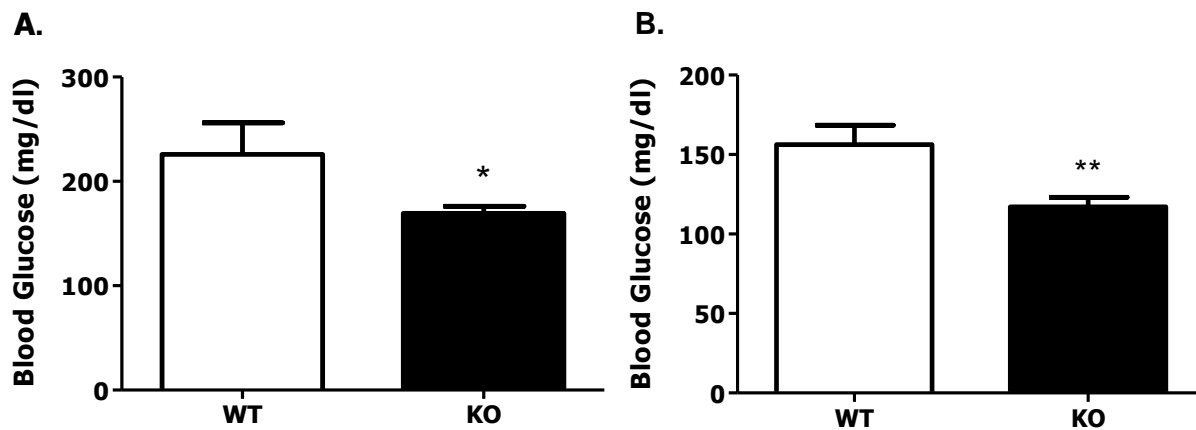


Figure 7: Male PANKO-C57 Mice have Lower Fasting Glycemia Short and Long Term. (A): Blood glucose measurements (mg/dl) obtained from a tail vein poke after a short term fast for 4 hours and measured using standard glucometer, $n = 8-11$, $P < 0.05$. (B): Blood glucose measurements (mg/dl) measured after an overnight (long-term) fast from tail vein poke as previously described, $n = 12-15$, $P < 0.01$.

The same procedure to measure fasting glycemia was performed with female PANKO-C57 and WT mice that were 4 months of age. After a short-term fast, blood glucose concentrations of PANKO-C57 and WT females were very similar, where the average PANKO-C57 concentration was $169.7 \text{ mg/dl} \pm 30.38$ versus WT blood glucose concentrations of $181.1 \text{ mg/dl} \pm 39.10$ (n.s.) (Figure 8A). Greater differences were observed in female blood glucose concentrations after a long-term overnight fast, though differences were not significant.

PANKO-C57 females blood glucose average concentrations were $139.4 \text{ mg/dl} \pm 20.90$ versus $189.8 \text{ mg/dl} \pm 30.88$ female WT average blood glucose concentration (n.s.) (Figure 8B).

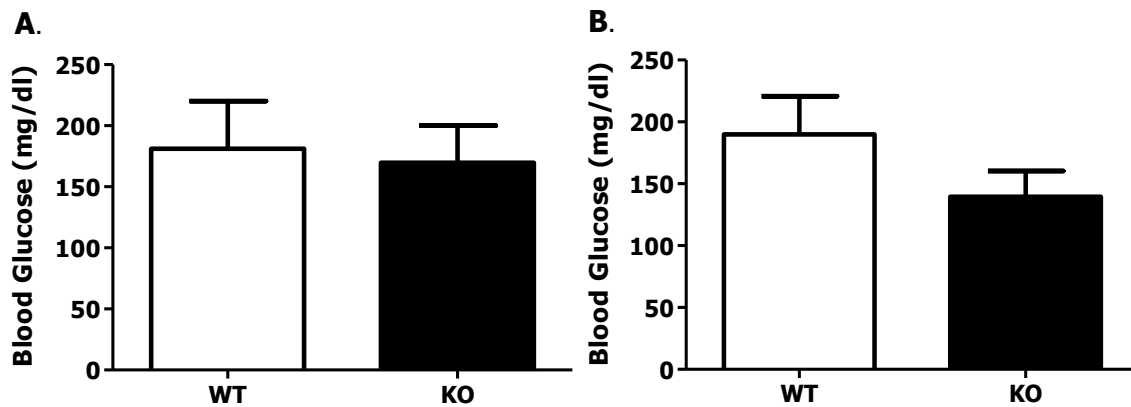


Figure 8: Female PANKO-C57 Display Lower Average Fasting Glycemia Trend After Short and Long Term Fast. (A) Blood glucose concentrations were measured (mg/dl) from PANKO-C57 and WT female mice after 4 hour fast through a tail vein poke and measured using a glucometer (n= 6-10). (B) Following a long-term overnight fast, female PANKO-C57 and WT mice blood glucose concentrations were measured via tail vein (n= 7-12).

PANKO-C57 Mice Display Increased Body Weights Longitudinally

In order to characterize any effect that PANDER has *in-vivo* in terms of weight and weight gain, body weights of both male and female PANKO-C57 and WT mice were measured as described above in Experimental Design & Methods. PANTG pancreatic overexpressors displayed an increase in overall weight gain, whereas PANKO C57/129 mice were shown to have similar weights to WT when fed HFD. This lead us to determine if the knockout of PANDER in C57BL/6 mice would induce a difference in murine body weights that was not previously noted in any previous PANDER knockdown/knockout model [61, 82]. Beginning at 8 weeks of age, male PANKO-C57 mice displayed a significant increase in body weight at an average of $25.16 \text{ g} \pm 0.35$ compared to male WT mice averaging $23.32 \text{ g} \pm 0.3$ ($P < 0.001$). This trend continued every 2-3 weeks weight was measured up to 23 weeks of age where PANKO-C57 mice averaged $37.20 \text{ g} \pm 1.05$ versus WT mice averaging $30.59 \text{ g} \pm 0.45$ ($P < 0.001$) (Figure 9A).

Longitudinal body weight measurements were also performed every 2-3 weeks for female PANKO-C57 and WT mice to determine any significant differences as there were in the male mice. It was found that at 8 weeks of age, female PANKO-C57 mice were also significantly heavier than WT mice, where the average PANKO-C57 weight was $20.18 \text{ g} \pm 0.5$ versus an average weight of $18.20 \text{ g} \pm 0.26$ for WT mice ($P < 0.001$). The trend, though diminishing in its significance, also continued through to 21 weeks of age in the females where PANKO-C57 females weighed an average of $25.84 \text{ g} \pm 1.17$ compared to WT average weight of $23.01 \text{ g} \pm 0.52$ ($P < 0.05$) (Figure 9B).

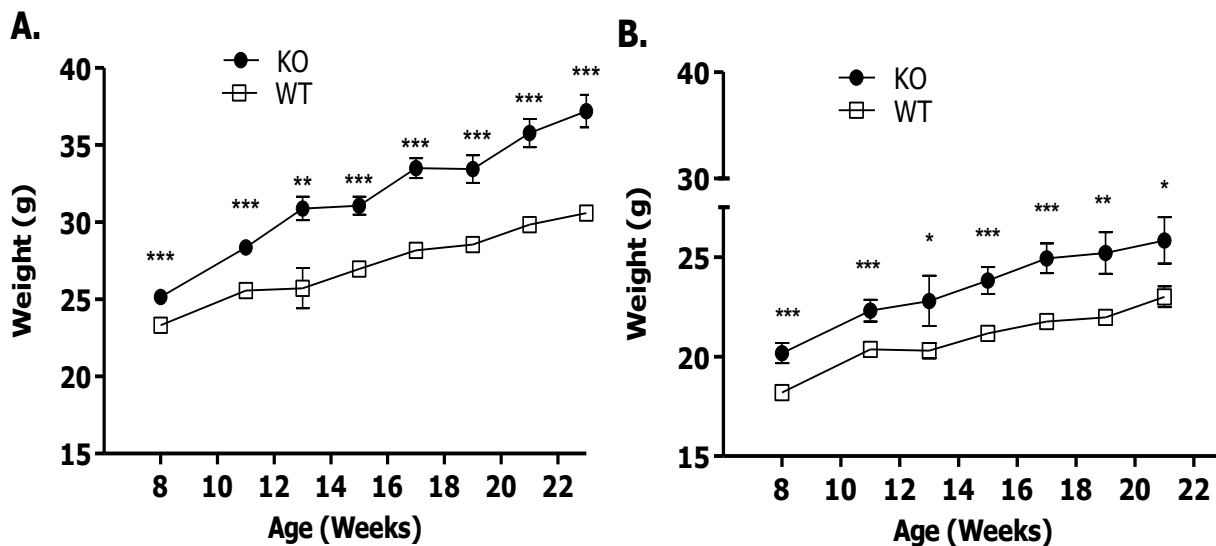


Figure 9: PANKO-C57 Mice Body Weight Measurements Trend Heavier than WT Mice. (A) Male longitudinal weights of PANKO-C57 and WT mice (in grams) obtained every 2-3 weeks from 8-23 weeks of age using a Beckman digital scale each time weights were obtained ($n = 10-27$). (B) Comparison of female PANKO-C57 and WT mice obtained beginning at 8 weeks of age through to 21 weeks of age, weighing every 2-3 weeks as described in Experimental Design & Methods ($n = 9-22$).

Differential Expression of Metabolic Hormonal Analytes in PANKO-C57

To elucidate the mechanism of the significant observed decreased fasting glycemia in the male PANKO-C57 mice, a MAGPIX® Luminex (Austin, TX) Multiplexing approach was employed to determine concentrations of the fasting concentrations of the hormones insulin, glucagon, leptin, c-peptide, amylin, and resistin as described in Experimental Design & Methods.

While the previous PANKO C57/129 mice displayed an increase serum insulin concentration only measured during metabolic testing with no differences in leptin, c-peptide, glucagon or amylin and an ad-PANDER overexpressor model showed no difference in glucagon levels, neither contributed to an explanation for overall fasting glycemia, perhaps due to their genetic backgrounds [52, 54, 60].

To begin, overnight fasting plasma obtained from male PANKO-C57 and WT mice at 2 months of age revealed significantly decreased insulin content in PANKO-C57 plasma compared to WT at $105.4 \text{ pg/mL} \pm 36.4$ versus $487.8 \text{ pg/mL} \pm 34.6$ ($P < 0.001$), respectively, with the same trend at 5 months of age, though not significant (Figure 10). Plasma glucagon levels were similar in PANKO-C57 and WT mice at both 2 and 5 months of age, where levels in WT at 2 months and PANKO-C57 and WT at 5 months of age were below the minimal detectable content for the assay and therefore could not be quantified (Figure 10). Leptin, an adipose tissue-derived hormone known to be elevated in the plasma with increasing fat mass and obesity, was significantly elevated in the plasma of PANKO-C57 mouse at both 2 and 5 months of age (Figure 10) [93, 94]. At 2 months old, PANKO-C57 mice plasma leptin levels were $779.7 \text{ pg/mL} \pm 76.6$ versus WT plasma leptin levels of $253.3 \text{ pg/mL} \pm 84.8$ ($P < 0.01$), and though significance was lost at 5 months of age, plasma leptin concentrations in PANKO-C57 mice remained nearly 5 times higher than levels in WT mice. Lastly, c-peptide, the connecting peptide between insulin's A and B chain in the proinsulin molecule used as a diagnostic tool for the measure of insulin in diabetes, was significantly decreased in PANKO-C57 at 2 months of age compared to WT mice, $386.0 \text{ pg/mL} \pm 104.9$ vs. $830.8 \text{ pg/mL} \pm 46.98$, respectively ($P < 0.01$), coinciding with the decreased insulin levels at 2 months (Figure 10) [95]. Interestingly, when plasma c-peptide levels were evaluated at 5 months of age, PANKO-C57 mice displayed a significant increase in c-peptide concentration at $686.5 \text{ pg/mL} \pm 100.8$ compared to WT c-

peptide levels of $388.0 \text{ pg/mL} \pm 40.84$ ($P < 0.05$) where they displayed a decrease in insulin levels from 2 to 5 months. Amylin and resistin, the last 2 hormones analyzed, were not able to be quantified due to the constraints of the assay in terms of quality controls and concentrations of both analytes fell below the minimal detectable range on the standard curve.

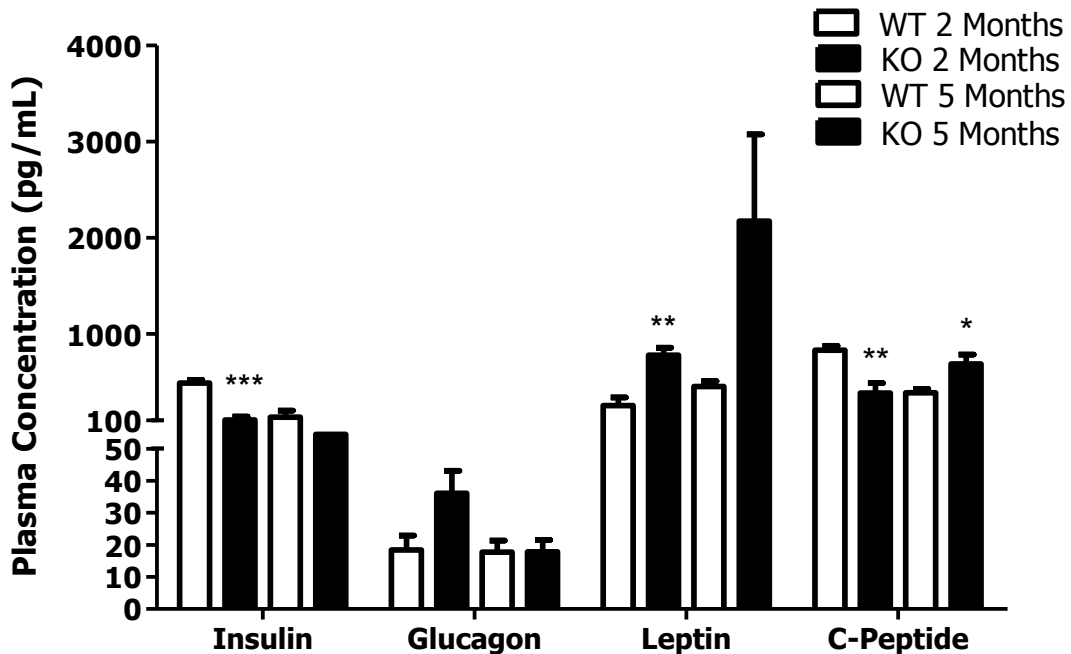


Figure 10: Longitudinal Serum Hormonal Analyte Concentrations in PANKO-C57 and WT Mice. 2 and 5 month longitudinal Luminex multiplexing analysis of insulin, glucagon, leptin, and c-peptide in PANKO-C57 and WT plasma fasted overnight, concentrations shown in pg/mL (n= 4-6). Not included: amylin and resistin, as concentrations were too low to quantify.

Similar Corticosterone and Plasma Triglyceride Concentrations in PANKO-C57

Corticosterones, the murine version of glucocorticoids, were previously shown to be the primary cause of fasting hyperglycemia in ad-PANDER overexpressing mice compared to WT mice [52, 54]. Further, Li *et al.* reported that in their ad-PANDER hepatic overexpressor, there was an increase in serum triglycerides [51]. To further determine if plasma corticosterone levels contributed to the lower fasting glycemia in the PANKO-C57 and if increased serum triglycerides potentially contributed to the increased body weight with the plasma levels of leptin, assays were conducted to measure each in PANKO-C57 and WT fasting plasma. Corticosterone levels

were almost identical between PANKO-C57 and WT mice at both 2 and 5 months of age, where fasting corticosterone averages were lower at 5 months than at 2 months of age (Figure 11A). At 2 months, PANKO-C57 fasting corticosterone concentrations averaged $54.74 \text{ ng/mL} \pm 1.65$ versus WT averages of $57.00 \text{ ng/mL} \pm 10.31$ (n.s.). These averages decreased in each cohort to $40.48 \text{ ng/mL} \pm 11.75$ in PANKO-C57 mice versus $41.11 \text{ ng/mL} \pm 17.96$ in WT mice at 5 months of age (n.s.).

When examining plasma triglyceride content, at 2 months of age, PANKO-C57 mice presented with significantly higher plasma triglycerides at an average of $164.9 \text{ nM} \pm 7.939$ compared to WT mice at $140.7 \text{ nM} \pm 7.716$ ($P < 0.05$) (Figure 11B). There was a switch in trend of longitudinal plasma triglyceride content at 5 months of age in the same PANKO-C57 and WT mice, where PANKO-C57 mice displayed a lower plasma triglyceride concentration than WT mice, $147.2 \text{ nM} \pm 11.93$ versus $158.7 \text{ nM} \pm 10.97$ (n.s.), respectively. Interestingly, not only did PANKO-C57 plasma triglyceride content decrease longitudinally, but WT plasma triglyceride content increased longitudinally from 2 to 5 months of age (Figure 11B).

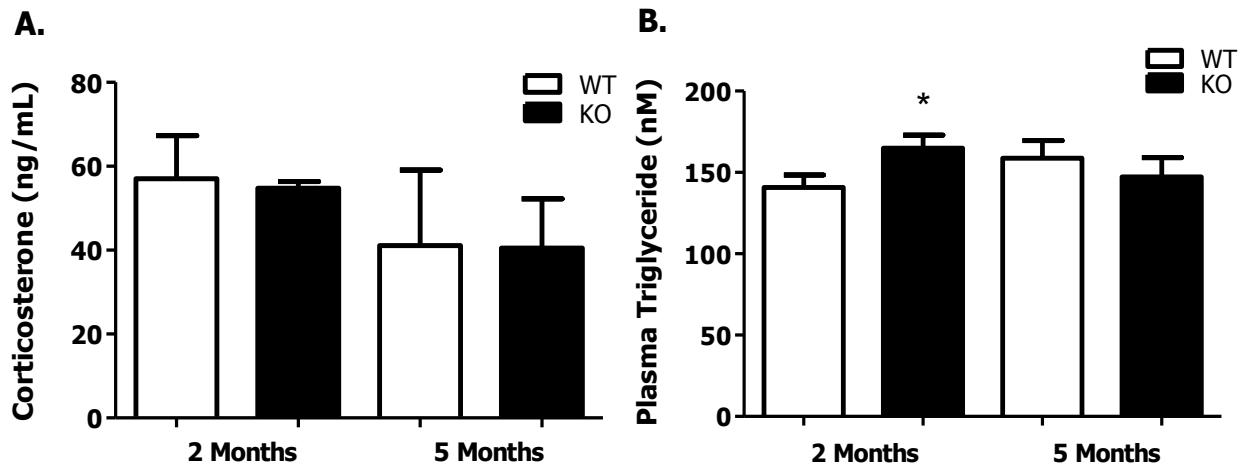


Figure 11: Plasma Corticosterone and Triglyceride Levels in PANKO-C57 and WT Mice. (A) Overnight fasting plasma obtained from both PANKO-C57 and WT mice longitudinally at 2 and 5 months of age were analyzed for corticosterone content using Corticosterone ELISA Kit (ADI-900-097) (Farmingdale, NY), shown in ng/mL (n= 4). (B) Plasma triglyceride content from overnight fasting PANKO-C57 and WT mice was analyzed using Triglyceride Quantification Kit (Abcam- ab65336, Cambridge, MA), presented in nM (n= 5).

PANKO-C57 Mice Display Enhanced Glucose Tolerance in Metabolic Tests

GTTs previously performed on male PANKO mice on C57/129 background revealed significant glucose intolerance as evidenced by increased blood glucose levels during GTT [60]. This glucose intolerance was accompanied by increased insulin levels at every time point during the GTT, both the result of impaired Ca²⁺ handling in pancreatic islets and impaired insulin clearance, respectively [60]. To explore whether these same traits were also apparent in PANKO-C57 mice, both male and female PANKO-C57 and WT mice underwent GTTs at 4 months of age. Male PANKO-C57 mice displayed lower blood glucose levels at every time point during the GTT, 3 of which were significantly lower- 15 minutes, where PANKO-C57 blood glucose levels were 415.9 mg/dL \pm 45.9 versus WT blood glucose levels of 561.1 mg/dL \pm 33.2 (P < 0.05), 60 minutes, where PANKO-C57 mice had blood glucose levels of 397.7 mg/dL \pm 46.3 versus WT blood glucose levels 592.8 mg/dL \pm 8.3 (P < 0.01), and at the final time point in the GTT at 120 minutes where PANKO-C57 mice presented with blood glucose readings of 290.1 mg/dL \pm 48.2 versus WT blood glucose levels of 472.3 mg/dL \pm 37.1 (P < 0.05) (Figure 12A). This trend was confirmed by area under the curve (AUC) determination, where the PANKO-C57 AUC was significantly lower than WT (P < 0.01), a further indication that male PANKO-C57 mice are more glucose tolerant than male WT mice (Figure 12B).

This trend of enhanced glucose tolerance was also observed to a milder extent in PANKO-C57 females where, at the first 4 time points during the GTT, female PANKO-C57 blood glucose levels were decreased, and significantly decreased at 30 minutes post i.p. glucose injection where female PANKO-C57 blood glucose concentration averaged 378.4 mg/dl \pm 72.79 versus WT at 531.3 mg/dl \pm 33.88 (P < 0.05) (Figure 12C). This mild enhancement in glucose tolerance was also corroborated by a decrease in PANKO-C57 GTT AUC, though it was not significant (Figure 12D).

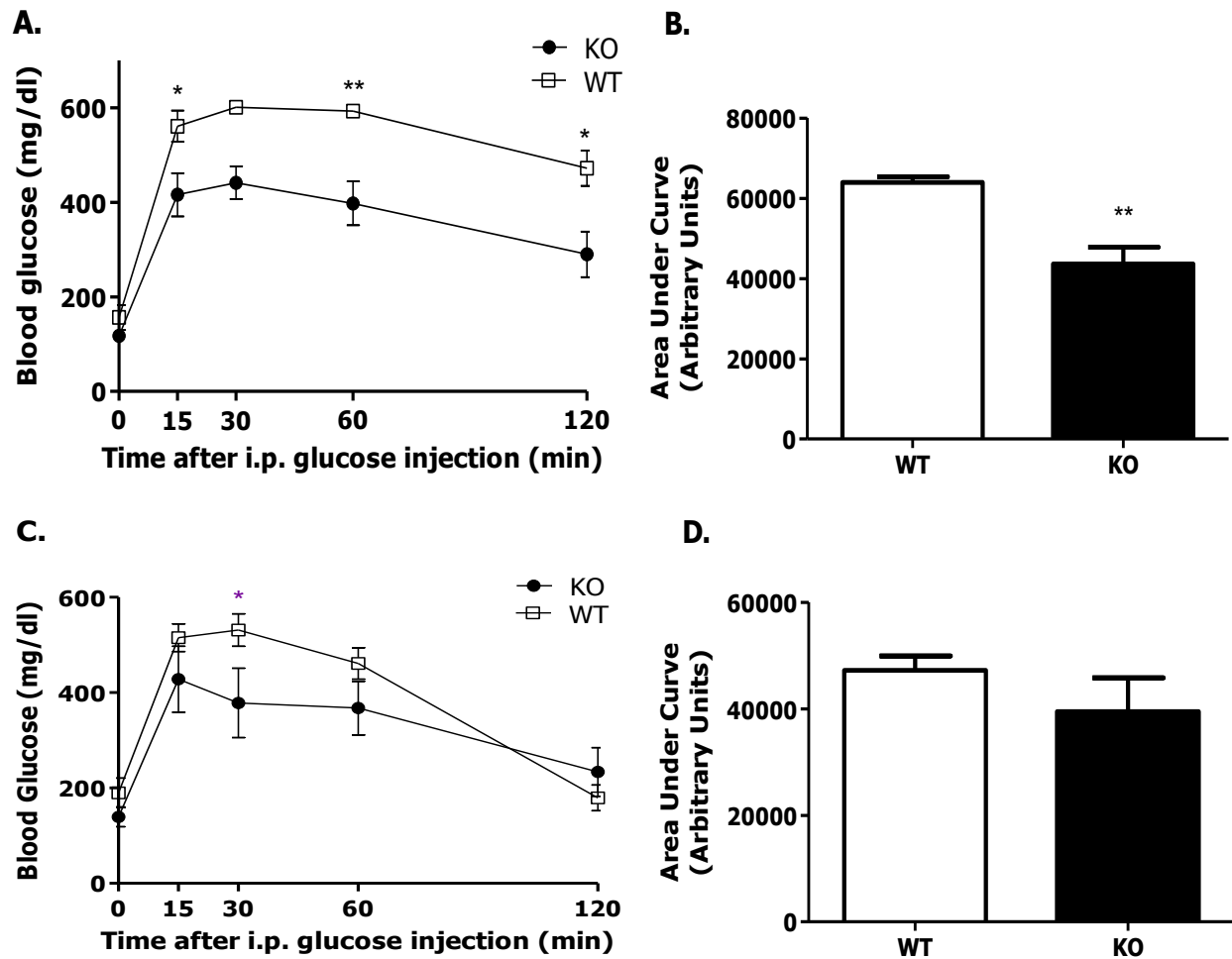


Figure 12: GTT of PANKO-C57 Male and Female Mice Reveals Enhanced Glucose Tolerance. (A) glucose tolerance test (GTT) of male PANKO-C57 and WT mice showing average blood glucose (mg/dl) at each time point (in minutes) post 2 g/kg intraperitoneal glucose injection (n= 8-13). (B) Area under the curve (AUC) of male GTT shown in A. (C) GTT of female PANKO-C57 and WT mice depicting blood glucose readings (mg/dl) using glucometer at 0, 15, 30, 60, and 120 minutes post intraperitoneal glucose injection at 2g/kg concentration (n= 7-12). (D) AUC of female GTT shown in C.

PANKO-C57 Mice Reveal Similar Insulin Sensitivity in Insulin Tolerance Test (ITT)

In addition to GTTs done at 4 months of age to characterize overall glucose tolerance, the same PANKO-C57 and WT mice underwent ITTs to characterize their peripheral sensitivity in response to a bolus injection of insulin on the C57BL/6 background. The previous PANKO C57/129 mouse were shown to have no difference in peripheral insulin sensitivity shown by ITT when fed both HFD for 5 and 10 weeks and normal chow, though generally, blood glucose levels were slightly higher in the PANKO C57/129 at each time point [60, 61]. The same was

also true for Ad-PANDER overexpressing mice and the PANTG mouse, where blood glucose levels (shown as % of baseline) were similar to WT during a GTT [52, 81, 82]. Additionally, another hepatic Ad-PANDER overexpressing model showed via a minimal model analysis, where mice are anesthetized during experimentation, that PANDER ultimately contributed to an overall decrease in insulin sensitivity [51].

Like the PANKO C57/129 mice, PANKO-C57 males showed no significant difference in raw blood glucose concentrations from 0-60 minutes during the ITT, though their blood glucose levels were trending lower than WT. Interesting, at 90 and 120 minutes of the ITT, the trend switched and the PANKO-C57 blood glucose average was higher than that of the WT mice, though differences in blood glucose measurements were not significantly different (Figure 13A). The similarity in blood glucose levels during the ITT was confirmed by AUC analysis, where the AUC for PANKO-C57 and WT were virtually the same 24490 ± 2048 versus 25610 ± 3558 , respectively (n.s.), though PANKO-C57 AUC was slightly lower (Figure 13B). When evaluating the % from baseline change in blood glucose concentrations during the ITT, where timepoint 0 is considered 100%, or baseline, the similarity between PANKO-C57 and WT insulin sensitivity became more profound, as did the trend reversal at 90 minutes, where PANKO-C57 mice average blood glucose % from baseline, $121.8 \% \pm 13.76$, was significantly higher than WT at $73.38 \% \pm 15.01$ ($P < 0.05$) (Figure 13C). % from baseline change in blood glucose in PANKO-C57 mice remained elevated at 120 minutes compared to WT, as well, though the difference was not considered significant. The AUC of % from baseline change in blood glucose of PANKO-C57 and WT mice was also not significantly different, though PANKO-C57 AUC was slightly elevated compared to WT (13320 ± 1205 versus 12080 ± 2192 , respectively), potentially due to the trend reversal at 90 and 120 minutes (Figure 13D).

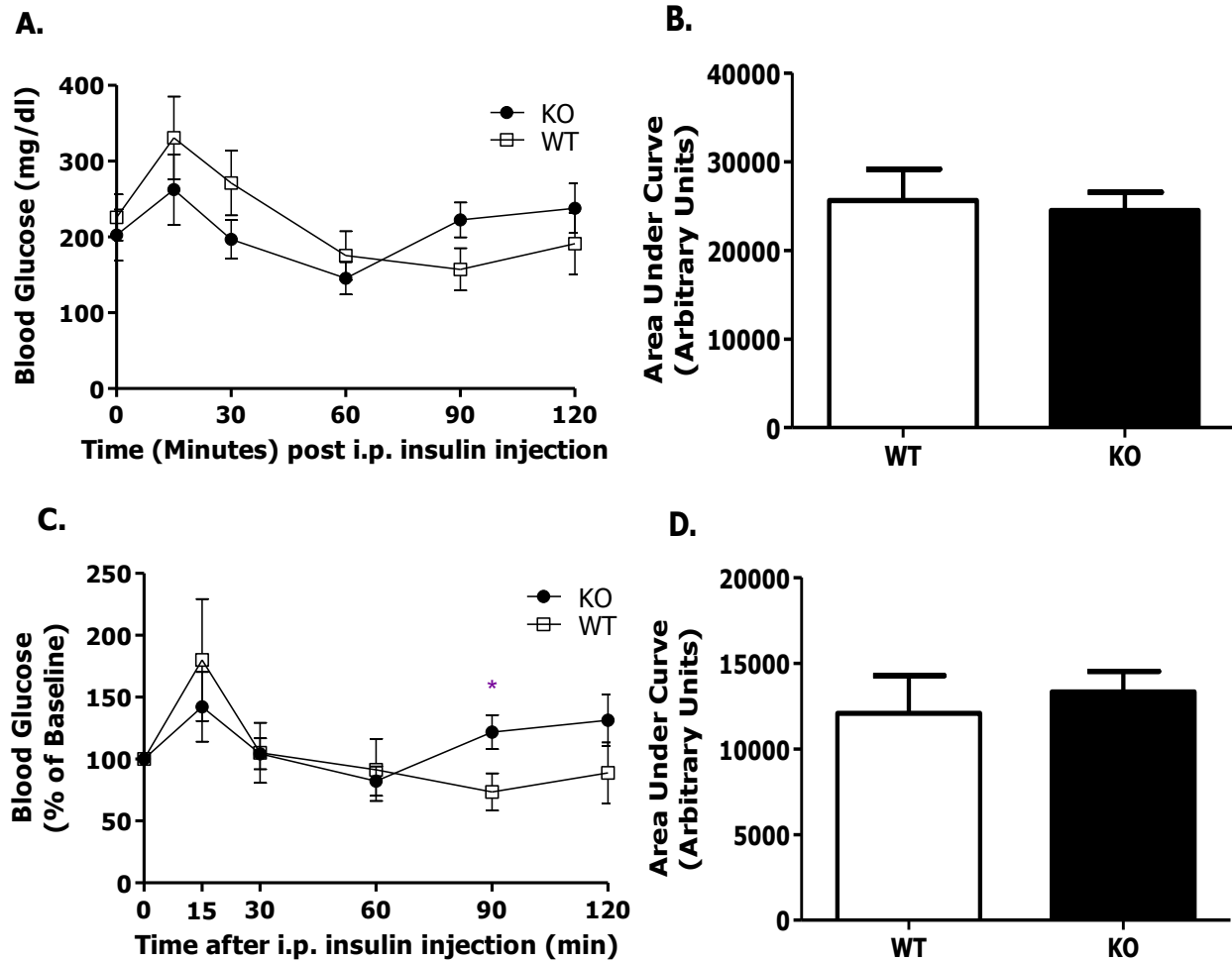


Figure 13: Male PANKO-C57 and WT Similarities of Blood Glucose in ITT. (A) Male PANKO-C57 and WT raw blood glucose numbers (mg/dl) during ITT at 0, 30, 60, 90, and 120 minutes post intraperitoneal insulin (1U/kg) injection recorded using glucometer (n= 8-12). (B) AUC of male ITT raw blood glucose readings in Figure A. (C) Male PANKO-C57 and WT blood glucoses as % from baseline during ITT, where 0 minute reading was baseline, calculated from values at each timepoint in Figure A (P < 0.05) (n= 8-12). (D) AUC of % from baseline blood glucose values during ITT for males shown in Figure C.

Though female mice previously showed no gross differences in metabolic analysis regarding PANDER *in-vivo*, differences in insulin sensitivity via ITTs have not been reported in C57BL/6 PANDER knockout mice [60]. Overall, when evaluating insulin sensitivity in female PANKO-C57 mice during an ITT and observing the raw blood glucose readings at each time point, there was no difference compared to female WT mice (Figure 14A). This was confirmed by differences in AUC of the ITT that were not significant, though PANKO-C57 average AUC was

slightly higher than WT (Figure 14B). Further, the same was true for female blood glucose concentrations during an ITT calculated as % change from baseline, where measurements at all time points were highly similar and correlated with the raw data (Figure 14C). The AUC for female blood glucose during an ITT as % change from baseline was also similar, despite the increase in WT AUC compared to PANKO-C57 (Figure 14D).

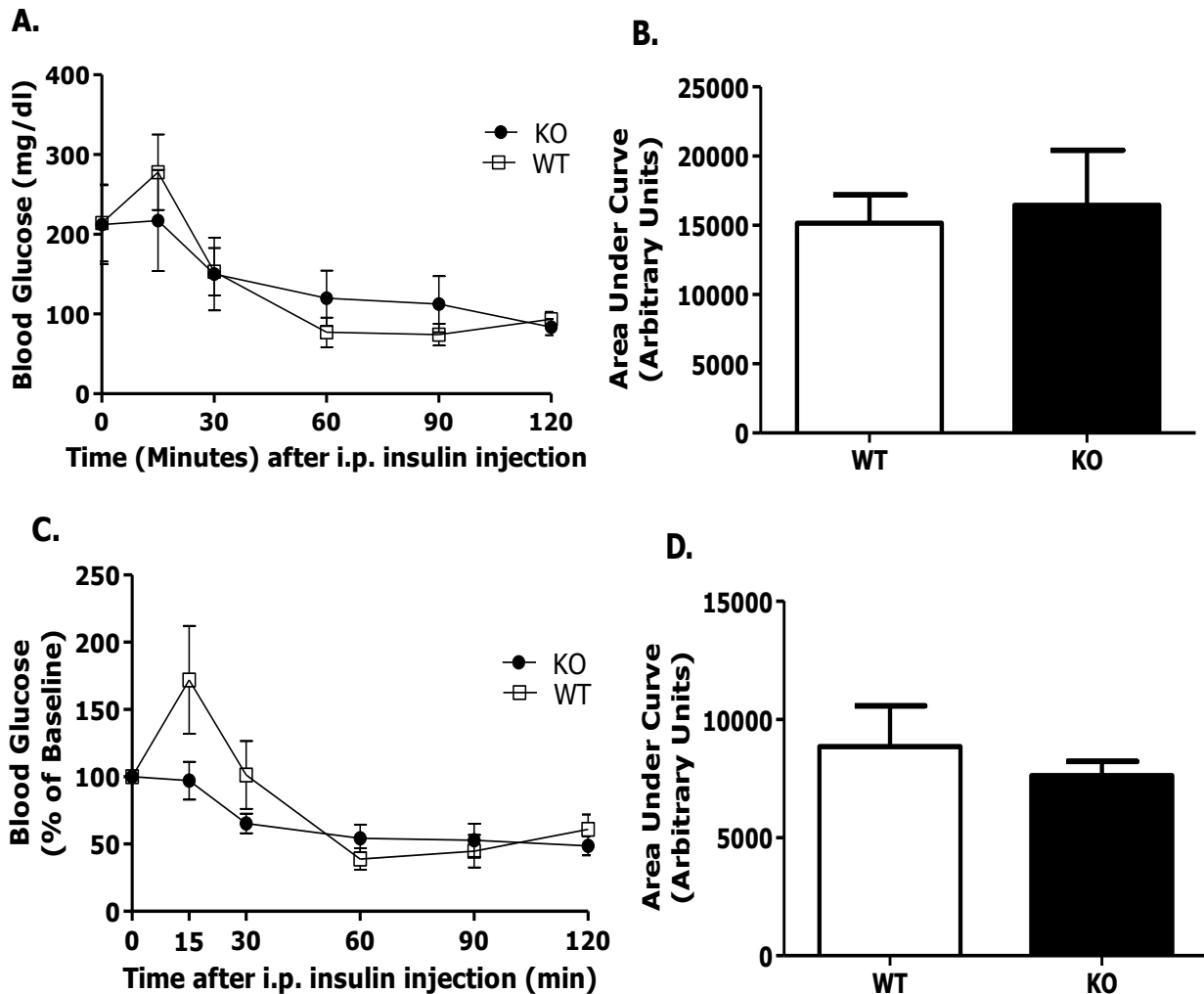


Figure 14: ITT Measurement of Insulin Sensitivity in Female PANKO-C57 and WT Mice. (A) Raw blood glucose numbers (mg/dl) from female PANKO-C57 and WT after 4 hours of fasting during ITT at 0, 30, 60, 90, and 120 minutes post intraperitoneal insulin (1U/kg) injection recorded using glucometer (n= 7-11). (B) AUC of female ITT raw blood glucose readings in Figure A. (C) Female PANKO-C57 and WT blood glucoses as % from baseline during ITT, where 0 minute reading was baseline, calculated from values at each timepoint in Figure A (n= 7-11). (D) AUC of % from baseline blood glucose values during ITT for males shown in Figure C.

Summary of Initial PANKO-C57 Phenotypic & Metabolic Characterization

At the conclusion of the initial phenotyping experiments on the PANKO-C57 mice, several novel findings were observed when taking into consideration previous *in-vivo* PANDER studies. First, PANKO-C57 male mice have a significantly lower overall fasting glycemia compared to WT mice after fasting for both 4 hours and overnight. This is in contrast to the female PANKO-C57 fasting glycemias, which, though had a decreased trend, were not significantly lower. When the decrease in fasting glycemia was discovered at 4-5 months of age in the males, it was also accompanied by a decrease in overnight fasting insulin with a surprising increase in c-peptide, increased leptin, and no difference in glucagon or corticosterone levels compared to WT mice. When measured in plasma from the same PANKO-C57 mice at 2 months of age in comparison to age and sex-matched WT mice, insulin was also decreased with the concordant decrease in c-peptide, leptin trended to be increased as well as glucagon, and corticosterone levels were also no different. Plasma triglyceride content was also significantly increased at 2 months old in the PANKO-C57 compared to 5 months old, where plasma triglycerides trended decreased.

The male specificity of PANDER's role *in-vivo*, as first evidenced by the measurement of fasting glycemias, was also corroborated with enhanced glucose tolerance shown by GTTs and significantly increased weight of male PANKO-C57s compared to WT. Though PANKO-C57 females also displayed significantly increased weights from 8-21 weeks of age, the trend of enhanced glucose tolerance shown by GTT was not as pronounced. Peripheral insulin sensitivity, however, was unaffected by the knockout of PANDER in both males and females as ITTs showed similar blood glucose levels and % change from baseline in response to a bolus injection of insulin.

This initial phenotype, being male-dominant, suggests that the knockout of PANDER not only decreases fasting glycemia and increases glucose tolerance through hormonal analytes such as insulin, but it also facilitates a significant increase in weight, possibly through significant increases in plasma leptin and triglyceride concentrations.

CHAPTER THREE: HEPATIC INSULIN SIGNALING IN PANDER KNOCKOUT C57BL/6 MOUSE

Rationale

In-vitro, PANDER has been shown to bind to the liver membrane in HepG2 cells and inhibit insulin signaling at the liver by preventing the phosphorylation of both the Insulin Receptor (IR) and Insulin Receptor Substrate-1 (IRS-1) under insulin-stimulated conditions [39, 62, 72]. Further down the insulin signaling cascade, PANDER was also shown to inhibit the insulin-stimulated activation of PI3K and phosphorylation of Akt, both critical insulin signaling molecules, in a dose- and time-dependent manner [39, 62, 72]. These results were exacerbated in *in-vivo* animal models of PANDER where different ad-PANDER overexpressors presented with an increase in lipogenic (SREBP-1, FAS, PPAR γ) and gluconeogenic enzyme expression (G6Pase and PEPCCK), and a decrease in phosphorylated Akt, AMPK, and FOXO1 protein expression [51, 54]. The first PANTG overexpressing mouse also displayed a decrease in phosphorylated hepatic AMPK and ACC as well [82]. The initial phenotypes of various PANDER overexpressors has been shown to both support and contradict the phenotype of the initial PANDER knockout models. Concordant with the characterized overexpressing or transgenic models, PANDER knockout mice on mixed genetic background or siRNA models present with a lower HGP with higher % HGP suppression, lower expression of gluconeogenic enzymes and enhanced hepatic insulin signaling (in siRNA knockdown models), but with glucose intolerance and hyperinsulinemia [51, 52, 54, 60]. The observed glucose intolerance in the previous PANDER knockout was attributed to impaired insulin secretion and hepatic insulin clearance. However, these studies lack a

concrete mechanism of action of hepatic signaling in a genetically pure model, like our PANKO-C57 model. In addition, the mixed genetic background PANDER knockout mouse was never thoroughly investigated in the context of altered hepatic signaling despite the presence of increased HGP suppression.

Using the genetically pure PANDER knockout mouse on a C57BL/6 background (PANKO-C57), the effect PANDER is having on the mechanism of hepatic insulin signaling, hepatic gluconeogenic enzyme expression, and glycogen content under fed and fasting conditions was ultimately determined. We hypothesized that the PANKO-C57 mice would have enhanced hepatic insulin signaling as demonstrated by increased phosphorylation of critical signaling molecules such as p-PI3K, Akt, and AMPK, along with increased downstream effector pathways such as in regard to increased glycogen synthesis and lipogenesis.

Experimental Design & Methods

SDS-PAGE Western Blotting of Fasting and Fed Liver Protein

The liver tissue was obtained from male PANKO-C57 and WT mice at 5 months of age in the fasting (>16 hrs, overnight) or fed (insulin-stimulated) state. For fasting samples, mice were fasted overnight by removing all food and livers were extracted the next day after humane euthanization in accordance with experimental IACUC compliance (Appendix C). Livers were placed in CryoTube Vials (Thermo Scientific) and were subsequently flash frozen in liquid nitrogen and stored at -80°C until use. For insulin-stimulated livers, mice were fasted for 4 hours and injected with 2 units/kilogram of insulin (NovoLog) before humane euthanization and flash freezing of whole livers. Serum was also collected 15-minutes post-injection of insulin in insulin-stimulated mice and just prior to euthanization in fasted mice. The SDS-PAGE gels were prepared using 100 mg of liver tissue homogenized using a TissueRuptor (Qiagen) in a

TPER/HALT Protease and Phosphatase inhibitor cocktail (Thermo Scientific). The supernatant of the liver lysate was quantified using a Pierce BCA Protein Assay (Thermo Scientific) following manufacturer's protocol and analyzed using a VersaMax Microplate Reader (Molecular Devices). 20-50 μ g of the liver lysate was then loaded into a 10% tris/glycine Mini-PROTEAN® TGX™ Precast Gel (BioRad) SDS-PAGE with Precision Plus Protein™ WesternC™ Ladder (BioRad) to determine protein size. Transferring of the gel to a PVDF membrane was then performed using iBlot® semi-dry transfer technology per the manufacturer's protocol provided (Invitrogen). The membrane was then blocked overnight at 4° (or for 2 hours at room temperature), rocking constantly, using StartingBlock Blocking Buffer (Thermo Scientific) and was probed for the presence of IRS-1, p-IRS-1, p-PI3K, SREBP-1 (all 4 from SantaCruz Biotechnologies), Akt, p-Akt, AMPK α , p-AMPK α , Acetyl CoA (ACC), p-Acetyl CoA (p-ACC), CREB, p-CREB, p-FOXO1, Glycogen Synthase, p-Glycogen Synthase, and GAPDH as a loading control (all 12 from Cell Signaling Technology) (Appendix A) at a 1:1,000 dilution in 10 mLs of StartingBlock Blocking Buffer overnight at 4°C. Blots were then washed and respective secondary antibodies, whether anti-rabbit (BioRad), anti-mouse (BioRad) or rabbit-anti-goat (Santa Cruz) were added at a 1:3,000-1:5,000 dilution in 10 mLs of StartingBlock Blocking Buffer with 1 μ l of Precision Protein StrepTactin-HRP conjugate (BioRad) for illumination of the protein ladder for 1 hr at RT. Blots were then washed and developed using Pierce ECL Western Blotting Substrate (Thermo Scientific) and imaged using a Fuji LAS4000 imager (FujiFilm GE Healthcare). Once imaged, the blots were then stripped using Restore Western Blot Stripping Buffer (Thermo Scientific), shaking, at 37°C, blocked for > 2 hours at room temperature, rocking, and re-probed using another antibody. ImageJ was used in densitometric analysis of western blot images and all values and concentrations were analyzed via GraphPad Prizm (Version 5) and statistical significance ($p < 0.05$) between KO and WT was determined using 2-tailed Student t-test.

Measurement of Hepatic Triglyceride Content

To measure hepatic triglyceride content in PANKO-C57 and WT livers, fasting and insulin-stimulated liver samples were obtained from PANKO-C57 and WT mice as described above for *SDS-PAGE western blotting*. 100 mg of liver tissue was homogenized in 1 mL of 5% Triton X-100 and heated at 99°C for 5 minutes before being cooled to room temperature, then heated again for solubilization of all triglycerides and centrifuged for 2 minutes at top speed. Samples were then diluted 10-fold and used in the Triglyceride Quantification Kit (Abcam-ab65336) following manufacturer's protocol in triplicate for each sample and at dilutions of 1:10 and 1:100. The colorimetric assay was utilized and samples were analyzed using a VersaMax Microplate Reader (Molecular Devices) with SoftMax® Pro software at a wavelength of 570 nm for optimal absorbance, as it was for serum triglyceride measurement described previously. All values and concentrations, presented in nM, were analyzed via GraphPad Prizm (Version 5) and statistical significance ($p < 0.05$) between KO and WT was determined using 2-tailed Student t-test.

Evaluation of Hepatic Glycogen Content

To measure the differences in hepatic glycogen content between PANKO-C57 and WT mice, 10 mg of previously collected liver tissue from overnight fasted and insulin-stimulated mice was used. The 10 mg of liver tissue was homogenized in 200 μ l of deionized water. The liver homogenate was then boiled, centrifuged, and the supernatant was collected and frozen at -80°C until use in accordance with the manufacturer protocol provided in the Glycogen Assay Kit (Abcam- ab65620). The assay was completed according to manufacturer's protocol for the colorimetric assay and samples were read at 570 nm using VersaMax Microplate Reader (Molecular Devices). The assay was performed in triplicate for every sample using water as a control, and each sample was analyzed not only quantitatively but qualitatively observing color

change for samples that appeared off the standard curve. Each sample was also analyzed in dilutions of 1:10 and 1:100 as to ensure that one of the two data sets coincide with the standard curve (0.0004 mg/mL – 2 mg/mL). All values and concentrations (presented in µg/µl or in fold change) were analyzed via GraphPad Prizm and statistical significance ($p < 0.05$) between KO and WT was determined using 2-tailed Student t-test.

Measurement of PEPCK and G6Pase Expression via RT-PCR

To examine the expression of gluconeogenic enzymes within the livers of the PANKO-C57 and WT mice, livers were harvested and flash frozen from fasting and insulin-stimulated mice as described in *SDS-PAGE Western Blotting* methods. In order to prepare the lysate for RNA extraction, approximately 20 mg of liver tissue was homogenized in a mixture of Buffer RLT (Qiagen) & BME in a 1:100 dilution BME:RLT Buffer using a TissueRuptor (Qiagen). The supernatant, as a result of centrifuging, was then transferred to a gDNA eliminator column provided in the RNeasy Plus Mini Kit (Qiagen) to rid the sample of any remaining genomic DNA contaminants. Then, after a series of washes using ethanol and buffers provided with the kit according to the manufacturer's protocol, the RNA was eluted using RNase-free water (Thermo Scientific). The RNA was then quantified along with determination of their purity using a NanoDrop (Thermo Scientific), and then subsequently frozen in the -80°C freezer until use. For real-time RT-PCR analysis, primer/probes for G6Pase, PEPCK, and 18s rRNA internal control (Applied Biosystems, Life Technologies, Grand Islands, NY) were used with the TaqMan Reverse Transcriptase systems (Applied Biosystems) and StepOne Plus™ Systems (Life Technologies) for mRNA detection. All samples were run in triplicate with deionized water serving as a negative control to ensure there is no false amplification. Expression results were normalized to the 18s rRNA expression and relative levels were determined using the $2^{-\Delta\Delta Ct}$ method [9]. All values were analyzed via GraphPad Prizm (Version 5) and statistical significance ($p < 0.05$)

between KO and WT was determined using 2-tailed Student t-test, presented as fold change from WT.

Measurement of Plasma High-Density Lipoprotein (HDL) and Low-Density Lipoprotein (LDL) Cholesterol

Plasma was obtained from 2 month old fasting PANKO-C57 and WT mice as previously described in *Measurement of Hormonal Analytes* and used in HDL and LDL/VLDL Cholesterol Assay Kit (Abcam- kit ab65390) according to manufacturer's protocol. HDL and LDL were separated in the beginning of the assay and analyzed separately to ensure accurate concentration determination of each. Each sample was run in triplicate with a water control and concentration was analyzed using a VersaMax Microplate Reader (Molecular Devices) at 570 nm. All values and concentrations (presented in $\mu\text{g}/\mu\text{l}$) were analyzed via GraphPad Prizm and statistical significance ($p < 0.05$) between KO and WT was determined using 2-tailed Student t-test.

Fasting PANKO-C57 Mice Exhibit Enhanced Hepatic Insulin Signaling

Previous data regarding PANDER murine models and insulin signaling have thus far been convoluted and inconclusive due to overall differences in models where signaling was characterized. 2 different ad-PANDER overexpressing models suggested that PANDER disrupts the activation of FOXO1, AMPK, and Akt, in addition to enhancing signaling through CREB to induce fasting hyperglycemia [51, 54, 62]. Additionally, these accounts were further corroborated by the PANTG where levels of phosphorylated AMPK and ACC were decreased due to PANDER overexpression [96]. However, the complete elucidation of PANDER's effects on the entire insulin signaling cascade has never been fully evaluated in any *in-vivo* model until this PANKO-C57 characterization.

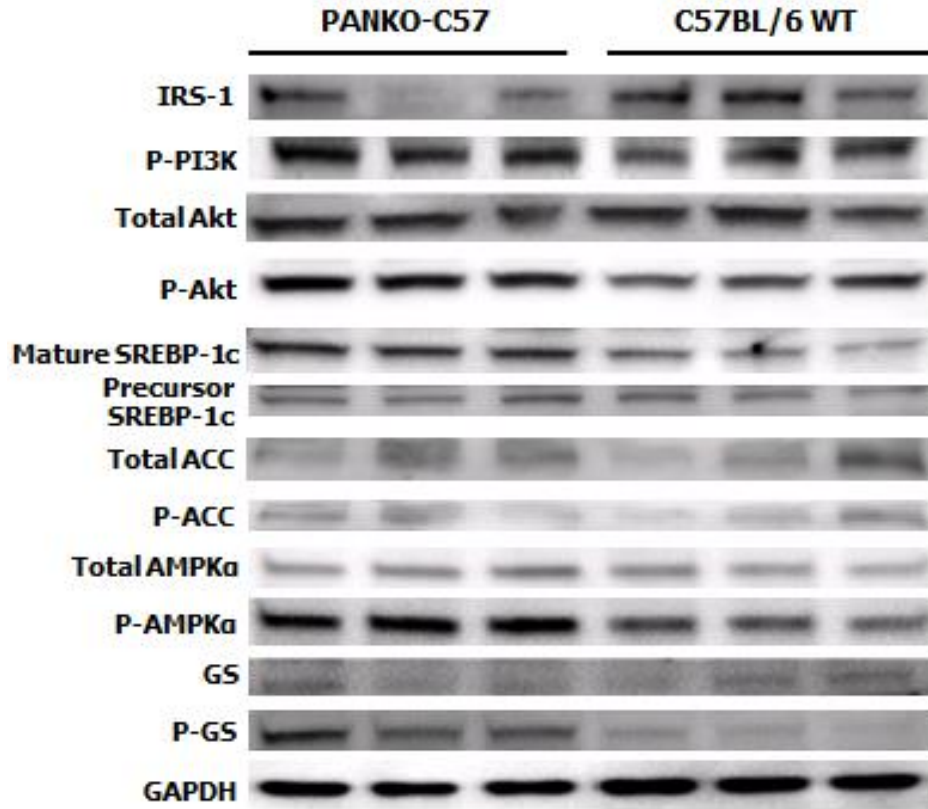


Figure 15: Overnight Fasting Hepatic Signaling in PANKO-C57 and WT Mice. Figure depiction of 10% SDS-PAGE gels loaded with 20-50 μ g of liver lysate protein from overnight fasted PANKO-C57 and WT mice outlined in Experimental Design & Methods above. All primary antibody dilutions presented were 1:1000 with goat-anti-rabbit (BioRad) secondary antibody dilutions of 1:3000-1:5000. Images presented are representative of multiple replicate western blots that were analyzed ($n=3$).

After fasting overnight, PANKO-C57 mice display an overall decrease in protein expression levels of IRS-1 (Figure 15). However, beginning at phosphorylated-PI3K and continuing down through p-Akt, p-ACC, p-AMPK, p-GS and mature SREBP-1c, all protein expressions are increased, indicating an enhancement of phosphorylation activity in the insulin signaling cascade (Figure 15). All of these increases in protein phosphorylation between PANKO-C57 and WT mice are relative to total levels of each respective target protein and normalized to GAPDH levels serving as loading control for each individual mouse. Additionally, levels of SREBP-1c precursor, the transcription factor attached to the endoplasmic reticulum (ER) and nuclear envelope released in times of sterol-depletion to generate the mature SREBP-1, were similar between PANKO-C57 and WT mice (Figure 15) [103]. Glycogen Synthase (GS)

levels appeared similar between both groups, but when comparing phosphorylated-GS levels, PANKO-C57 mice displayed an overall increase in protein expression, indicating that in the fasting state in these mice, the GS protein is inactivated and glycogenolysis is occurring. The increase in phosphorylation of these insulin signaling proteins, including GS, indicates an enhancement in overall insulin signaling in PANKO-C57 mice in the fasting state. Unfortunately, due to technical limitations with regard to lack of successful detection of target protein by western analysis, phosphorylated IRS-1, total CREB, phosphorylated CREB, and phosphorylated FOXO1 protein levels were unable to be properly measured despite utilizing commercially available antibodies that were generated for detection of target proteins and previous reports were unable to be corroborated in PANKO-C57 and WT C57BL/6 mice.

Insulin-Stimulation Enhances Hepatic Insulin Signaling in PANKO-C57

Expression of insulin signaling proteins in response to insulin stimulation in the PANTG murine model revealed an overall decrease in expression levels of both phosphorylated AMPK and ACC, as it did in the fasted state, compared to total levels of the same proteins [96]. Apart from *in-vivo* models, HepG2 cells infected with ad-PANDER for only 48 hours displayed a significant decrease in levels of phosphorylated Akt and FOXO1 after various lengths of times of insulin treatment, further demonstrating PANDER's negative regulatory effects on insulin signaling on the liver *in-vitro* [51]. However, any further characterization of affected protein levels of insulin signaling proteins post-insulin stimulation has remained to be characterized compared to fasting levels in the same murine models, especially in the PANKO-C57 pure PANDER knockout model.

15 minutes after insulin stimulation in PANKO-C57 mice, expression of IRS-1 appears to be slightly decreased compared to WT mice (Figure 16).

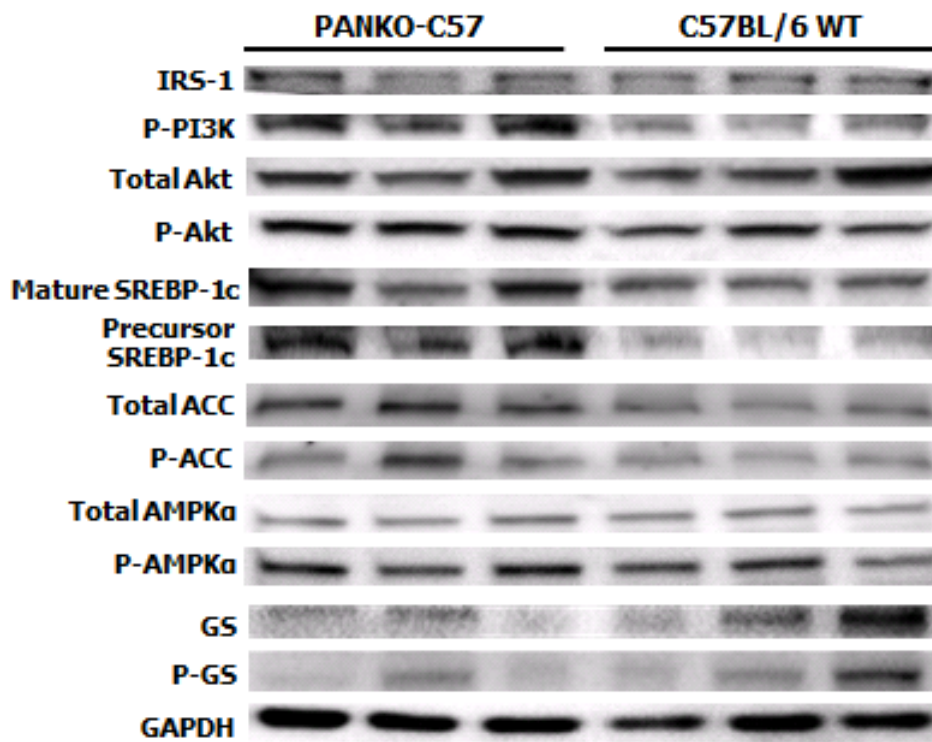


Figure 16: Insulin-Stimulated Effect on Hepatic Signaling Protein Expression in PANKO-C57.

Protein expression measured as outlined in Experimental Design & Methods using 20-50 μ g of liver protein lysate from PANKO-C57 and WT mice injected with insulin. PVDF membranes with transferred proteins were incubated with primary antibodies at 1:1000 dilution and goat-anti-rabbit secondary antibody (BioRad) at 1:3000-1:5000 dilution in StartBlock (Thermo Scientific).

However, insulin-stimulated levels of p-PI3K were highly upregulated in the PANKO-C57 with an unexpected minimal decrease in p-Akt levels compared to WT mice, though protein expression levels are different in each mouse compared to total Akt levels (Figure 16). Both mature SREBP-1c and SREBP-1c precursor expression levels were increased in the PANKO-C57 when stimulated with insulin in striking difference to fasting levels, where there was no difference in SREBP-1c precursor expression between the PANKO-C57 and WT mice. Further, insulin-stimulated p-AMPK and p-ACC expression levels appeared to be similar in both PANKO-C57 and WT mice (Figure 16). Lastly, expression of phosphorylated GS was lesser in PANKO-C57 mice compared to WT mice where there appeared to be no significant differences, if any, in non-phosphorylated GS levels in both cohorts of mice. All protein expression intensities were compared to their respective total protein levels for each mouse when examining

phosphorylated protein expression and all proteins were normalized to GAPDH protein loading control (Figure 16).

Decreased Fasting Hepatic Triglyceride Content in PANKO-C57 Mice

The PANTG overexpressing mouse was recently shown to display an increase in hepatic triglyceride concentration while fed a normal chow diet compared to WT mice, much like that of an Ad-PANDER overexpressing model that revealed significantly higher liver triglyceride content [51, 82]. Surprisingly, an additional Ad-PANDER murine model revealed decreased liver triglycerides while fasting, opposite of what was observed in the hepatic Ad-PANDER overexpressor [51, 54]. Further, the siRNA PANDER knockdown model revealed a reversal of hepatic steatosis in *db/db* mice, but hepatic triglyceride concentration has never been evaluated in a C57BL/6 PANDER knockout, or the previously characterized PANKO C57/129 model until now [51, 54].

Evaluation of hepatic triglyceride content in male PANKO-C57 mice revealed an approximate 4-fold increase in triglyceride concentration when stimulated with insulin, where concentrations were $6.149 \text{ nM} \pm 1.595$ versus WT concentrations of $1.517 \text{ nM} \pm 0.7263$, though values were not significant (Figure 17). After fasting overnight, interestingly, the PANKO-C57 male mice displayed a significant decrease in hepatic triglyceride content compared to WT mice, $7.021 \text{ nM} \pm 1.131$ versus $10.87 \text{ nM} \pm 0.2170$, respectively ($P < 0.05$) (Figure 17). Also interesting to note, hepatic triglyceride content of WT mice was significantly increased ($P < 0.01$) in the fasting state compared to insulin-stimulated hepatic triglyceride concentrations. WT triglyceride concentration was approximately 6-fold higher in fasting compared to insulin-stimulated conditions, whereas PANKO-C57 hepatic triglyceride content was similar in fasting and fed conditions.

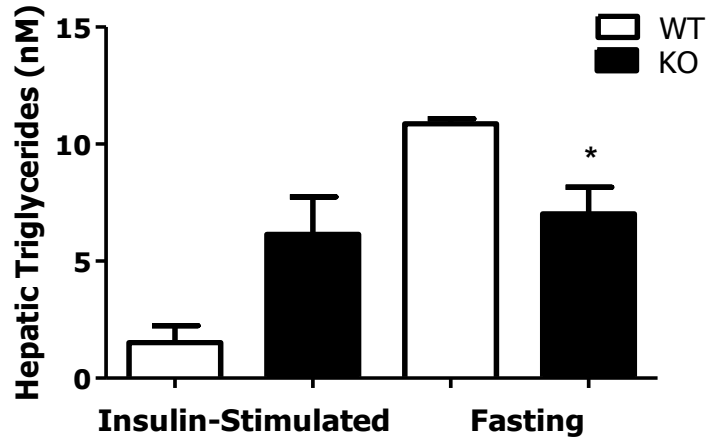


Figure 17: PANKO-C57 Mice Hepatic Triglyceride Concentrations Fasted and Insulin-Stimulated. Comparisons of PANKO-C57 and WT hepatic triglycerides using 100 mg of either overnight fasting or insulin-stimulated liver sample and measured via Triglyceride Quantification Kit (Abcam-ab65336). Concentrations presented in nM, P < 0.05 denoted by single asterisk (n = 3 for each group).

PANKO-C57 Mice Exhibit Increased Fed Hepatic Glycogen Stores

To date, the only differences observed in glycogen stores in PANDER murine models has been in the PANTG model, where glycogen stores were significantly increased while being fed HFD [82]. No differences in glycogen stores were observed in the previous PANKO C57/129 mouse, prompting the measurement of glycogen concentrations in the PANKO-C57 in both the fasting and insulin-stimulated conditions, as glycogen storage and glycogenolysis are central hepatic metabolic processes [54].

Insulin-stimulated hepatic glycogen concentrations were significantly increased in the PANKO-C57 mice where their glycogen concentrations were $142.7 \mu\text{g}/\mu\text{l} \pm 17.16$ versus WT glycogen concentration at $1.169 \mu\text{g}/\mu\text{l} \pm 0.1085$ (P < 0.01) which correlated to a 122.1 fold increase in glycogen stores over WT (P < 0.01) (Figure 18 A & B). After having been fasted overnight, glycogen stores were depleted in both PANKO-C57 and WT mice, where PANKO-C57 mice had a lower concentration of hepatic glycogen at $1.737 \mu\text{g}/\mu\text{l} \pm 0.4636$ versus WT mice with fasting hepatic glycogen concentration at $3.226 \mu\text{g}/\mu\text{l} \pm 0.4003$ (n.s.) which resulted in an almost 2 fold increase in glycogen stores within WT mice (Figure 18 A & C).

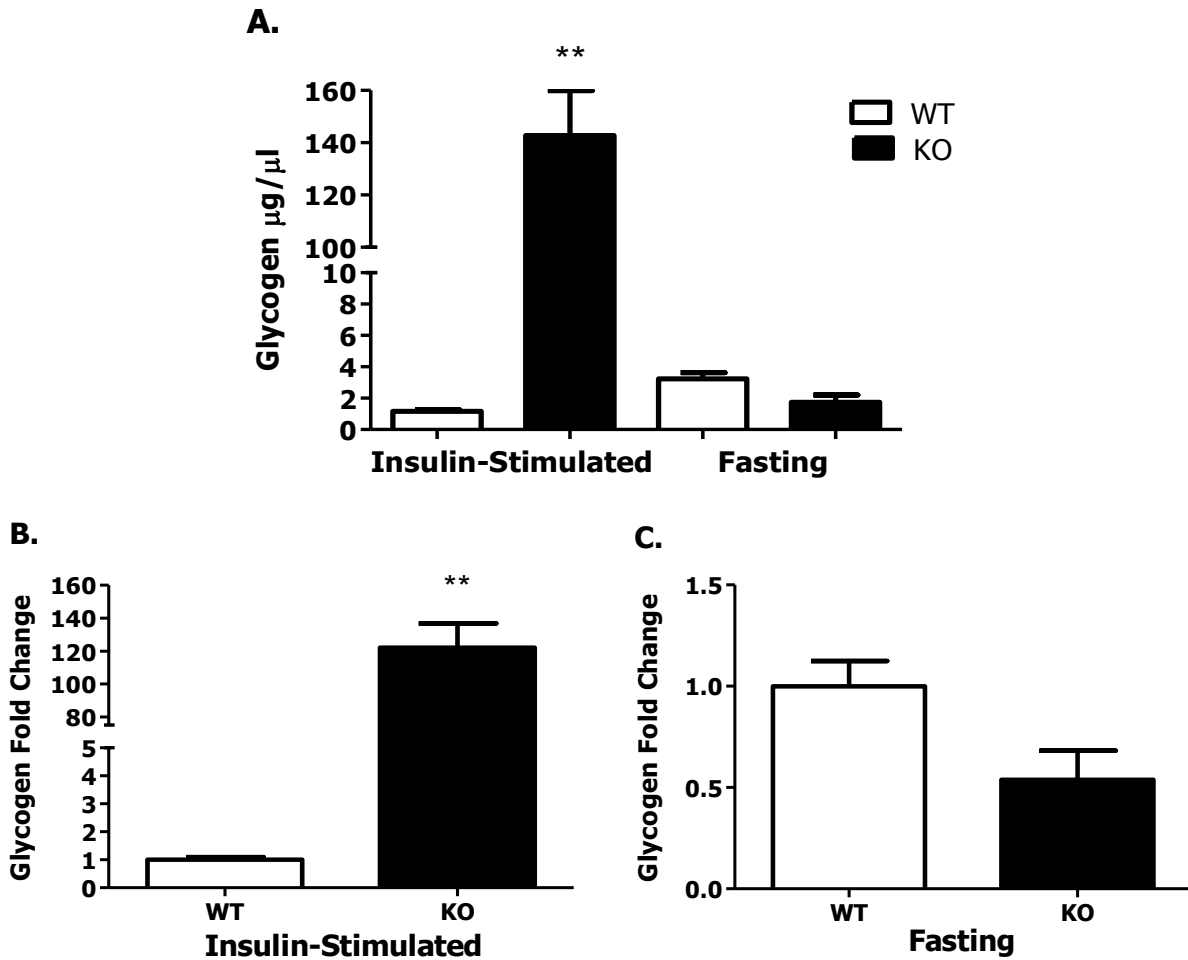


Figure 18: Hepatic Glycogen Stores in PANKO-C57 and WT Mice. (A) Comparison of hepatic glycogen concentration between PANKO-C57 and WT mice, presented in $\mu\text{g}/\mu\text{l}$, in the insulin-stimulated (2U/kg of insulin) and overnight fasting conditions ($n=3$). (B) Fold change between WT and PANKO-C57 hepatic glycogen stores, presented in fold change above WT, in the insulin-stimulated state shown on the left in A. (C) Fold change in hepatic glycogen concentrations, given in fold change above/below WT, in the fasting state shown on the right in A.

Gluconeogenic Enzyme Expression is Upregulated in Fed PANKO-C57 Mice

Gluconeogenesis is the main contributor to HGP after approximately 8-12 hours of fasting, and PANDER has been linked to upregulating expression of gluconeogenic enzymes, G6Pase and PEPCK, in ad-PANDER overexpressing mice after only 3-4 hours of fasting after a GTT, contributing to an overall increased fasting glycemia [2, 25, 54]. siRNA PANDER knockdown *db/db* mice and the C57/129 PANKO mouse displayed a decrease in both G6Pase and PEPCK, and this decrease was observed in the PANKO C57/129 mouse after an overnight

fast, surprisingly, with no reports of gluconeogenic enzyme expression while insulin-stimulated [51, 54].

Surprisingly, when evaluated under insulin-stimulated conditions, PANKO-C57 mice displayed not only a significant increase in G6Pase expression compared to WT (45.36 ± 10.71 vs. 3.807 ± 1.160 , $P < 0.01$), but an almost 8-fold higher relative gene expression of PEPCK (86.28 ± 49.8 vs. 11.08 ± 4.452 , respectively), though not significant (Figure 19A). Interestingly, as opposed to the significant decrease in expression of G6Pase and PEPCK in the C57/129 PANKO mice observed after an overnight fast, the PANKO-C57 mice displayed no significant difference in expression of either G6Pase or PEPCK, though PEPCK expression was trending lower than that of WT (Figure 19B) [52]. Fasting relative expression levels of G6Pase in PANKO-C57 mice were similar to that of WT mice where relative gene expression was 3.117 ± 1.215 versus WT G6Pase expression levels of 2.956 ± 1.062 (n.s.). Further, fasting expression levels of PEPCK in PANKO-C57 averaged 3.756 ± 1.339 versus WT mice at 5.105 ± 1.378 (n.s.).

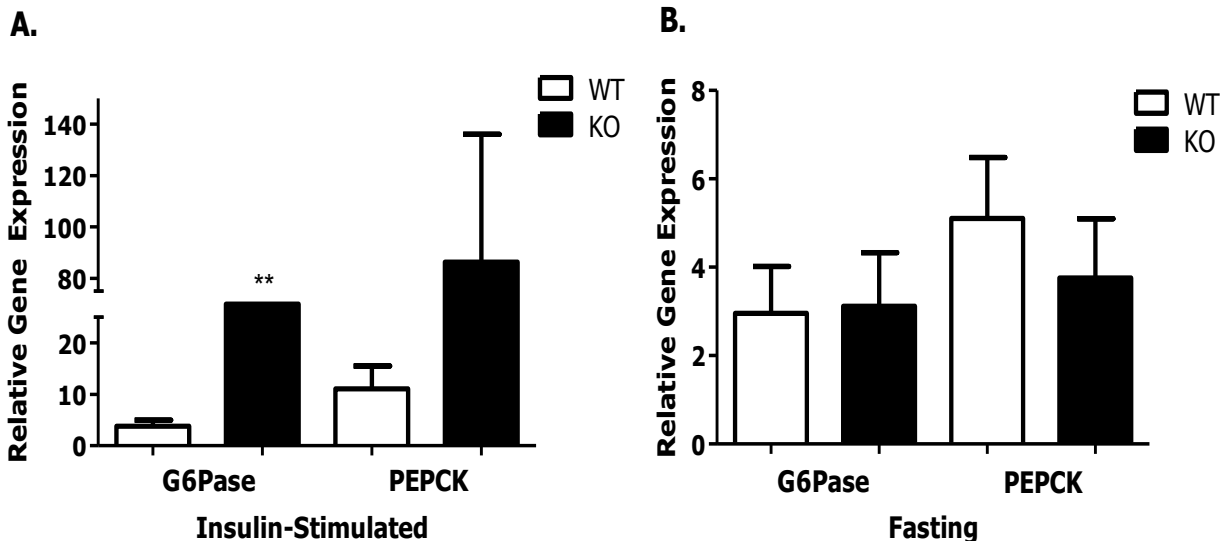


Figure 19: Fasting and Insulin-Stimulated Relative Gene Expression of G6Pase and PEPCK in PANKO-C57 Mice. (A) Using the $2^{-\Delta\Delta Ct}$ method for determination of relative expression levels, insulin-stimulated expression of G6Pase and PEPCK was measured in RNA isolated from 10 mg of liver tissue

from PANKO-C57 and WT mice (n= 4-6). (B) Overnight fasting relative expression of G6Pase and PEPCK measured in isolated hepatic RNA and calculated using $2^{-\Delta\Delta Ct}$ relative gene expression calculation (n= 6).

Higher HDL and Lower LDL Plasma Cholesterol in PANKO-C57 Mice

Overexpression of hepatic PANDER was previously shown to have little effect on HDL/LDL cholesterol concentrations specifically within the liver, though the same hepatic PANDER overexpressing mice interestingly displayed a significant increase in serum VLDL concentrations [51]. Hepatic PANDER siRNA knockdown in *db/db* mice also revealed significantly lower circulating VLDL in contrast to hepatic overexpressors [51]. The PANTG mouse, on the other hand, was reported to display an increase in plasma HDL cholesterol with similar LDL plasma cholesterol levels, perhaps suggesting a role for PANDER in maintaining circulating cholesterol biosynthesis, which we evaluated in fasting PANKO-C57 plasma obtained from mice at 2 months of age [82]. Like the PANTG, the PANKO-C57 presented with an increase in plasma HDL cholesterol with a concentration of 0.701 $\mu\text{g}/\mu\text{l}$ versus WT plasma HDL concentration of 0.480 $\mu\text{g}/\mu\text{l}$ (Figure 20). Plasma LDL cholesterol, on the other hand, and unlike that of the previous PANDER siRNA knockdown model, trended slightly lower in the PANKO-C57 at a concentration of 0.075 $\mu\text{g}/\mu\text{l}$ versus WT plasma LDL cholesterol concentration of 0.103 $\mu\text{g}/\mu\text{l}$ (Figure 20).

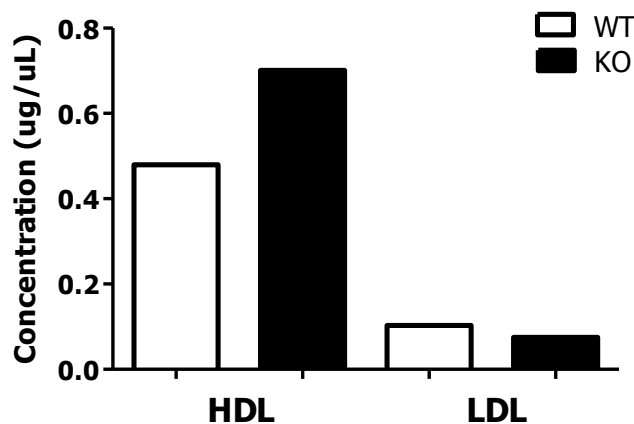


Figure 20: Plasma HDL/LDL Cholesterol Concentrations in PANKO-C57 and WT Mice. 2 months HDL (left) and LDL (right) cholesterol measurement from fasting plasma of PANKO-C57 and WT mice

shown in concentration of $\mu\text{g}/\mu\text{l}$ using HDL and LDL/VLDL Cholesterol Assay Kit (Abcam- kit ab65390) (n= 1).

Summary of Hepatic Signaling Mechanisms in PANKO-C57 Mice

The complete elucidation of hepatic insulin signaling in PANKO-C57 mice provides not only clarity to earlier contradictory evidence, but also novel findings regarding PANDER's role in effecting hepatic insulin signaling, particularly during the fasted state. The PANKO-C57 mice displayed an upregulation of all of the critical insulin signaling molecules in the insulin signaling pathway after an overnight fast, where 3 of the 5 protein expression differences were significant when analyzed using densitometry, denoted by asterisks and shaded dark green in a heat map (Table 1). This supports the idea that PANDER's most severe effects are in the fasted state as opposed to in insulin-stimulated conditions. When stimulated with insulin, the PANKO-C57 mice displayed selectively different trends in protein expression within the insulin signaling cascade as in the fasted state, though no values were significant or expression levels were not different compared to WT (Table 1).

Table 1: Summary of Western Results Comparing Hepatic Signaling in PANKO-C57 versus WT as a Heat Map Representation

Signaling Molecule	Fasting	Insulin Stimulated
IRS-1	↓	↓*
p-PI3K	↑	↑
p-Akt	↑*	↓
p-AMPK	↑*	NC
p-ACC	↑	NC
mSREBP-1	↑*	↑
p-GS	↑**	↓

* Western results are shown in a heat map with up arrows (shaded in green) or down arrows (shaded in red) denoting increased or decreased phosphorylation (normalized to total target protein and loading) or abundance (for IRS-1), respectively. * denotes statistical significance according to densitometry and are highlighted by a darker shade of red or green. NC refers to no change measured and is shaded in yellow.

Beyond insulin signaling, the PANKO-C57 mice presented with increased hepatic triglyceride content post-insulin stimulation but lower hepatic triglyceride content after an overnight fast compared to WT mice. Glycogen stores were also significantly increased along with hepatic triglycerides after insulin stimulation and were almost depleted after fasting overnight. Interestingly, as opposed to previous PANKO C57/129 and siRNA PANDER knockdown models, expression of gluconeogenic enzymes G6Pase and PEPCCK were increased in the PANKO-C57 after insulin stimulation and were similar to WT after fasting, though PEPCCK was evidenced to be slight decreased. Lastly, plasma levels of HDL cholesterol were higher with decreased levels of plasma LDL cholesterol in the PANKO-C57 mice at 2 months of age compared to age and sex matched C57BL/6 WT mice.

These novel findings discovered as a result of the elucidation of hepatic signaling both fasting and insulin stimulated (fed) along with glycogen, triglyceride, and cholesterol measurement in the PANKO-C57 indicate PANDER plays a significant role in affecting glycemetic regulation, particularly in the fasting state. Furthermore, PANDER also potentially affects hepatic stores of glycogen and differentially affects gluconeogenic enzyme expression and HGP under conditions of insulin abundance.

CHAPTER FOUR: CONCLUSIONS

PANKO-C57 Compared to Previous PANDER Knockout/Knockdown Models

After complete phenotypic and hepatic signaling characterization of the global PANDER knockout mouse on a C57BL/6 genetic background, the PANKO-C57 mouse, several similarities and differences were discovered between the PANKO-C57, the previous PANKO C57/129 mixed genetic PANDER knockout, and the acute ad-PANDER *db/db* siRNA PANDER knockdown mouse (Table 2). The PANKO-C57, devoid of any circulating PANDER, exhibited an enhanced glucose tolerance and decreased fasting glycemia, like that of the siRNA PANDER knockdown, but unlike that of the PANKO C57/129 [51, 54, 60]. Interestingly, in full contrast to the siRNA knockdown model, the PANKO-C57 presented with an overall increase in both plasma and hepatic triglycerides, neither of which were even evaluated in the PANKO C57/129, suggesting that PANDER may work through alternate mechanisms up or downregulate triglyceride synthesis under different conditions [51, 60]. The fact that none of the 3 PANDER knockout/down models display an enhanced peripheral insulin sensitivity indicates that PANDER's effects are solely focused on the liver to upregulate glucose output, as evidenced by the decrease in gluconeogenic enzyme expression in both the PANKO C57/129 and the siRNA knockdown, but not in the PANKO-C57, indicating an additional mechanism for their decreased fasting glycemia [51, 54]. However, in light of the lack of decreased gluconeogenic enzyme expression, the PANKO-C57 has, thus far, been the only model to exhibit a decrease in fasting glycemia, increase in hepatic glycogen stores, and enhanced hepatic signaling through critical insulin signaling molecules involving p-PI3K, p-Akt, and SREBP-1, among others, which was not fully

characterized in the siRNA knockdown model and not attempted in the PANKO C57/129 [51]. This suggests that the PANKO-C57, as opposed to comparable models, represents a more enhanced phenotype for identification of PANDER function.

Table 2: Comparisons of PANDER Knockout C57/129 & *db/db* siRNA Knockdown Murine Models to PANKO-C57

	PANKO-C57	PANKO C57/129	<i>db/db</i> siRNA PANDER
↑ Glucose Tolerance	✓	X	✓
↓ Fasting Glycemia	✓	X (on normal chow)	✓
↓ Fasting Insulinemia	✓	X	N/A
↓ Gluconeogenic Enzymes	X	✓	✓
↓ Corticosterones	X	N/A	N/A
↑ Plasma Triglycerides	✓	X	X
↑ Insulin Sensitivity	X	X	X
↑ Hepatic Glycogen	✓	X	N/A
↑ Hepatic Triglycerides	✓	N/A	X
↑ Critical Insulin Signaling Molecules	✓	N/A	✓ (Akt, AMPK, FOXO1)

PANKO-C57 as an Improved PANDER Murine Model

Advantages

The PANKO-C57 mouse offered great advantages in terms of phenotypic characterization and offered clarity, in addition to further understanding, of PANDER's role *in-vivo*. First, this PANKO-C57 mouse was the first and only PANDER model to depict significant phenotypic differences between female PANKO-C57s and WT mice, including increases in body weights and enhanced glucose tolerances, in addition to trending decreased fasting glycemia. Though PANDER's effects were ultimately determined to be male-dominant, as they are regarding other PANDER murine models, shown by significant decreases in fasting glycemia and

significant enhances in glucose tolerance in male PANKO-C57 mice, the differences observed here in female PANKO-C57s is novel [54, 60, 82, 96]. Additionally, given that these PANKO-C57s are on a purebred C57BL/6 genetic background, any abnormalities due to the genetic background with heterozygosity and gene expression, which was the case with the PANKO C57/129 co-isogenic strain, are abolished, ensuring in excess of 99% homology within the breeding colony of the congenic PANKO-C57 strain [91, 92]. When compared to the mixed genetic PANKO C57/129, the pure bred PANKO-C57 was able to exhibit traits such as enhanced glucose tolerance, decreased fasting insulinemia, and differences in body weight and fasting glycemic levels not previously observed in the PANKO C57/129 [54, 60, 61]. These observed differences can only be attributed to the different genetic backgrounds, PANKO C57/129 versus PANKO-C57, and suggest that the PANKO-C57 is the optimal PANDER knockout model. Also, because the PANKO C57/129 mixed genetic mouse revealed defects in insulin secretion due to improper calcium handling, it is possible that those defects are also present in the PANKO-C57 [60]. However, any of the possible effects of defective insulin secretion in the PANKO-C57 were completely masked by the significantly enhanced hepatic insulin sensitivity that was not observed in the PANKO C57/129.

Additionally, because the PANKO-C57 has integrated the null PANDER mutation into its genome for transmission to all generations, there are multiple advantages to the PANKO-C57 over the acute siRNA PANDER knockdown *db/db* model. First, not only was siRNA knockdown performed in a mouse accepted as a suitable model for type 2 diabetes, but siRNA knockdown via tail vein injection was only performed 3 days prior to all experimentation [51, 53]. Because knockdown of a gene via siRNA is considered transient in the case of this PANDER model, not only is continuous application of the siRNA needed to elicit a long-term effect, but the efficiency of delivery and off-target effects of the siRNA need to be taken into consideration as well [51,

98]. The PANKO-C57 offers an advantage to this model in that the effects of the null PANDER mutation are able to be studied longitudinally in these mice throughout their lifespan, from weaning to euthanization. This allows us to observe not only the effects of globally knocking out PANDER in these purebred C57BL/6 mice, but also to observe how the aging process effects PANDER and perhaps the development of type 2 diabetes, considered an adult-onset disorder [12-15]. Several assays and screenings presented in this study were able to be performed at 2 and 5 months in the same mice, whereas siRNA knockdown models were not due to the short-term longevity of the siRNA effects [51, 98]. Further, the *db/db* mouse is known as a model of type 2 diabetes because of a point mutation in the leptin receptor that results in abnormal signal transduction along with gross obesity, leptin resistance, and type 2 diabetic hallmarks [53]. It is potentially for this reason that such a difference in fasting plasma leptin concentrations were observed in the PANKO-C57 that could not possibly be observed in the siRNA knockdown model being that the siRNA was performed on a *db/db* mouse.

Limitations

Though the PANKO-C57 is considered to be on an optimal background to observe the effects of and phenotype null mutations, there are limitations to this study [91, 92]. First, the lack of a tissue-specific PANKO-C57 is a potential drawback to completely characterizing PANDER's implications *in-vivo*. To delineate the relative contribution of various tissue-derived PANDER from the liver, intestine, and pancreas, an argument could be made that tissue-specific knockouts pertaining to these PANDER producing tissues would further refine the synergistic role of this molecule. Thus far, the PANTG has been the only tissue-specific PANDER overexpressing murine model created apart from other transient/acute ad-PANDER models [81, 82, 96]. The PANTG, a pancreas-specific PANDER overexpressor, has shed light on many inconsistencies presented in other PANDER overexpressing models, and the creation of either a

pancreas or liver-specific PANDER knockout would allow for improved clarity regarding PANDER's effects on/in specific organs and tissues [81, 82, 96]. Additionally, the PANDER receptor has yet to be elucidated. Though the crystal structure of PANDER was discovered early this year, the lack of a definitive PANDER receptor greatly hinders not only characterizing PANDER's interactions, but also potential novel therapeutics in preventing PANDER's actions [40]. That's not to say that the PANKO-C57 was lacking, in any way, valuable evidence that its phenotypic characterization adds to our knowledge regarding PANDER.

Further limitations regarding this study involve the n , or the number of mice, involved in each analysis. Though an n value of 3 is able to generate statistical significance, perhaps using more mice in each of the studies would reduce the standard error from the mean (SEM) values and allow for greater significance to be reached. Many of the PANKO-C57 studies presented including body weight measurements, GTTs, ITTs, and fasting glycemic measurements here involved up to 10-15 mice and sometimes greater, where the greatest differences to WT were observed, but technical limitations involving multiple assay optimizations hindered the ability to assess more mice. Further, PANKO C57/129 mice displayed decreased fasting glycemia with decreased insulinemia when stimulated with glucose and decreased fasting G6Pase and PEPCk when fed HFD for up to 10 weeks [61]. This insinuates that these PANKO C57/129 mice could be offered some protection to developing fasting hyperglycemia, a hallmark of type 2 diabetes and an effect of PANDER, by ingestion of a HFD [52, 61]. As a result of these findings in the mixed genetic PANKO C57/129, it is plausible to say that the effects of HFD feeding should be evaluated on PANKO-C57 mice also. The genomic deletion of PANDER in C57BL/6 mice could potentially offer an even higher degree of protection against hyperglycemia and hyperinsulinemia brought on by a HFD that was observed in the PANKO C57/129, given that the PANKO-C57s already display a decreased fasting glycemia and insulinemia. Unfortunately, due

to the time constraints regarding this project, the effects of HFD on PANKO-C57 glycemic regulation and glucose homeostasis was not able to be determined (although initiated), but should be considered in future directions regarding PANKO-C57 characterization.

Lastly, though hepatic insulin signaling was determined to be enhanced in the PANKO-C57 in this study, inconsistencies remained regarding increased and similar gluconeogenic enzyme expression in insulin-stimulated and fasting conditions, respectively. Previously, the PANKO C57/129 and siRNA PANDER knockdown presented with decreased gluconeogenic enzyme expression which was corroborated in the PANKO-C57 only in the fasted state based on a non-statistical trend [51, 54]. To circumvent these inconsistencies and better understand HGP within the PANKO-C57, a hyperinsulinemic-euglycemic clamp study should be performed and this model may eventually be sent for clamp studies for this purpose. HEC studies are considered to be the gold standard and optimal method for determining hepatic insulin sensitivity, peripheral glucose utilization, insulin action, and HGP [97]. HECs were performed on both the PANTG and the PANKO C57/129 mice and revealed increased and decreased HGP, respectively, along with decreased and increased % HGP suppression, respectively, which greatly added to the overall phenotypes observed in each mouse [60, 81]. These HEC studies should optimally be utilized as a confirmatory measure for enhanced hepatic insulin sensitivity observed in the PANKO-C57 via multiple western blots, however, due to technical and monetary limitations, HEC studies were not able to be completed within the realm of this study. Nevertheless, the findings regarding PANDER and the characterization of the PANKO-C57 murine model that were gained from this study, in light of the few limitations, are novel and further corroborate evidence that PANDER plays a major role in glycemic regulation, particularly at the hepatic level.

PANDER's Role in Glycemic Regulation & Type 2 Diabetes Based on PANKO-C57

PANDER's association with type 2 diabetes has been characterized thus far in terms of *in-vitro* data and findings primarily from acute ad-PANDER overexpressors and knockdown models. However, with the characterization of the PANKO-C57 presented in this study, clarity has been gained regarding PANDER's actions in the fed, fasting, and type 2 diabetic states.

PANDER in the Fed State

In the fed state, based on previous PANDER data combined with novel findings from this PANKO-C57 phenotypic characterization, upon ingestion of a meal, blood glucose will rise by the release of broken down sugars and carbohydrates into the bloodstream, or glucose appearance [1, 4, 5]. The rising blood glucose stimulates pancreatic islets to secrete both PANDER and insulin from β -cells [66]. Given that exogenously produced PANDER does not affect insulin levels or secretion *in-vivo* and PANKO C57/129 mice islets reveal improper calcium handling resulting in decreased glucose stimulated insulin secretion, PANDER seems to further enhance insulin secretion from pancreatic islets [52, 54, 60]. Insulin, being the dominate molecule, and being further facilitated by PANDER, will bind to its respective IR on the hepatic membrane and enhances insulin signaling, lipogenesis, and enhance hepatic glycogen stores [51, 72]. Additionally, insulin enhances PANDER secretion from α -cells, further allowing PANDER to augment the effects of insulin and insulin sensitivity [52, 69]. All of these factors contribute to the maintenance of euglycemia after meal ingestion when all other contributions to blood glucose and glycemia are normal (Figure 21).

Interestingly, in the PANKO-C57, though there is no circulating PANDER to facilitate insulin secretion and action, the mice display enhanced hepatic insulin sensitivity in the insulin-stimulated (fed) state and respond greater to insulin than C57BL/6 WT mice. This is shown through an upregulation of critical insulin signaling molecules including p-PI3K, p-Akt, and

SREBP-1, stimulating increased hepatic triglyceride content, and significantly higher glycogen stores. This could potentially be due to the fact that though PANDER assists insulin and promotes its secretion from β -cells, insulin plays a counterregulatory role to PANDER. When PANDER is no longer present, insulin's effects are potent and unrivaled *in-vivo*, leading to the fact that fasting PANKO-C57 mice are particularly more insulin sensitive than WT mice. Additionally, when PANDER is knocked out on a pure C57BL/6 background and all other genetic inconsistencies are eliminated, insulin is able to work maximally to enhance glucose disappearance, observed in the PANKO-C57 mice where they exhibit enhanced glucose tolerance through lower blood glucose levels during a GTT.

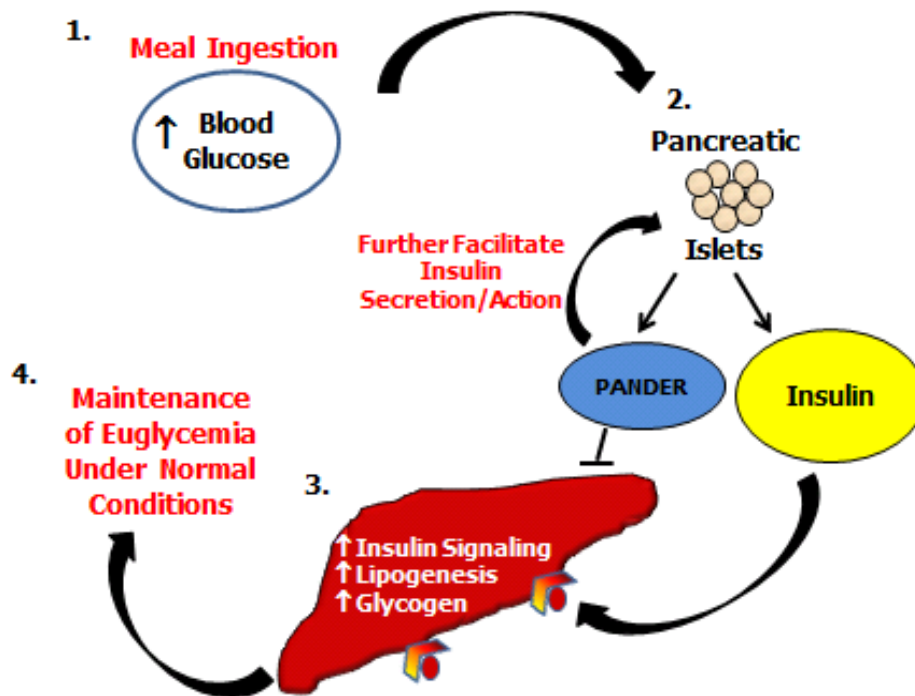


Figure 21: PANDER's Predicted Actions in the Fed State Based on PANKO-C57 Model. Depiction of PANDER's role in the fed states where (1) ingestion of a meal increases blood glucose levels, stimulating (2) pancreatic islets to secrete PANDER and insulin, where PANDER further allows for insulin secretion and action from the islets and insulin's effects dominate that of PANDER's at the hepatic level and allow for (3) enhanced insulin signaling, increased lipogenesis, and enhanced glycogen storage, leading to (4) the further maintenance of euglycemia and insulin sensitivity (adapted from Wilson *et al.* 2011) [52].

PANDER in the Fasting State

When fasting, PANDER's mechanism of action is slightly less understood, but it has appeared as though PANDER exerts a greater negative role on glycemia under fasting conditions. Decreasing blood glucose levels stimulate the release of glucagon from α -cells in pancreatic islets [1]. With regard to PANDER secretion from pancreatic α -cells, L-arginine, a stimulator of glucagon, highly upregulates PANDER secretion in a dose-dependent manner [52, 69, 70, 71]. Surprisingly, insulin was also found to upregulate PANDER secretion from pancreatic α -cells as well [69]. With the increase in glucagon and subsequent decrease in circulating insulin, PANDER is allowed to dominate glycemic regulation over glucagon via either a FOXO1 or CREB dependent pathway [51, 52, 54]. PANDER levels have been evidenced to be increased in fasting *db/db* mice, and this increase in PANDER negatively impacts the liver through FOXO1 and/or CREB to decrease basal insulin signaling and enhance HGP [51]. This increase in HGP seen in the PANTG via HEC clamp studies and evidenced through increased expression in gluconeogenic enzyme expression in ad-PANDER overexpressors, contributes to an overall increase in fasting hyperglycemia and plasma insulin content [54, 82] (Figure 22).

The PANKO-C57 corroborates the siRNA PANDER knockdown model where decreased fasting blood glucose levels were observed, though glucagon levels were similar in the PANKO-C57 [51]. Although differences in FOXO1 and CREB (and p-CREB) levels were not able to be observed in the PANKO-C57 due to technical limitations, hepatic insulin signaling was upregulated, and levels of PEPCK were shown to be trending lower in PANKO-C57, indicating that when fasting; PANDER does, in fact, dominate basal levels of insulin to increase HGP. Because fasting plasma insulin levels were lower in the PANKO-C57 compared to WT, PANDER could potentially be working through an alternate mechanism to enhance HGP and increase fasting glycemia. Being that there was no significant difference in fasting plasma leptin levels in

the PANTG overexpressor and the PANKO-C57 exhibited significantly increased plasma leptin levels, this offers a suitable route for PANDER. Increases in leptin and leptin signaling in the brain are associated not only with increased fat mass, but with enhances in hepatic signaling through PI3K, suppression of HGP, and increased hepatic insulin sensitivity [96, 99, 100]. This presents an attractive mechanism for PANDER to act through, where PANDER could potentially act on/be secreted from the brain and decrease leptin signaling, ultimately leading to an increase in HGP and decrease in hepatic insulin sensitivity. Further, the siRNA PANDER knockdown db/db model with a known defect in leptin receptor signal transduction failed to report an enhancement of expression in all insulin proteins, perhaps due to the fact that they are lacking the synergism that exists between leptin and hepatic insulin sensitivity [51, 53]. As a whole, evidence from the PANKO-C57 phenotype indicates that the complete knockout of PANDER allows for enhanced basal insulin sensitivity when fasting, contributing to an overall decrease in fasting glycemia.

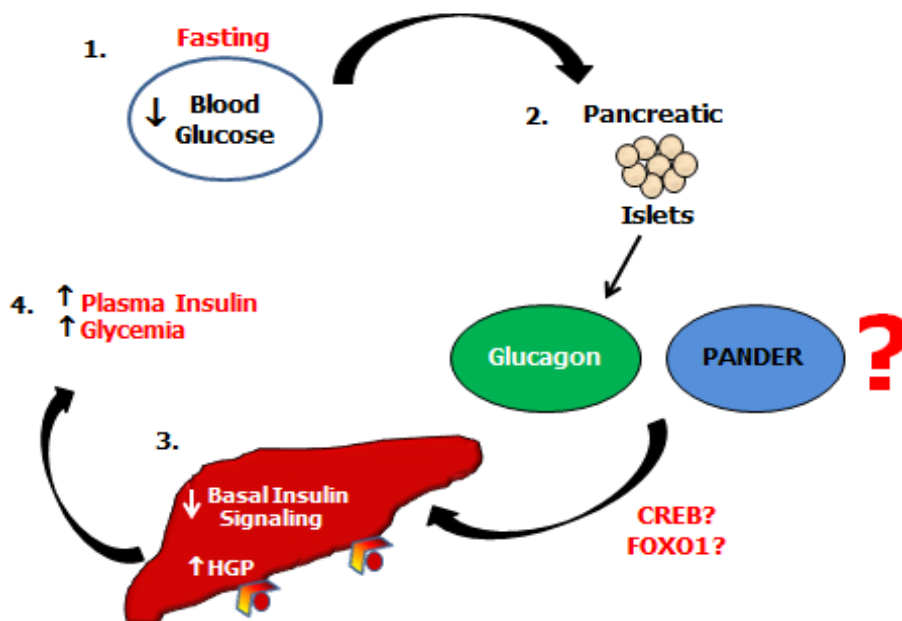


Figure 22: PANDER’s Predicted Role in Glycemic Regulation in the Fasted State Based on PANKO-C57. (1) When fasting, blood glucose levels decrease, which (2) stimulate α -cells in pancreatic islets to secrete glucagon. Meanwhile, PANDER works either through a CREB or FOXO1 dependent

pathway to (3) decrease hepatic basal insulin signaling and increase HGP leading to (4) an increase in plasma insulin and increased glycemia.

PANDER in Type 2 Diabetes

Type 2 diabetes is a disease primarily characterized by 3 hallmarks- hyperglycemia, hyperinsulinemia, and hyperlipidemia, all of which are caused by secretagogues that have been shown to stimulate PANDER transcription and secretion [65, 66, 68, 69, 90]. When any/all of these disease states and secretagogues are present, the pancreatic islets are stimulated to further secrete PANDER and maintain basal levels of insulin. Because of the hyper conditions and given that PANDER levels are increased in mice modeling type 2 diabetes, PANDER could potentially stimulate its own secretion from both the pancreatic islets and hepatocytes, where PANDER is also present [51, 62]. This allows PANDER to impart its counterregulatory actions on insulin and bind to its putative target receptor on the liver to decrease insulin signaling, increase HGP, and decrease glycogen stores. The culmination of these events further perpetuates hyperinsulinemia, hyperglycemia, and hyperlipidemia as insulin and glucose are not being utilized, but instead remain in circulation. Thus, it appears that PANDER promotes a vicious cycle with regard to type 2 diabetes and facilitates the progression and potentially onset of the disease hallmarks (Figure 23).

PANKO-C57 mice, to begin, present with not only decreased fasting glucose levels, but also decreased fasting plasma insulin levels. This further supports the notion that PANDER is a main causative agent of fasting hyperglycemia and the subsequent hyperinsulinemia (due in part to counteraction of insulin resistance or potentially facilitation of insulin secretion), as was observed in young PANTG mice [96]. In terms of hyperlipidemia, PANKO-C57 mice, though they appear to be hyperlipidemic, they retain their hepatic insulin sensitivity, and the improved hepatic insulin signaling through SREBP-1 accounts for this observed hyperlipidemia both hepatically and in the plasma. In the fed, insulin-sensitive state, PANDER's effects on glucose

homeostasis are minimal, as insulin imparts inhibitory effects on PANDER action perhaps simply by a concentration dependence. But when insulin resistance sets in, it appears as though insulin is potentially no longer capable of sufficiently counterracting PANDER. Instead, it appears that PANDER operates in a positive-feedback loop to enhance its own production from the pancreatic islets. PANDER binding to the liver membrane may also further stimulate PANDER expression and secretion from the liver in a similar positive feedback loop. PANKO-C57 mice are a model of insulin sensitivity and glucose tolerance compared to the PANTG and other PANDER overexpressors being that the PANKO-C57 mice, with no PANDER expression or secretion from any tissues, display reversal of a majority of metabolic abnormalities present in these overexpressors. With excess PANDER in circulation due to these disease hallmarks, all evidence points to PANDER as a causative factor in the progression of type 2 diabetes by continually increasing the severity of hyperinsulinemia, hyperlipidemia, and hyperglycemia and an attractive target for therapeutics in the treatment of type 2 diabetes.

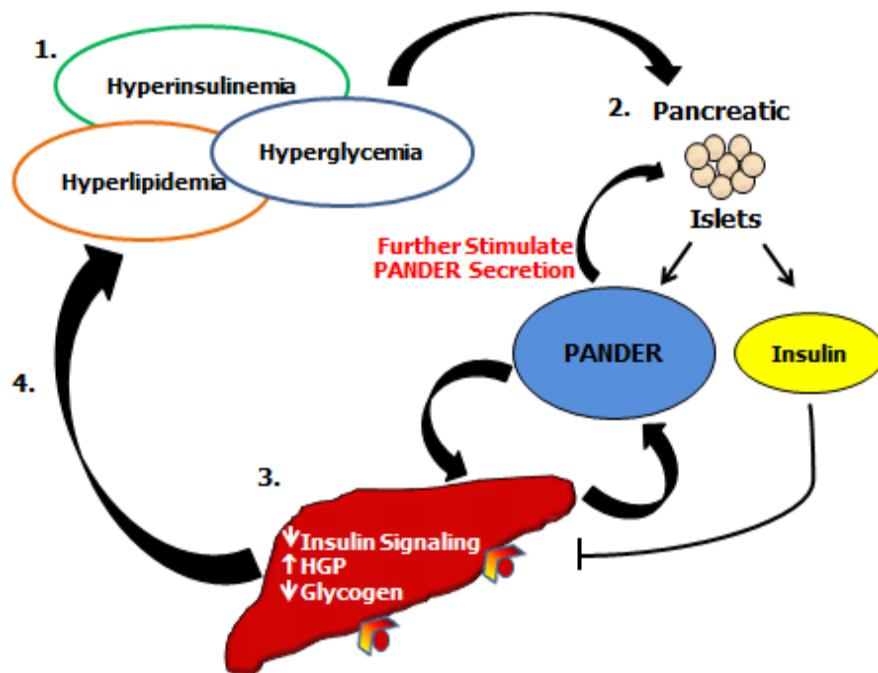


Figure 23: PANDER's Predicted Role in Insulin Resistance and Type 2 Diabetes. In insulin resistant and type 2 diabetic individuals, where (1) hyperinsulinemia, hyperglycemia, and hyperlipidemia are present, (2) pancreatic islets secrete PANDER and insulin where PANDER is the dominant over insulin

and leads to an increase in PANDER secretion from pancreatic islets and the liver. (3) PANDER will decrease insulin sensitivity by decreasing hepatic insulin signaling, increasing HGP, and decreasing glycogen stores contributing to (4) a vicious cycle of hyperinsulinemia, hyperglycemia, and hyperlipidemia (adapted from Wilson, *et al.* 2011) [52].

Perhaps the most telling data regarding PANDER and its negative regulatory effects on hepatic insulin sensitivity and fasting glycemia is its severe depleting effects on hepatic glycogen stores. Being that the PANKO-C57 had an over 100-fold greater amount of glycogen in the liver compared to WT and the PANTG revealed significantly decreased glycogen stores, this could potentially represent an additional mechanism of PANDER to induce fasting hyperglycemia [96]. We have concluded that the PANKO-C57 resembles that of an animal model of Glycogen Storage Disease (GSD). GSD, specifically Type 1 GSD, is a disorder caused by deficiency of G6Pase, an enzyme which performs the last step of gluconeogenesis and glycogenolysis to hydrolyze a phosphate group from glucose, leaving free glucose to be exported into the bloodstream [1, 2, 101, 102]. The disease, both in humans and in murine G6Pase^{-/-} models, ends up manifesting itself through the following symptoms: hypoglycemia, significant liver enlargement, and hyperlipidemia both hepatically and in the serum, all of which were evident in the PANKO-C57 [101, 102]. The striking similarities between GSD Type 1 models and the PANKO-C57 could offer a potential mechanism for PANDER in increasing both fasting glycemia and gluconeogenic enzyme expression apart from increases in corticosterones and CREB signaling previously described [52, 54]. Additionally, GSD Type 1a is defined by a deficiency in the catalytic activity of G6Pase, which could be represented in the PANKO-C57 in that though the mice are not deficient in G6Pase expression (or PEPCK) in fasting or fed conditions shown via RT-PCR, perhaps G6Pase is building up due to a defect in its activity but not in its production [101, 102]. This then leads to a decrease in HGP, subsequent hypoglycemia, build-up of glycogen in the liver with an increased liver mass, and increased triglycerides in the PANKO-C57. Lastly, with the recent findings involving PANDER and its role in various cancers

including oral squamous cell carcinoma and gastric cancer, this PANKO-C57 mouse model may offer future resources in the field of oncology [73, 77]. Given that PANDER expression was recently discovered to be downregulated in both of the aforementioned cancer types, our PANKO-C57 offers an optimal model to potentially study the progression of each cancer type *in-vivo* [73, 77].

Final Thoughts and Summary

In conclusion, this novel phenotypic characterization of the first PANDER knockout mouse on a C57BL/6J background offers valuable information regarding PANDER's role in glucose homeostasis and insulin sensitivity. Not only do these PANKO-C57 mice display a significant increase in glucose tolerance and hepatic insulin sensitivity, but they exhibit an enhanced expression of key insulin signaling molecules throughout the entire insulin signaling cascade, indicating that PANDER disrupts insulin signaling as part of its detrimental actions on insulin sensitivity. Further, PANKO-C57 mice exhibit lower fasting glycemic measurements with decreased insulinemia and increased weights, perhaps to compensatory mechanisms involving leptin signaling and glycogen storage. Taken together, the characterization of this PANKO-C57 model further indicates that PANDER plays a significant role in promoting the advancement and worsening of type 2 diabetes and its associated abnormalities during pathological states of dysregulation.

LITERATURE CITED

1. Aronoff, S. L., Berkowitz, K., Shreiner, B., Want, L. (2004). Glucose Metabolism and Regulation: Beyond Insulin and Glucagon. *Diabetes Spectrum*, 17. 183-190.
2. Tirone, T. A., & Brunicardi, F. C. (2001). Overview of glucose regulation. *World J Surg*, 25 (4), 461-467.
3. Vaulont, S., Vasseur-Cognet, M., & Kahn, A. (2000). Glucose regulation of gene transcription. *J Biol Chem*, 275 (41), 31555-31558.
4. Baggio, L. L., & Drucker, D. J. (2007). Biology of incretins: GLP-1 and GIP. *Gastroenterology*, 132 (6), 2131-2157.
5. Yip, R. G., & Wolfe, M. M. (2000). GIP biology and fat metabolism. *Life Sci*, 66 (2), 91-103.
6. Saltiel, A. R., & Kahn, C. R. (2001). Insulin signalling and the regulation of glucose and lipid metabolism. *Nature*, 414 (6865), 799-806.
7. Myers, M. G., Jr., Backer, J. M., Sun, X. J., Shoelson, S., Hu, P., Schlessinger, J., Yoakim, M., Schaffhausen, B., White, M. F. (1992). IRS-1 activates phosphatidylinositol 3'-kinase by associating with src homology 2 domains of p85. *Proc Natl Acad Sci U S A*, 89 (21)
8. Weyer, C., Maggs, D. G., Young, A. A., & Kolterman, O. G. (2001). Amylin replacement with pramlintide as an adjunct to insulin therapy in type 1 and type 2 diabetes mellitus: a physiological approach toward improved metabolic control. *Curr Pharm Des*, 7 (14), 1353-1373.
9. Unger, R. H., & Orci, L. (1976). Physiology and pathophysiology of glucagon. *Physiol Rev*, 56 (4), 778-826.
10. International Diabetes Federation. IDF Diabetes Atlas Poster Update 2012. 2012. Brussels, Belgium.
11. Hu, F. B. (2011). Globalization of diabetes: the role of diet, lifestyle, and genes. *Diabetes Care*, 34 (6), 1249-1257.

12. Center for Disease Control and Prevention. National diabetes fact sheet: national estimates and general information on diabetes and prediabetes in the United States, 2011. Atlanta, GA: U.S. Department of Health and Human Services, CDC, 2011.
13. Zimmet, P., Alberti, K. G., & Shaw, J. (2001). Global and societal implications of the diabetes epidemic. *Nature*, *414* (6865), 782-787.
14. Lin, Y., & Sun, Z. (2010). Current views on type 2 diabetes. *J Endocrinol*, *204* (1), 1- 11.
15. Albright, A. L., & Gregg, E. W. (2013). Preventing type 2 diabetes in communities across the U.S.: the National Diabetes Prevention Program. *Am J Prev Med*, *44* (4 Suppl 4), S346-351.
16. Zierath, J. R., Krook, A., & Wallberg-Henriksson, H. (2000). Insulin action and insulin resistance in human skeletal muscle. *Diabetologia*, *43* (7), 821-835.
17. Webb, G. C., Akbar, M. S., Zhao, C., & Steiner, D. F. (2000). Expression profiling of pancreatic beta cells: glucose regulation of secretory and metabolic pathway genes. *Proc Natl Acad Sci U S A*, *97* (11), 5773-5778.
18. Kahn, S. E. (2003). The relative contributions of insulin resistance and beta-cell dysfunction to the pathophysiology of Type 2 diabetes. *Diabetologia*, *46* (1), 3- 19.
19. Zierath, J. R., Galuska, D., Nolte, L. A., Thorne, A., Kristensen, J. S., & Wallberg-Henriksson, H. (1994). Effects of glycaemia on glucose transport in isolated skeletal muscle from patients with NIDDM: in vitro reversal of muscular insulin resistance. *Diabetologia*, *37* (3), 270-277.
20. Krook, A., Roth, R. A., Jiang, X. J., Zierath, J. R., & Wallberg-Henriksson, H. (1998). Insulin-stimulated Akt kinase activity is reduced in skeletal muscle from NIDDM subjects. *Diabetes*, *47* (8), 1281-1286.
21. Bjornholm, M., Kawano, Y., Lehtihet, M., & Zierath, J. R. (1997). Insulin receptor substrate-1 phosphorylation and phosphatidylinositol 3-kinase activity in skeletal muscle from NIDDM subjects after in vivo insulin stimulation. *Diabetes*, *46* (3), 524-527.
22. Burgering, B. M., & Coffey, P. J. (1995). Protein kinase B (c-Akt) in phosphatidylinositol-3-OH kinase signal transduction. *Nature*, *376* (6541), 599- 602.
23. Datta, K., Bellacosa, A., Chan, T. O., & Tsichlis, P. N. (1996). Akt is a direct target of the phosphatidylinositol 3-kinase. Activation by growth factors, v-src and v-Ha- ras, in Sf9 and mammalian cells. *J Biol Chem*, *271* (48), 30835-30839.
24. Rhodes, C. J. (2005). Type 2 diabetes-a matter of beta-cell life and death? *Science*, *307* (5708), 380-384.

25. Fritsche, L., Weigert, C., Haring, H. U., & Lehmann, R. (2008). How insulin receptor substrate proteins regulate the metabolic capacity of the liver--implications for health and disease. *Curr Med Chem*, *15*(13), 1316-1329.
26. Rena, G., Guo, S., Cichy, S. C., Unterman, T. G., & Cohen, P. (1999). Phosphorylation of the transcription factor forkhead family member FKHR by protein kinase B. *J Biol Chem*, *274*(24), 17179-17183.
27. Michael, M. D., Kulkarni, R. N., Postic, C., Previs, S. F., Shulman, G. I., Magnuson, M. A., & Kahn, C. R. (2000). Loss of insulin signaling in hepatocytes leads to severe insulin resistance and progressive hepatic dysfunction. *Mol Cell*, *6*(1), 87-97.
28. Edgerton, D. S., Lautz, M., Scott, M., Everett, C. A., Stettler, K. M., Neal, D. W., Chu, C. A., Cherrington, A. D. (2006). Insulin's direct effects on the liver dominate the control of hepatic glucose production. *J Clin Invest*, *116*(2), 521-527.
29. DeFronzo, R. A. (1992). Pathogenesis of type 2 (non-insulin dependent) diabetes mellitus: a balanced overview. *Diabetologia*, *35*(4), 389-397.
30. DeFronzo, R. A., & Ferrannini, E. (1987). Regulation of hepatic glucose metabolism in humans. *Diabetes Metab Rev*, *3*(2), 415-459.
31. DeFronzo, R. A., Gunnarsson, R., Bjorkman, O., Olsson, M., & Wahren, J. (1985). Effects of insulin on peripheral and splanchnic glucose metabolism in noninsulin-dependent (type II) diabetes mellitus. *J Clin Invest*, *76*(1), 149-155.
32. Aurora, R., & Rose, G. D. (1998). Seeking an ancient enzyme in *Methanococcus jannaschii* using ORF, a program based on predicted secondary structure comparisons. *Proc Natl Acad Sci U S A*, *95*(6), 2818-2823.
33. Abdel-Meguid, S. S., Shieh, H. S., Smith, W. W., Dayringer, H. E., Violand, B. N., & Bentle, L. A. (1987). Three-dimensional structure of a genetically engineered variant of porcine growth hormone. *Proc Natl Acad Sci U S A*, *84*(18), 6434-6437.
34. Zhu, Y., Xu, G., Patel, A., McLaughlin, M. M., Silverman, C., Knecht, K., Sweitzer, S., Li, X., McDonnell, P., Mirabile, R., Zimmerman, D., Boyce, R., Tierney, L. A., Hu, E., Livi, G. P., Wolf, B., Abdel-Meguid, S. S., Rose, G. D., Aurora, R., Hensley, P., Briggs, M., Young, P. R. (2002). Cloning, expression, and initial characterization of a novel cytokine-like gene family. *Genomics*, *80*(2), 144-150.
35. Zhou, Y., Jia, S., Wang, C., Chen, Z., Chi, Y., Li, J., Xu, G., Guan, Y., Yang, J. (2013). FAM3A is a target gene of peroxisome proliferator-activated receptor gamma. *Biochim Biophys Acta*, *1830*(8), 4160-4170.
36. Pilipenko, V. V., Reece, A., Choo, D. I., & Greinwald, J. H., Jr. (2004). Genomic organization and expression analysis of the murine Fam3c gene. *Gene*, *335*, 159-168.

37. Katahira, T., Nakagiri, S., Terada, K., & Furukawa, T. (2010). Secreted factor FAM3C (ILEI) is involved in retinal laminar formation. *Biochem Biophys Res Commun*, *392* (3), 301-306.
38. Xu, H., Aurora, R., Rose, G. D., & White, R. H. (1999). Identifying two ancient enzymes in Archaea using predicted secondary structure alignment. *Nat Struct Biol*, *6* (8), 750-754.
39. Yang, J., & Guan, Y. (2013). Family with sequence similarity 3 gene family and nonalcoholic fatty liver disease. *J Gastroenterol Hepatol*, *28 Suppl 1*, 105-111.
40. Johansson, P., Bernstrom, J., Gorman, T., Oster, L., Backstrom, S., Schweikart, F., Xu, B., Xue, Y., Schiavone, L. H. (2013). FAM3B PANDER and FAM3C ILEI Represent a Distinct Class of Signaling Molecules with a Non-Cytokine-like Fold. *Structure*.
41. Kuhlman, B., Dantas, G., Ireton, G. C., Varani, G., Stoddard, B. L., & Baker, D. (2003). Design of a novel globular protein fold with atomic-level accuracy. *Science*, *302* (5649), 1364-1368.
42. Sandberg, W. S., & Terwilliger, T. C. (1989). Influence of interior packing and hydrophobicity on the stability of a protein. *Science*, *245* (4913), 54-57.
43. Yang, J., Gao, Z., Robert, C. E., Burkhardt, B. R., Gaweska, H., Wagner, A., Wu, J., Greene, S., Young, R., Wolf, B. A. (2005). Structure-function studies of PANDER, an islet specific cytokine inducing cell death of insulin-secreting beta cells. *Biochemistry*, *44* (34), 11342-11352.
44. Cao, X., Gao, Z., Robert, C. E., Greene, S., Xu, G., Xu, W., Bell, E., Campbell, D., Zhu, Y., Young, R., Trucco, M., Markmann, J., Najj, A., Wolf, B. A. (2003). Pancreatic-derived factor (FAM3B), a novel islet cytokine, induces apoptosis of insulin-secreting beta-cells. *Diabetes*, *52* (9), 2296-2303.
45. Burkhardt, B. R., Yang, M. C., Robert, C. E., Greene, S. R., McFadden, K. K., Yang, J. C., Wu, J. M., Gao, Z. Y., Wolf, B. A. (2005). Tissue-specific and glucose-responsive expression of the pancreatic derived factor (PANDER) promoter. *Biochimica Et Biophysica Acta-Gene Structure and Expression*, *1730* (3), 215-225.
46. German, M., Ashcroft, S., Docherty, K., Edlund, H., Edlund, T., Goodison, S., Imura, H., Kennedy, G., Madsen, O., Melloul, D., Moss, L., Olson, K., Permutt, M., Philippe, J., Robertson, B., Rutter, W., Serup, P., Stein, R., Steiner, D., Tsai, M., Walker, M. (1995). The insulin gene promoter. A simplified nomenclature. *Diabetes*, *44* (8), 1002-1004.
47. Drucker, D. J., Philippe, J., Jepeal, L., & Habener, J. F. (1987). Glucagon gene 5'-flanking sequences promote islet cell-specific gene transcription. *J Biol Chem*, *262* (32), 15659-15665.
48. Odagiri, H., Wang, J., & German, M. S. (1996). Function of the human insulin promoter in primary cultured islet cells. *J Biol Chem*, *271* (4), 1909-1915.

49. Burkhardt, B. R., Cook, J. R., Young, R. A., & Wolf, B. A. (2008). PDX-1 interaction and regulation of the Pancreatic Derived Factor (PANDER, FAM3B) promoter. *Biochimica Et Biophysica Acta-Gene Regulatory Mechanisms*, 1779 (10), 645-651.
50. Peshavaria, M., Henderson, E., Sharma, A., Wright, C. V., & Stein, R. (1997). Functional characterization of the transactivation properties of the PDX-1 homeodomain protein. *Mol Cell Biol*, 17 (7), 3987-3996.
51. Li, J., Chi, Y., Wang, C., Wu, J., Yang, H., Zhang, D., Zhu, Y., Wang, N., Yang, J., Guan, Y. (2011). Pancreatic-derived factor promotes lipogenesis in the mouse liver: role of the Forkhead box 1 signaling pathway. *Hepatology*, 53 (6), 1906-1916.
52. Wilson, C. G., Robert-Cooperman, C. E., & Burkhardt, B. R. (2011). PANcreatic-DERived factor: Novel hormone PANDERing to glucose regulation. *Febs Letters*, 585 (14), 2137-2143.
53. Kobayashi, K., Forte, T. M., Taniguchi, S., Ishida, B. Y., Oka, K., & Chan, L. (2000). The db/db mouse, a model for diabetic dyslipidemia: molecular characterization and effects of Western diet feeding. *Metabolism*, 49 (1), 22-31.
54. Wilson, C. G., Schupp, M., Burkhardt, B. R., Wu, J. M., Young, R. A., & Wolf, B. A. (2010). Liver-Specific Overexpression of Pancreatic-Derived Factor (PANDER) Induces Fasting Hyperglycemia in Mice. *Endocrinology*, 151 (11), 5174-5184.
55. Gonzalez, G. A., & Montminy, M. R. (1989). Cyclic AMP stimulates somatostatin gene transcription by phosphorylation of CREB at serine 133. *Cell*, 59 (4), 675-680.
56. Jelinek, L. J., Lok, S., Rosenberg, G. B., Smith, R. A., Grant, F. J., Biggs, S., Bensch, P., Kuijper, J., Sheppard, P., Sprecher, C., O'Hara P., Foster, D., Walker, K., Chen, L., McKernan, P., Kindsvogel, W. (1993). Expression cloning and signaling properties of the rat glucagon receptor. *Science*, 259 (5101), 1614-1616.
57. Mayr, B., & Montminy, M. (2001). Transcriptional regulation by the phosphorylation-dependent factor CREB. *Nat Rev Mol Cell Biol*, 2 (8), 599-609.
58. Livingstone, D. E., Jones, G. C., Smith, K., Jamieson, P. M., Andrew, R., Kenyon, C. J., & Walker, B. R. (2000). Understanding the role of glucocorticoids in obesity: tissue-specific alterations of corticosterone metabolism in obese Zucker rats. *Endocrinology*, 141 (2), 560-563.
59. Olefsky, J. M., & Kimmerling, G. (1976). Effects of glucocorticoids on carbohydrate metabolism. *Am J Med Sci*, 271 (2), 202-210.
60. Robert-Cooperman, C. E., Carnegie, J. R., Wilson, C. G., Yang, J. C., Cook, J. R., Wu, J. M., Young, R. A., Wolf, B. A., Burkhardt, B. R. (2010). Targeted Disruption of Pancreatic-Derived Factor (PANDER, FAM3B) Impairs Pancreatic beta-Cell Function. *Diabetes*, 59 (9), 2209-2218.

61. Robert-Cooperman, C. E., Wilson, C. G., & Burkhardt, B. R. (2011). PANDER KO mice on high-fat diet are glucose intolerant yet resistant to fasting hyperglycemia and hyperinsulinemia. *Febs Letters*, *585*(9), 1345-1349.
62. Wang, C. J., Burkhardt, B. R., Guan, Y. F., & Yang, J. C. (2012). Role of pancreatic-derived factor in type 2 diabetes: evidence from pancreatic beta cells and liver. *Nutrition Reviews*, *70*(2), 100-106.
63. Liu, X., & Gorovsky, M. A. (1993). Mapping the 5' and 3' ends of *Tetrahymena thermophila* mRNAs using RNA ligase mediated amplification of cDNA ends (RLM-RACE). *Nucleic Acids Res*, *21*(21), 4954-4960.
64. Zhang, C., Moriguchi, T., Kajihara, M., Esaki, R., Harada, A., Shimohata, H., Oishi, H., Hamada, M., Morito, N., Hasegawa, K., Kudo, T., Engel, J., Yamamoto, M., Takahashi, S. (2005). MafA is a key regulator of glucose-stimulated insulin secretion. *Mol Cell Biol*, *25*(12), 4969-4976.
65. Wang, O., Cai, K., Pang, S., Wang, T., Qi, D., Zhu, Q., Ni, Z., Le, Y. (2008). Mechanisms of glucose-induced expression of pancreatic-derived factor in pancreatic beta-cells. *Endocrinology*, *149*(2), 672-680.
66. Yang, J. C., Robert, C. E., Burkhardt, B. R., Young, R. A., Wu, J. M., Gao, Z. Y., & Wolf, B. A. (2005). Mechanisms of glucose-induced secretion of pancreatic-derived factor (PANDER or FAM3B) in pancreatic beta-cells. *Diabetes*, *54*(11), 3217-3228.
67. Cao, X. P., Yang, J. C., Burkhardt, B. R., Gao, Z. Y., Wong, R. K., Greene, S. R., Wu, J., Wolf, B. A. (2005). Effects of overexpression of pancreatic derived factor (FAM3B) in isolated mouse islets and insulin-secreting beta TC3 cells. *American Journal of Physiology-Endocrinology and Metabolism*, *289*(4), E543-E550.
68. Xu, W., Gao, Z., Wu, J., & Wolf, B. A. (2005). Interferon-gamma-induced regulation of the pancreatic derived cytokine FAM3B in islets and insulin-secreting betaTC3 cells. *Mol Cell Endocrinol*, *240*(1-2), 74-81.
69. Carnegie, J. R., Robert-Cooperman, C. E., Wu, J. M., Young, R. A., Wolf, B. A., & Burkhardt, B. R. (2010). Characterization of the expression, localization, and secretion of PANDER in alpha-cells. *Molecular and Cellular Endocrinology*, *325*(1-2), 36-45.
70. Gromada, J., Franklin, I., & Wollheim, C. B. (2007). Alpha-cells of the endocrine pancreas: 35 years of research but the enigma remains. *Endocr Rev*, *28*(1), 84-116.
71. Pipeleers, D. G., Schuit, F. C., Van Schravendijk, C. F., & Van de Winkel, M. (1985). Interplay of nutrients and hormones in the regulation of glucagon release. *Endocrinology*, *117*(3), 817-823.
72. Yang, J. C., Wang, C. J., Li, J., Burkhardt, B. R., Robert-Cooperman, C. E., Wilson, C., Gao, Z., Wolf, B. A. (2009). PANDER binds to the liver cell membrane and inhibits insulin signaling in HepG2 cells. *Febs Letters*, *583*(18), 3009-3015.

73. Shiiba, M., Ishige, S., Saito, Y., Shimizu, T., Minakawa, Y., Kasamatsu, A., Ogawara, K., Uzawa, K., Tanzawa, H. (2012). Down-regulated expression of family with sequence similarity 3, member B (FAM3B), in oral squamous cell carcinoma. *Oral Science International*, 9(1), 9-16.
74. Li, Z., Mou, H., Wang, T., Xue, J., Deng, B., Qian, L., Zhou, Y., Gong, W., Wang, J., Wu, G., Zhou, C., Fang, J., Le, Y. (2013). A non-secretory form of FAM3B promotes invasion and metastasis of human colon cancer cells by upregulating Slug expression. *Cancer Lett*, 328(2), 278-284.
75. Mou, H., Li, Z., Yao, P., Zhuo, S., Luan, W., Deng, B., Qian, L., Yang, M., Mei, H., Le, Y. (2013). Knockdown of FAM3B triggers cell apoptosis through p53-dependent pathway. *Int J Biochem Cell Biol*, 45(3), 684-691.
76. Burkhardt, B. R., Greene, S. R., White, P., Wong, R. K., Brestelli, J. E., Yang, J., Robert, C., Brusko, T., Wasserfall, C., Wu, J., Atkinson, M., Gao, Z., Kaestner, K., Wolf, B. A. (2006). PANDER-induced cell-death genetic networks in islets reveal central role for caspase-3 and cyclin-dependent kinase inhibitor 1A (p21). *Gene*, 369, 134-141.
77. Huang, H., Wu, B., Yang, S., Shao, Y., You, W., Wang, W., & Wang, M. (2008). Downregulation of PANDER expression in gastric cancer. *World Chin. J. Digestol.*, 16, 1513-1518.
78. Hajra, K. M., Chen, D. Y., & Fearon, E. R. (2002). The SLUG zinc-finger protein represses E-cadherin in breast cancer. *Cancer Res*, 62(6), 1613-1618.
79. Cano, A., Perez-Moreno, M. A., Rodrigo, I., Locascio, A., Blanco, M. J., del Barrio, M. G., Portillo, F., Nieto, M. A. (2000). The transcription factor snail controls epithelial-mesenchymal transitions by repressing E-cadherin expression. *Nat Cell Biol*, 2(2), 76-83.
80. Robert, C., Wu, J., Burkhardt, B., Wolf, B. Transgenic Mice Overexpressing the Novel Islet Specific Cytokine, PANDER, Exhibit Glucose Intolerance and Decreased beta Cell Mass. [abstract]. 2005; 54 (suppl 1): 74-LB.
81. Dougan, G., Moak, S., Athanason, M., Danse, W., Kuehl, M., Robert-Cooperman, C., Burkhardt, B. Pancreas-Specific PANDER Over Expression Induces Hepatic Insulin Resistance. [abstract]. 2012; 61 (suppl 1): 1765-P.
82. Dougan, G., Moak, S., Burkhardt, B. Glucose Intolerance and Hepatic Lipidemia with Decreased Phospho-AMPK α in PANDER Transgenic Mice. [abstract]. 2013; 62 (suppl 1): 1984-P.
83. de Wit, N. J., N, I. Jssennagger, Oosterink, E., Keshtkar, S., Hooiveld, G. J., Mensink, R. P., Hammer, S., Smit, J., Muller, M., van der Meer, R. (2012). Oit1/Fam3D, a gut-secreted protein displaying nutritional status-dependent regulation. *J Nutr Biochem*, 23(11), 1425-1433.

84. Souza, J. J. S., Machado, M. M. C., Fortez, M. A. H., Giorgi, R. R., Cunha, J. E. M., Jukemura, J., Nery, M., Wajchenberg, B., Siqueira, Giannella-Neto, D. et al. (2006). Cytokine-like Fam3d gene is associated to diabetes mellitus in pancreatic adenocarcinoma. *Pancreas*, *33* (4), 498.
85. Yang, J., Zhang, D., Li, J., Zhang, X., Fan, F., & Guan, Y. (2009). Role of PPARgamma in renoprotection in Type 2 diabetes: molecular mechanisms and therapeutic potential. *Clin Sci (Lond)*, *116* (1), 17-26.
86. Waerner, T., Alacakaptan, M., Tamir, I., Oberauer, R., Gal, A., Brabletz, T., Schreiber, M., Jechlinger, M., Beug, H. (2006). ILEI: a cytokine essential for EMT, tumor formation, and late events in metastasis in epithelial cells. *Cancer Cell*, *10* (3), 227-239.
87. Greinwald, J. H., Jr., Wayne, S., Chen, A. H., Scott, D. A., Zbar, R. I., Kraft, M. L., Prasad, S., Ramesh, A., Coucke, P., Srisailapathy, C., Lovett, M., Van Camp, G. Smith, R. J. (1998). Localization of a novel gene for nonsyndromic hearing loss (DFNB17) to chromosome region 7q31. *Am J Med Genet*, *78* (2), 107-113.
88. Chaudhury, A., Hussey, G. S., Ray, P. S., Jin, G., Fox, P. L., & Howe, P. H. (2010). TGF-beta-mediated phosphorylation of hnRNP E1 induces EMT via transcript-selective translational induction of Dab2 and ILEI. *Nat Cell Biol*, *12* (3), 286-293.
89. Hussey, G. S., Chaudhury, A., Dawson, A. E., Lindner, D. J., Knudsen, C. R., Wilce, M. C., Merrick, W. C., Howe, P. H. (2011). Identification of an mRNP complex regulating tumorigenesis at the translational elongation step. *Mol Cell*, *41* (4), 419-431.
90. Xiang, J. N., Chen, D. L., & Yang, L. Y. (2012). Effect of PANDER in betaTC6-cell lipoapoptosis and the protective role of exendin-4. *Biochem Biophys Res Commun*, *421* (4), 701-706.
91. Wolfer, D. P., Crusio, W. E., & Lipp, H. P. (2002). Knockout mice: simple solutions to the problems of genetic background and flanking genes. *Trends Neurosci*, *25* (7), 336-340.
92. Seong, E., Saunders, T. L., Stewart, C. L., & Burmeister, M. (2004). To knockout in 129 or in C57BL/6: that is the question. *Trends Genet*, *20* (2), 59-62.
93. Friedman, J. M., & Halaas, J. L. (1998). Leptin and the regulation of body weight in mammals. *Nature*, *395* (6704), 763-770.
94. Ahima, R. S., & Flier, J. S. (2000). Leptin. *Annu Rev Physiol*, *62*, 413-437.
95. Horwitz, D. L., Starr, J. I., Mako, M. E., Blackard, W. G., & Rubenstein, A. H. (1975). Proinsulin, insulin, and C-peptide concentrations in human portal and peripheral blood. *J Clin Invest*, *55*(6), 1278-1283.

96. Robert-Cooperman, C. E., Dougan, G. C., Moak, S. L., Athanason, M. G., Kuehl, M. N., & Burkhardt, B. R. (2013). PANDER Transgenic Mice Display Fasting Hyperglycemia and Hepatic Insulin Resistance. In Review. *Journal of Endocrinology*.
97. Kim, J. K. (2009). Hyperinsulinemic-euglycemic clamp to assess insulin sensitivity in vivo. *Methods Mol Biol*, 560, 221-238.
98. Scherer, L. J., & Rossi, J. J. (2003). Approaches for the sequence-specific knockdown of mRNA. *Nat Biotechnol*, 21(12), 1457-1465.
99. German, J. P., Wisse, B. E., Thaler, J. P., Matsen, M. E., Taborsky, G. J., Jr, Schwartz, M. W., Morton, G, J. Leptin action in the brain normalizes diabetic hyperglycemia via insulin-independent mechanisms. [abstract]. 2010; 59 (suppl 1): 1638-P.
100. German, J., Kim, F., Schwartz, G. J., Havel, P. J., Rhodes, C. J., Schwartz, M. W., & Morton, G. J. (2009). Hypothalamic leptin signaling regulates hepatic insulin sensitivity via a neurocircuit involving the vagus nerve. *Endocrinology*, 150 (10), 4502-4511.
101. Zingone, A., Hiraiwa, H., Pan, C. J., Lin, B., Chen, H., Ward, J. M., & Chou, J. Y. (2000). Correction of glycogen storage disease type 1a in a mouse model by gene therapy. *J Biol Chem*, 275 (2), 828-832.
102. Wolfsdorf, J. I., & Weinstein, D. A. (2003). Glycogen storage diseases. *Rev Endocr Metab Disord*, 4 (1), 95-102.
103. Wang, X., Sato, R., Brown, M. S., Hua, X., & Goldstein, J. L. (1994). SREBP-1, a membrane-bound transcription factor released by sterol-regulated proteolysis. *Cell*, 77 (1), 53-62.

APPENDICES

Appendix A: Primary Antibodies Utilized

Table A1. Primary Antibodies and their Respective Catalog Numbers Used in SDS-PAGE in Chapter 3.


Primary Antibody Used	Source
IRS-1 (C-20)	Santa Cruz Biotechnologies, Cat. # sc-559
p-IRS-1 (Tyr 989)	Santa Cruz Biotechnologies, Cat. # sc-17200
p-PI3K p85 α	Santa Cruz Biotechnologies, Cat. # sc-12929
Total Akt	Cell Signaling Technology, Cat. # 4691
p-Akt Thr 308 (244F9)	Cell Signaling Technology, Cat. # 4056
SREBP-1C (Mature & Precursor) (H-160)	Santa Cruz Biotechnologies, Cat. # sc-8984
Total ACC (C83B10)	Cell Signaling Technology, Cat. # 3676
p-ACC (Ser79)	Cell Signaling Technology, Cat. # 3661
Total AMPK α (23A3)	Cell Signaling Technology, Cat. # 2603
p-AMPK α (Thr172)	Cell Signaling Technology, Cat. # 2535
GAPDH (14C10)	Cell Signaling Technology, Cat. # 2118
Total Glycogen Synthase (15B1)	Cell Signaling Technology, Cat. # 3886
p-Glycogen Synthase (Ser641)	Cell Signaling Technology, Cat. # 3891
Total CREB	Cell Signaling Technology, Cat. # 4820
p-CREB (Ser133)	Cell Signaling Technology, Cat. # 4276
p-FOXO1 (Thr24)/FoxO3a (Thr32)	Cell Signaling Technology, Cat. # 9464

Appendix B: 4005M Breeding Protocol for PANKO-C57 IACUC Approval



MEMORANDUM

TO: Brant Burkhardt, PhD
Dept. of Biology
BSF_213

FROM: Jay B. Dean, Ph.D., Chairperson 
Institutional Animal Care & Use Committee
Division of Research Integrity and Compliance

DATE: 6/23/2011

PROJECT TITLE: Colonies for Evaluating the Cytokine-Like Pancreatic-Derived Factor

AGENCY/SOURCE OF SUPPORT: Departmental

IACUC PROTOCOL#: M 4005

PROTOCOL STATUS: APPROVED

The Institutional Animal Care and Use Committee (IACUC) received your *Request to Amend An Animal Use Protocol* application concerning the above referenced IACUC Protocol.

The following amendment(s) were reviewed and **APPROVED** by the IACUC on 6/23/2011:

Additional Strain of Mice: JAX strain B6.129S6-Fam3b^{tm1Bkht}/J (Stock# 013788).

cc: Comparative Medicine

Appendix C: Experimental 4071 R Protocol IACUC Approval



DIVISION OF RESEARCH INTEGRITY AND COMPLIANCE
INSTITUTIONAL ANIMAL CARE USE COMMITTEE

MEMORANDUM

TO: Brant Burkhardt, PhD
Dept. of Biology
BSF_213

FROM: Jay B. Dean, Ph.D., Chairperson
Institutional Animal Care & Use Committee
Division of Research Integrity and Compliance 

DATE: 9/28/2011

PROJECT TITLE: Mechanism of Pancreatic-Derived Factor (PANDER) Induced Glycemic Regulation

AGENCY/SOURCE OF SUPPORT: Departmental

LACUC PROTOCOL#: R 4071

PROTOCOL STATUS: APPROVED

The Institutional Animal Care and Use Committee (IACUC) reviewed your application requesting the use of animals in research for the above-entitled study. The IACUC APPROVED your request to use the following animals in your protocol for a one-year period beginning 9/23/2011 :

- * 320 Mice

Please reference the above IACUC protocol number in all correspondence regarding this project with the IACUC, Comparative Medicine, or the Division of Research Integrity and Compliance. In addition, please take note of the following:

- IACUC approval is granted for a one-year period at the end of which, an annual renewal form must be submitted for years two (2) and three (3) of the protocol. After three years all continuing studies must be completely re-described in a new application and submitted to IACUC for review.
- All Comparative Medicine pre-performance safety and logistic meetings must occur prior to implementation of this protocol [IACUC policy V.10]. Please contact the program coordinator at compmed@research.usf.edu, to schedule a pre-performance meeting.
- All changes to the IACUC-Approved Protocol must be pre-approved by the IACUC [IACUC policy III.11]. Minor changes can be submitted to the IACUC for review and approval as an amendment or procedural change, whereas major changes to the protocol require submission of a new IACUC application. Minor changes are changes considered to be within the scope of the original research hypothesis or involve the original species and are submitted to the IACUC as an Amendment or Procedural change. Any change in the IACUC-approved protocol that does not meet the latter definition is considered a major protocol change and requires the submission of a new application. More information on what constitutes a minor versus major protocol change and procedural steps necessary for IACUC review and approval are available on the Comparative Medicine web site at <http://www.research.usf.edu/cm/amendments.htm>
- All costs invoiced to a grant account must be allocable to the purpose of the grant [IACUC policies IV.5 and V.10]. allocable to one protocol may not be shifted to another in order to meet deficiencies caused by overruns, or for other reasons@66ts convenience. Rotation of charges among protocols by month without establishing that the rotation schedule credibly reflects the relative benefit to each protocol is unacceptable.

For more information on IACUC policies and procedures, please visit the Comparative Medicine web site at <http://www.research.usf.edu/cm/default.htm>.

cc: Comparative Medicine
Division of Research Grants

OFFICE OF RESEARCH · DIVISION OF RESEARCH INTEGRITY AND COMPLIANCE
INSTITUTIONAL ANIMAL CARE AND USE COMMITTEE
PHS No. A4100-01, AAALAC No. 58-15, USDA No. 58-15
University of South Florida · 12901 Bruce B. Downs Blvd., MDC35 · Tampa, FL 33612-4799
(813) 974-7106 · FAX (813) 974-7091